NASA TECHNICAL MEMORANDUM

NASA TM X-73450

CENTAUR D-1A NOSE FAIRING JETTISON TEST

by W. M. Prati
Lewis Research Center
Cleveland, Ohio 44135

June 1976

1. Report No. NASA TM X-73450	2. Government Accession No.	3. Recipient's Catalog No.
4. Title and Subtitle CENTAUR D-1A NOSE FAIRING JETTISON TEST		5. Report Date
		6. Performing Organization Code
7. Author(s) W. M. Prati		8. Performing Organization Report No. E-8808
		10. Work Unit No.
9. Performing Organization Name and Address Lewis Research Center National Aeronautics and Space Administration Cleveland, Ohio 44135		11. Contract or Grant No.
		13. Type of Report and Period Covered Technical Memorandum
12. Sponsoring Agency Name and Address National Aeronautics and Space Administration Washington, D.C. 20546		14. Sponsoring Agency Code
15. Supplementary Notes		

16. Abstract

An experimental investigation was conducted to verify the functional and structural capability of the Centaur D-1A nose fairing. A full-scale flight-type nose fairing was jettisoned at the Lewis Research Center Space Power Chamber at simulated altitude. Two complete jettisons of the nose fairing were performed, one without aft helper springs and one with aft helper springs. A "static" rotation test was also performed to verify the capability of the helper springs and to allow clearance measurements between the nose fairing and spacecraft envelope mock-up at certain discrete nose fairing rotation angles. Nose fairing trajectories, structural deflections, clearances, and hinge forces during jettison are presented. Data from subsequent Centaur D-1A flights, relative to nose fairing jettisons, are compared with the experimental results.

17. Key Words (Suggested by Author(s))	18. Distribution Statement
Nose fairing; Altitude jettison test; Nose fairing jettison deflections; Nose fairing to spacecraft clearances; Aft helper springs	Unclassified - unlimited

19. Security Classif. (of this report)	20. Security Classif. (of this page)	21. No. of Pages	22. Price*
Unclassified	Unclassified		

* For sale by the National Technical Information Service, Springfield, Virginia 22161

NASA-C-168 (Rev. 10-75)

Table of Contents

Tables

Figures

Plotted Data

ABBREVIATIONS

MVM	Mariner-Venus-Mercury
D-1A	Atlas/Centaur Configuration
g	Gravitational force at earth's surface
OAO	Orbiting Astronomical Observatory
AC-22, AC-31, etc.	Specific Atlas/Centaur Vehicle
LeRC	Lewis Research Center
SPC	Space Power Chamber
NASA	National Aeronautics and Space Administration
EED	Electro-Explosive Device, Squib
Quad	Quadrant
o-p	Zero to Peak
Stringer ID	Specific Stringer Location, Str
HSL	Horizontal Split Line
VSL	Vertical Split Line
LPOF	Lowpass Output Filter
NFJ	Nose Fairing Jettison
FPA	Forward Payload Adapter
Hz	Cycle per Second
N/A	Not Applicable
A/C	Air Conditioning
N/F	Nose Fairing
S/N	Serial Number
Lbs.	Pounds
RFI	Radiated Frequency Interference

D-1A N/F JETTISON TEST

Summary

The Atlas/Centaur aerospace vehicle employs a jettisonable nose fairing to encapsulate and protect various spacecraft from aerodynamic forces during ascent through the earth's atmosphere (Figure 1). When the vehicle has attained an altitude above the denser atmosphere, the clamshell-type fairing is jettisoned from the second stage Centaur. This event separates the fairing weight from the second stage, as well as deencapsulating the spacecraft preparatory to later spacecraft separation from the vehicle.

In order to verify the structural integrity of the fairing and the functional capability of the separation system at altitude, an experimental investigation was conducted at the Lewis Research Center (December 1972). A flight-type D-1A nose fairing assembly encapsulating mock-ups of the Intelsat and Mariner-Venus-Mercury (MVM) spacecraft was subjected to a simulated altitude test in a vacuum chamber. Vehicle axial acceleration was not duplicated exactly; the earth's 1-g surface gravity was a close approximation to the 0.75g acceleration field during flight jettison. The fairing pyrotechnics were activated and the nose fairing was jettisoned from a mock-up of the Centaur forward end. Catch nets were utilized to decelerate and capture the fairing halves. One "static" rotation test and two "all-up" systems jettison tests were performed.

Each of the test runs was successful in demonstrating the structural and functional capability of the nose fairing system during jettison. There were no structural failures of the system and the separation and jettison characteristics of the fairing halves were verified to occur at the predicted velocities and accelerations.

All pyrotechnic detonators in the explosive bolts fired properly. One anomaly occurred in the pyrotechnic harnesses at the harness connector. Data presented in the text show that the two electric detonators in each of the bolts did not fire simultaneously. The firing of one detonator severed the bolt and propelled each bolt half into a deceleration block. When the bolt halves reached the deceleration blocks, the firing of the second detonator while its bolt half was engaged in the deceleration block increased the deceleration forces and caused the wire harness pins to be pulled free of the connector exposing the two pins. Since the harnesses are still connected to the pyro batteries at this time, a short across these two exposed pins could generate RFI detrimental to the vehicle's electronic systems. Table 1, page 16, shows the detonator locations that had this pin/connector problem. This pin exposure problem was solved by the use of a specially-designed clamshell retainer. These retainers, used on Test No. 3, were successful in precluding harness damage.

Fairing trajectories and clearances were within design limits. The hinge load data indicated acceptable levels of force transferred into the supporting stub adapter section. Fairing structural deflections during the jettison event were as predicted. Data relating to trajectories, dynamic characteristics, hinge loads, and clearances from each test are presented in this report.

With one design fix incorporated into the pyrotechnic harness, the results of the test program indicate that all components and subsystems of the nose fairing in the flight configuration are suitable for their required functions.

Introduction

A nose fairing 10 feet in diameter and 33.6 feet long is used with the Atlas/Centaur launch vehicles. The fairing is a low-drag cylindrical conical lightweight shell assembled from fiberglas and metallic sections. It is mounted on the forward end of the Centaur stage and encapsulates the payload and the forward mounted vehicle equipment. The primary functions of the fairing are to minimize the aerodynamic forces on the vehicle and to completely protect the spacecraft and vehicle equipment from these forces during ascent through the atmosphere. At an altitude above the dense atmosphere, the jettisonable bisegment section of the fairing is jettisoned from the Centaur vehicle. This eliminates the weight of the functionally expended fairing and deencapsulates the spacecraft in preparation for separation from the Centaur. The separation systems must unlatch the fairing halves and jettison them clear of the vehicle. Simultaneously, the fairing halves must retain their structural integrity while subjected to the jettison forces.

The nose fairing is a composite of existing and new designs. It incorporates the existing design of the AC-22 (OAO) nose fairing along with some design changes required for the D-1A configuration. A comparison of the AC-22/D-1A nose fairing systems is given in the text of this report.

Analysis of the design indicated that the fairing system would perform satisfactorily at jettison. The calculated fairing separation forces, structural capabilities, dynamic characteristics, hardware clearances, and jettison trajectories were adequate for the established requirements.

Component designs incorporated from other vehicle fairings had been previously evaluated and verified by ground testing and flight usage during their development. However, the component redesigns which were incorporated in the D-1A configuration negated use of the earlier test results in evaluating the new configuration. Since a satisfactory fairing jettison is required for a successful mission, verification of the design and analysis by functional testing of the complete fairing assembly was necessary to establish confidence for flight use. Therefore, a test program was initiated to qualify the composite design.

Valuable assistance was provided by the fairing contractor, Convair Division of General Dynamics Corporation, during the entire test program.

Test Objectives

The overall objective of the test program was to qualify the fairing system for flight use. A prototype flight fairing specimen was used in conjunction with an Intelsat and MVM spacecraft mock-up. The tests were conducted at a simulated altitude of approximately 90,000 feet with the fairing vertical to employ the 1-g surface gravity of the earth. The actual acceleration of the flight vehicle at the time of nose fairing jettison is approximately 0.75g's. Other environmental parameters of flight, such as ambient temperature, vehicle vibration, and lateral motion were not duplicated.

The primary objective of the test program was to successfully perform two jettison tests of the complete fairing system for verification of its functional and structural capability.

The secondary objectives of the test program were to define the following:

(1) Fairing jettison trajectories
(2) Fairing structural deflections during jettison
(3) Fairing hinge loads during jettison
(4) Behavior of the pyrotechnic electrical system during activation

Successful jettison was defined as: (1) all pyrotechnics must fire within 10 milliseconds after receiving firing voltage, (2) all jettisonable hardware must separate cleanly, and (3) functional or structural failures must not occur.

Test Facility Structure and Equipment

Testing was performed in the Space Power Chamber facility of the NASA Lewis Research Center. The facility consists of an operations building and an attached steel structure that houses two altitude test chambers. The tests were conducted in the center section of the test chamber as shown in Figure 3. Essentially, this part of the chamber is a large, steel, horizontal cylinder with an inside diameter of 51 feet and a length of 121 feet. The chamber has a total volume of 185,000 feet^3. It is connected to a large capacity-pumping system capable of reducing the chamber internal pressure to the equivalent of an altitude of 90,000 feet in approximately one hour. Facility services available within the chamber are area lighting, electrical power, compressed air, and monorail mounted hoists. An annular-shaped platform elevator with an inside diameter of 11 feet was installed in the center of the test area. This service platform could be

elevated on guide columns to any level between the floor and ceiling of the test chamber for ready access to the test article (of length 47.5 feet) during erection and servicing.

In order to decelerate and arrest the motion of the jettisoned fairing halves, a catcher and snubber system was installed in the test area. Two 50 feet long by 30 feet wide nylon nets were supported approximately 10 feet above the chamber floor to catch and decelerate the fairing halves after each jettison, as shown in Figure 2. To prevent excessive rebound of the fairings, each net had 12 snubber assemblies. Each assembly consisted of a rope bridle attached to the underside of the net, snubbed around a floor-mounted drum, and pretensioned with an elastic cord takeup line.

In addition to the general area lighting and the electrically operated hoists, electrical power was used for motion picture camera operation and floodlighting. Motion picture cameras were energized through an automatic switch operated by a test event sequencer located in the control room.

The control system consisted of the event sequencer and an event timer. The sequencer was programmed to initiate three events: (1) switch on the cameras and the oscillograph recorders prior to start of the test, (2) furnish a command signal to the event timer to start the test, and (3) switch off the cameras and recorders at test termination. The first event was initiated immediately following activation of the sequencer. Time delay relays in the sequencer initiated the second event 3 seconds later and the third event 13 seconds after sequencer start.

The event timer issued pulse signals to camera timing lights and to the oscillograph and magnetic tape recorders for correlation of data. The pulses were 16 2/3 milliseconds in duration at 100 millisecond intervals. An isolation circuit in the timer restrained the pulses from being issued prior to the start of the test. Upon receipt of the command signal from the sequencer, a holding circuit in the event timer restrained the signal until the next timing pulse was generated. At that instant, the command signal and the timing pulses were related simultaneously to the nose fairing jettison control unit and to the recorders and timing lights, respectively.

Test Hardware Description

The nose fairing was a 10-foot diameter cylindrical shell terminating in a cone at the forward end. It consisted of two major elements: the conical/cylindrical fiberglas section (nearly 29 feet long) and the aluminum split barrel. The fiberglas section is made from a 3/4 inch thick phenolic honeycomb core sandwiched between laminated glass cloth skins. The split barrel was attached to the stub adapter. It was 56 inches long, 10 feet in diameter,

was of aluminum skin/stringer construction, and had four doors (one in each quadrant for access to the Centaur equipment module). Each half of the split barrel contained two hinges which allowed the fairing halves to rotate from the vehicle. The stub adapter was installed on the forward tank ring and was not jettisoned. It supported the payload, payload adapter, equipment module structure, and the jettisonable nose fairing and split barrel structures. This adapter also contained the lower mating shelf of each of the separation hinges for the split barrel. The two fairing halves were held together by 12 explosive bolts mounted along the vertical split line. Eight explosive bolts attached the fairing to the stub adapter. Separation force was provided by two large springs near the dome held compressed by the shroud halves (AC-31 configuration). The MVM configuration has two additional aft mounted helper springs (Figure 4). The longerons at the vertical split line of both the fiberglas section and the split barrel contained shear pins along each split line that transferred flight loads between the shell halves. An inner seal between the longerons prevented leakage (Figure 5). The GDC part numbers and serial numbers of some of the hardware used for the test are listed in Table 1.

The major configuration differences between the "D-1A" (AC-31, MVM) configuration nose fairing and the OAO (AC-22) "D" configuration (tested previously at the LeRC SPC No. 2 in 1972) are the following:

1) The D-1A vertical split line separation plane is aligned with the Centaur vehicle X-axis. The AC-22 vertical split line place was rotated 25 degrees (CCW viewed aft) off the vehicle X-axis.

2) The D-1A fairing halves are fastened together along the vertical split line with six explosive bolts on each side. AC-22 had five explosive bolts on each side.

3) The D-1A nose fairing halves are fastened to the stub adapter at the horizontal split line plane with four explosive bolts on each half. AC-22 used three explosive bolts on each half in conjunction with a lap-joint at the circumferential junction of the horizontal and vertical split line planes.

4) The 56-inch-long aluminum "split barrel" aft section of the D-1A nose fairing is 20.5 inches longer than the corresponding "split fairing" aft section of the AC-22 nose fairing. The fiberglas/honeycomb forward section of both the D-1A and AC-22 fairing configuration is 347 inches long.

A typical explosive bolt installation is shown in Figure 6. A one amp one watt pressure cartridge is located in each end of the bolt. Spherical seats on the bolt ends and fittings allow fitting misalignment without bolt binding. Energy absorbers reduce the impact load that occurs when the bolt fractures and impacts the structure. The bolt fracture plane is located at the separation plane of the fittings. Each bolt will function properly when fired from either end with

one electric explosive device and with a tension load of 0 - 36,000 lbs. applied. Each bolt is a self-contained unit with no additional hardware or adjustment required except the electric explosive devices.

The fairing electrical pyrotechnic system (Figure 6) consists of two independent subsystems, each capable of supplying power to separate the nose fairing. Each subsystem consists of one 28 volt DC battery, two control units, and 20 electro-explosive devices (EEDs). A minimum of five amperes is supplied to each EED for a minimum of 50 milliseconds. Maximum time to fire with this current is 10 milliseconds. Basically, all EEDs receive current simultaneously. There have been time differences between subsystems in the order of 1.0 milliseconds. Each EED has a 1 amp, 1 watt, no fire capability.

As stated previously, the AC-31 (Intelsat) configuration uses only the forward spring actuators for jettison energy. Each actuator provides an initial force of from 1225 to 1450 lbs. with a stroke of 30.5 ± 1.5 inches. The compressed length is approximately 29 inches. Jettison force is applied for 2 1/2 degrees of fairing rotation. No contamination results from the actuator action as each is a self-contained unit. In the case of the MVM configuration, two additional aft mounted helper springs are used. Each helper spring provides an initial force of 1620 lbs. ± 200 lbs. with a stroke of approximately 10 inches. These springs were added to insure that a positive torque was applied to the nose fairing until the center of gravity of the fairing was past the hinge centerline. These springs are active for approximately 15 degrees of fairing rotation. The c.g. of the fairing rotates over the hinge centerline at approximately 12 degrees.

Upon issuance of the jettison command signal by the Centaur programmer, the relay assemblies mounted in the split barrels electrically complete the circuits from the split barrel-mounted batteries to the EEDs. At release of the separation latches, the energy furnished by the spring actuators forces the fairing halves to rotate outboard on the aft-mounted hinges. The hinges are of a fork and pivot pin design that permits hinge disengagement and separation after 30 degrees of rotation. Fairing design is such, however, that the forces during jettison will separate the fairings from the vehicle hinges at approximately 75 degrees of fairing rotation. One forward actuator will jettison both fairing halves and one aft actuator will jettison its corresponding fairing half.

The spacecraft mock-ups were fabricated from wood and simulated the maximum envelope each spacecraft would encompass. Static and dynamic clearance measurements were recorded relative to the fairing and mock-up.

Instrumentation and Data Recording

Electrical transducers, mechanical sensors, and high-speed motion picture cameras were used to measure and record the various events during the tests. (See Table 2 and Figures 7, 8, 9, 10, 11, and 12 for instrumentation definition.)

Five types of electrical transducers were used: 1) breakwire, 2) electrical bus disconnect, 3) strain gage, 4) accelerometer, and 5) extensometer. The flight-type breakwires were located at the hinge line and indicated the 45 degree angular position event time of the nose fairing halves during jettison. The bus disconnects were specific circuits (also used in flight) that terminated in electrical connectors located at the jettison hardware interface. Rotation of the fairing halves operated mechanical lanyards that caused the connectors to separate and open the circuits which indicated the event. The strain gages were of the biaxial type installed on each of the aft hinge fittings to measure jettison loads transmitted to the Centaur vehicle. The extensometers were used to determine fairing rotation angle and velocity. The pyrotechnic circuit battery currents and voltages were also measured.

The data from these transducers were recorded on magnetic tape and oscillographs.

Motion picture cameras (black-and-white) were used extensively to monitor the test. Most of the cameras were operated at 400 frames per second. Photographic targets were installed at various locations on the nose fairing for reference in the film. The data from several of the cameras were used for trajectory and shell deflection analyses.

Test Sequence Summary

Test No.	Date	Test Description
1	December 5, 1972	Separation and jettison test at altitude (79,500 feet) using the primary forward jettison actuators only (AC-31). No helper springs were used since this was a simulation of an AC-31 configuration jettison.
2a	December 14, 1972	"Static" rotation test of the Quad II/III fairing half using the aft mounted helper spring only. The fairing half was rotated incrementally (at atmospheric pressure) through 39 degrees. The MVM spacecraft mock-up, mission peculiar adapter, payload adapter with seal, thermal bulkhead, and partial air conditioning ducting and disconnect were used.

Test No.	Date	Test Description
2b	January 12, 1973	"Static" rotation test of the Quad I/IV fairing half using the aft-mounted helper spring only. The fairing half was rotated incrementally (at atmospheric pressure) through 30 degrees. The MVM configuration summarized in Test 2a was used.
3	January 30, 1973	Separation and jettison test, at altitude (91,000 feet), using the primary and aft helper springs. The MVM configuration summarized in Test 2a was used.

Results and Discussion

The test program was successfully accomplished. The test results verified that the nose fairing halves jettisoned satisfactorily and that no critical clearance problems existed with the Intelsat or MVM payload envelopes. Data obtained from the separation and jettison tests (Tests 1 and 3) were similar to data obtained during flight and during previous testing of the "D" configuration OAO nose fairing.

Analysis of the rotation data shows that the times for Tests 1 and 3 are approximately 0.1 to 0.2 seconds slower than comparable tests conducted on the AC-22 configuration at the SPC. The rotation data for the D-1A tests are presented in Tables 3 and 4. Data are presented in Figures 13 through 20 showing fairing rotation as a function of time. Figures 21 and 22 show rotation angle and angular velocity as a function of time for the MVM configuration. This configuration utilizes the helper springs and will be the configuration for all future D-1A nose fairing systems.

The rotation velocity presented in Figures 13 through 20 compares well with data obtained in the previous SPC testing of the AC-22 OAO fairing halves and was approximately 30 to 35 degrees per second when the primary jettison springs were fully extended (approximately 2 degrees of half fairing rotation). The magnitude of the rotation velocity was masked by a 34 Hz fairing mode. This 34 Hz high frequency mode was also present in the fairing accelerometer measurements and other data. (Note: The large transients exhibited by the velocity data at 0.76 seconds in Figure 17 and 0.78 seconds in Figure 19 were caused by instrumentation and are not actual structural test data.)

Operation of the electrical systems was satisfactory. Operation of battery systems 1 and 2 is summarized in Tables 5 and 6. Analysis of the data showed that the load was applied first at pyro relay boxes U3 and U4 of battery system 1 for both tests (hard load start times). Power demand at relay box U3 led the power demand at U5 by 1.1 and 0.9 milliseconds for Tests 1 and 3, respectively; power demand at relay box U4 led the power demand at U6 by 0.8 and 0.4 milliseconds for Test 1 and 3, respectively. Each relay box fired 10 of the 40 electro-explosive squibs, one on each end of the 20 explosive bolts. Relay boxes U3 and U5 fired either side of 10 explosive bolts, and relay boxes U4 and U6 fired either side of the other 10 explosive bolts. This data shows that the two electric detonators per bolt do not fire simultaneously. The time difference was such that the detonation of the second cartridge occurred while its bolt half was decelerating in the deceleration block. This increased the deceleration forces on the bolt half and caused the harness pins to be pulled free of the connector as stated in page 1 of this report.

The harness damage was experienced during Test No. 1 with the explosive bolt squib wiring at the squib connectors. This type of difficulty has occurred previously during LeRC SPC jettison tests, although not during every test. During Test No. 1, all the Battery 2 connectors (fired by Relay Boxes U5 and U6) had some damage. Fourteen of the squib connectors had minor pull damage; but the other six, all fired by Relay Box U5 and all on the vertical split lines of the Quad II/III fairing half, had the wires and attached pin connectors pulled out of the connector at the pyrotechnic squib. Exact location of the damaged wiring may be determined from Table 1. All 20 wiring harnesses at the squib connectors were reterminated with new connectors (flight-approved refurbishment) prior to Test No. 3 (per GDC memorandum 623-2-72-100, dated December 21, 1972).

To prevent harness damage at the squib connectors, pyro harness connector retainers were designed and used for Test No. 3. These clamshell-like metallic devices were installed with safety wire after the connectors had been attached to the squibs. No damage was evident in the pyro harness wiring after Test No. 3. The pyro harness connector retainers have been approved for flight.

After Test No. 3, an unusual profile was noted in the Battery System 1 ground path current measurement (measurement 24). Typically, the ground path current measurements indicate a peak current of 17 to 25 amperes immediately after detonation of the pyrotechnic cartridges (squibs), with a decay to approximately 5 to 10 amperes in 30 milliseconds. Data after this time usually indicates a smoothly varying low-level current profile until the pyro relays deactivate. The data from Test No. 3 indicated a smoothly increasing trend after 0.121 seconds (from 6.2 amperes and 26.4 VDC) which had reached 30 amperes and 14.7 VDC by 0.244 seconds. The current stayed above 25 amperes until 0.582 seconds when it decreased from 26.1 amperes (15.6 VDC) to 2.5 amperes (28.7 VDC). The current then further decreased to 0 amperes at 0.596 seconds (29.8 VDC). These current "drops" at 0.582 and 0.596 seconds were due to the denergization of relays B304U4 and B304U3, respectively.

The pyro relay U3 current data (measurement 22) also indicated a fault load in the Test No. 3 Battery System 1 data. Typically, the relay current measurements decay to near 0 amperes within 50 to 100 milliseconds after pyrotechnic detonation. After decaying to approximately 2 amperes as expected, the current started to increase at 0.154 seconds and remained at 11 to 15 amperes from 0.3 to 0.58 seconds. The maximum fault load was 20 amperes (14 VDC) at 0.501 seconds. At deenergization of the U4 pyro relay, the U3 current dropped to zero. No other relay current measurements showed any increase whatsoever after the initial post-detonation decay.

Prior to removal of the expended squibs after Test No. 3, a test check revealed a short-to-structure ground on pin 15 of B30456. This was the positive feedline to connector B304A145Q1 (power to squib 1 of explosive bolt No. 14 on the stub adapter, 180 degrees from -X axis). The expended squib on this connector was checked and found to have a 0.06 ohm short between pin A and the cartridge case. A large piece of slag was found inside across the base of the case. A check of the other 39 squibs showed no other squib with a shorted condition.

For bolts 11 through 20, ground loop paths for the squibs were provided by the pyro cable shields and the metal structure of the split barrel and equipment structure. The presence of transient ground plane currents in the equipment module was a definite possibility. For bolts 1 through 10 on the fiberglas structure, ground loop paths for the squibs were provided by the pyro cable shields.

The B304P/J4 and B304B/J6 lanyard connectors (vertical split line) carried power to the horizontal split line pyrotechnics. Power through B304P/J6 was removed before disconnect (at approximately 14.5 degrees of fairing rotation). residual current through B304P/J4 was broken at the time of disconnect (approximately 1 degree of fairing rotation; refer to Table 3, B304P3 disconnect). Data from Test No. 3 indicated a 5-ampere ground loop current was broken by B304P4.

Strain gage data obtained from the axial and radial measurements on each of the four nose fairing hinge brackets were satisfactory. Comparison of this data with similar data taken during previous testing at LeRC SPC No. 2 and during flight showed good agreement. The data are summarized in Table 7 and the raw analog data are presented in Figures 23 through 26. Analysis of the strain gage and motion picture data clearly showed that rocking motion of the nose fairing halves occurred during jettison. Motion picture and recorded instrumentation data also showed the breathing modes of the fairing halves during rotation (Figures 27 and 28).

Twelve accelerometers were installed on the fairing halves (four each at three different Station locations) on the vertical split line (S/L) to measure fairing "breathing" during rotation. Refer to Figure 12 for exact locations. These measurements provided valid data and indicated that the zero-to-peak (o-p) amplitudes experienced during rotation were greatest during early rotation. The maxima recorded ranged between 0.4 and 0.9 inches (o-p)

Analysis of these data was performed both manually and electronically. Slide rule computations were made of the raw accelerometer data presented in Figures 29 through 40 and zero-to-peak deflections were obtained for the greatest acceleration peaks. These data are summarized in Tables 8 and 9.

The accelerometer data was also double integrated using an analog computer at LeRC and these data are presented in Figures 29 through 40.

(The raw accelerometer data in Figures 29 through 40 were filtered using low pass output filters of 8 Hz to 20 Hz. This removed the higher frequencies, especially 34 Hz, which were present in these potentiometer-type accelerometer measurements. Apparent phase lags in the integrated data of Figures 29 through 40 were due to delays in the integration circuit.)

Insulation Panel Jettison Simulation

In order to more closely duplicate the flight loads on the nose fairing pyrotechnic batteries, 20 ampere loads were placed on each battery for 20 milliseconds at T-70 seconds using a pyro simulator box. This load simulated firing of the linear shaped charge at the time of insulation panel jettison. The actual magnitude and duration of the load is summarized in Tables 10 and 11.

Analysis of Tables 10 and 11 and all other test data indicated that the pyrotechnic batteries were "hotter" after discharge and recharge than when used after initial activation. The same batteries were used in System 1 and System 2 for both jettison tests (Test No. 1 and Test No. 3). Inspection of Tables 10 and 11 will show that the batteries were generally hotter during the load portion of the MVM test than they were during the load portion of the AC-31 test. Moreover, postload recovery after Test No. 3 was virtually a step function back to the pretest voltage, whereas the recovery after Test No. 1 was much more gradual.

Other data which substantiate that the recharged batteries were hotter than initial-use batteries were presented in the battery load test data (obtained prior to Test No. 1 and Test No. 3 during battery conditioning) and in the peak current and squib blowoff times of Tables 5 and 6. The pertinent values are summarized in Table 12. It can be seen in Table 12 that after discharge and recharge, the batteries delivered more current at a higher potential to the same load. Also, the current delivered during the second jettison test was in each case higher with a quicker squib blowoff time.

Nose Fairing Jettison Clearance Losses

The total payload clearance loss due to the fairing motion during jettison is made up of the following:

1) Split line flexing (breathing)
2) Nose fairing rocking
3) Nose fairing twisting

Figures 27 and 28 show the cyclic motion (6.7 Hz) of the nose fairing split line at Centaur station -14.58 (knee joint) during jettison. This motion is made up of items 1, 2, and 3 above. These curves were generated from film data taken during the test. The camera field of view dictated data cutoff at approximately 0.4 seconds after nose fairing jettison command. However, this time was ample to define the fairing split line motion. These curves and the hinge load data in Figures 23 and 24 show that shroud rocking motion was prevalent and indicate that the change of rocking direction occurred at approximately 0.4 to 0.5 seconds after nose fairing jettison command signal. The maximum total deflection of the split line longeron (knee joint) occurred during Test No. 1 (no helper springs) and was 2.1 inches outboard (increasing clearance). The maximum inboard motion (clearance loss) occurred during Test No. 3 (with helper springs) and was 1.8 inches. The portion of the total deflection due to breathing is approximately the same with and without helper springs. Therefore, the difference in the total deflection of the split line must be attributed to the rocking and twisting components. Since the direction of these components is difficult to predict and since the breathing portions of the deflections are nearly equal (with and without helper springs), one must assume that the total outboard deflection during Test No. 1 could have been inboard and could occur on nose fairings with helper springs. Therefore, this data verifies the validity of the following component worst-case clearance loss numbers (split line) previously published for a standard D-1A nose fairing:

D-1A NOSE FAIRING JETTISON CLEARANCE LOSSES

Location	Deflection Components*			
	Rock	Twist	Flex (Breathing)	Total**
Centaur Sta.				
-6.85	0.88 in.	0.39 in.	1.22 in.	2.49 in.

*Ref: GDC VS-0237, Drawing Addendum, Dated 8-2-71.
**Manufacturing tolerances not included.

Figures 41 through 56 show the MVM configuration static rotation test results. The clearances are marked on each figure. Tables 13 and 14 show the rotation angles and the events that occurred at the angles during the MVM static rotation test. Figures 57 through 61 show the clearances measured at discrete points for the Intelsat configuration jettison test (Test No. 1). All clearances are marked on the figures.

Figures 62 through 70 show the clearances measured at discrete points for the MVM configuration jettison test (Test No. 3). All clearances are marked on the figures.

It should be noted that the clearances shown in Figures 57 through 70 are minimum clearances since they were measured with a series of discrete length feeler wires. If no feelers were hit, the clearance would be greater than the longest feeler used at that point; if a feeler was hit, the clearance was assumed to be the length of the next untouched feeler which was shorter by some amount. The identification numbers (1 through 40) of the feeler wire blocks shown on figures 57 through 70 were used for block identification only and do not correspond to the measurement numbers called out in Table 2.

Conclusions

The D-1A nose fairing altitude jettison test results show that the separation system is capable of satisfactorily jettisoning the bi-segmented fairing at altitude and that the nose fairing has the structural capability to withstand the jettison forces. Previous altitude jettison tests (OAO-A2 and AC-22) showed that similar nose fairings having the same type jettison actuators (same jettison energy) did jettison satisfactorily without aft helper springs and with just one of the two forward actuators operative. Also, during those tests the fairings were jettisoned successfully with just the aft helper springs operative (forward actuators installed but inoperative). The results of the D-1A "static" rotation tests (Tests 2a and 2b) once again confirmed that the nose fairing halves would be successfully jettisoned with just the aft helper springs providing the jettison energy.

The fairing trajectories were satisfactory and within the predicted values. Table 15 shows the comparison of the test 45 degree rotation event time with several of the D-1A flight times. The clearances between the spacecraft envelope and the fairing during jettison including losses from dynamic deflections were adequate for worst-case conditions.

The pyrotechnic system operated satisfactorily. The results of Test No. 1 dictated a design modification to be utilized at the harness/connector interface. The modification, a clamshell retainer, was incorporated for Test No. 3 and successfully prevented the separation of the harness and connector. This design modification has been permanently incorporated for flight use.

As a result of the test program, the D-1A nose fairing is considered qualified for flight.

References

1. Eastwood, Charles W.: Centaur Orbiting Astronomoical Observatory Nose Fairing Altitude Jettison Test. NASA TMX-2096, Lewis Research Center, September 1970.

2. Staff of General Dynamics Convair Division: Centaur D-1A Systems Summary, Report No. GDC BNZ72-020, Contract NAS3-13514, September 1972.

TABLE 1 TEST CONFIGURATION

Item	Part Number	Serial Number	Comments		
System 1 Battery	69-06308-6	31-08327-053			
Pyro Relay Box U3	55-60662-5	T182836-001			
Pyro Relay Box U4	55-60662-5	T180739-001			
System 2 Battery	69-06308-6	31-08327-054			
Pyro Relay Box U5	55-60662-5	T180742-001			
Pyro Relay Box U6	55-60662-5	3710005			
			Load (lb.)		
			Test 1	Test 2	Test 3
Quad I/IV Forward Actuator	27-76275-6	TB06747-001	1290	N/A	1253
Quad II/III Forward Actuator	27-76275-6	TB06747-002	1380	N/A	1320
Quad I/IV Aft Actuator	55-79300-2	TD55223-001	N/A	1577	1557
Quad II/III Aft Actuator	55-79300-2	TD55223-002	N/A	1467	1557

TABLE 1 TEST CONFIGURATION (Cont'd)

AC-31 Configuration Jettison Test (Test No. 1)

	Explosive Bolt		Pressure Cartridge			
Position Number	Location	S/N (1)	Bolt End S/N (1)	BT (2)	Nut End S/N (1)	BT (2)
1	QI/II VSL, Sta-170	0230	0076	2*	0077	1
2	QIII/IV VSL, Sta-170	0231	0078	1	0080	2
3	QI/II VSL, Sta-67	0243	0081	2	0082	1
4	QIII/IV VSL, Sta-67	0044	0083	1	0084	2*
5	QI/II VSL, Sta-15	0245	0085	2*	0086	1
6	QIII/IV VSL, Sta-15	0246	0087	1	0088	2*
7	QI/II VSL, Sta 55	0247	0089	2	0090	1
8	QIII/IV VSL, Sta 55	0248	0092	1	0094	2*
9	QI/II VSL, Sta 126	0249	0095	2*	0096	1
10	QIII/IV VSL, Sta 126	0250	0100	1	0101	2
11	QI/II VSL, Sta 179	0253	0102	2	0239	1
12	QIII/IV VSL, Sta 179	0252	0240	1	0241	2
13	QI HSL, 18^{o} off-X (Str 48)	0288	0268	2	0269	1
14	QII HSL, 18^{o} off-X (Str 42)	0285	0260	2	0262	1
15	QI HSL, 18^{o} off+Y (Str 57)	0255	0249	2	0250	1
16	QII HSL, 18^{o} off-Y (Str 33)	0277	0255	2	0257	1
17	QIV HSL, 18^{o} off+Y (Str 3)	0283	0258	2	0259	1
18	QIII HSL, 18^{o} off-Y (Str 27)	0254	0243	2	0245	1
19	QIV HSL, 18^{o} off+X (Str 12)	0287	0264	2	0265	1
20	QIII HSL, 18^{o} off+X (Str 18)	0291	0270	2	0271	1

Notes:
(1) All components have the serial number 31-09777-XXXX.
(2) Denotes whether fired by Battery System 1 or 2.
HSL - Horizontal split line interface between split barrel and stub adapter.
VSL - Vertical split line interface between Quads I and II and between Quads III and IV.
Str - Split barrel section stringer ID number.
* Denotes squib which had wires and pins pulled out of plug connector.

TABLE 1 TEST CONFIGURATION (CONT'D.)

MVM Configuration Jettison Test (Test No. 3)

Explosive Bolt			Pressure Cartridge			
Position Number	Location	S/N (1)	Bolt End S/N (1)	BT (2)	Nut End S/N (1)	BT (2)
1	QI/II VSL, Sta-170	0009	0287	2	0289	1
2	QIII/IV VSL, Sta-170	0017	0290	1	0291	2
3	QI/II VSL, Sta-67	0029	0328	2	0329	1
4	QIII/IV VSL, Sta-67	0031	0330	1	0332	2
5	QI/II VSL, Sta-15	0036	0325	2	0327	1
6	QIII/IV VSL, Sta-15	0038	0319	1	0322	2
7	QI/II VSL, Sta 55	0078	0308	2	0307	1
8	QIII/IV VSL, Sta 55	0084	0313	1	0315	2
9	QI/II VSL, Sta 126	0107	0299	2	0301	1
10	QIII/IV VSL, Sta 126	0111	0303	1	0306	2
11	QI/II VSL, Sta 179	0112	0286	2	0297	1
12	QIII/IV VSL, Sta 179	0114	0283	1	0285	2
13	QI HSL, 18° off-X (Str 48)	0127	0282	2	0277	1
14	QII HSL, 18° off-X (Str 42)	0125	0274	2	0276	1**
15	QI HSL, 18° off+Y (Str 57)	0119	0272	2	0273	1
16	QII HSL, 18° off-Y (Str 33)	0120	0335	2	0283	1
17	QIV HSL, 18° off+Y (Str 3)	0123	0339	2	0338	1
18	QIII HSL, 18° off-Y (Str 27)	0118	0337	2	0336	1
19	QIV HSL, 18° off+X (Str 12)	0126	0342	2	0341	1
20	QIII HSL, 18° off+X (Str 18)	0129	0352	2	0347	1

Notes:
(1) All components have the serial number 31-09777-XXXX.
(2) Denotes whether fired by Battery System 1 or 2.
HSL - Horizontal split line interface between split barrel and stub adapter.
VSL - Vertical split line interface between Quads I and II and between Quads III and IV.
Str - Split barrel section stringer ID number.
** - Denotes squib which was found to be shorted after test completion (0.06 ohm, Pin A to Case).

TABLE 2. INSTRUMENTATION DEFINITION AND LOCATION

PARAMETER	MEASURE-MENT NO.	TYPE	RANGE	ACCURACY	FREQ. RESP.	RECORDER		AC-30 THRU AC-34 MEASUREMENT NO.
						TAPE	OSCILL	
QUAD II-III 45° FAIRING ROTATION	1	BREAKWIRE	EVENT	± 1/2%	330 Hz	X		CM293X
QUAD II-III FAIRING JETTISON	2	BUSS CONN.	EVENT	± 1/2%	330 Hz	X		
	3							
QUAD I-IV 45° FAIRING ROTATION	4	BREAKWIRE	EVENT	± 1/2%	330 Hz	X		CM267X
QUAD I-IV FAIRING JETTISON	5	BUSS CONN.	EVENT	± 1/2%	330 Hz	X		
	6							
NO. 1 HINGE AXIAL LOAD	7	STRAIN GAGE	±4K/LBS	± 2%	220 Hz	X		
NO. 2 HINGE AXIAL LOAD	8	STRAIN GAGE	±4K/LBS	± 2%	220 Hz	X		
NO. 3 HINGE AXIAL LOAD	9	STRAIN GAGE	±4K/LBS	± 2%	220 Hz	X		
NO. 4 HINGE AXIAL LOAD	10	STRAIN GAGE	±4K /LBS	± 2%	220 Hz	X		
NO. 1 HINGE RADIAL LOAD	11	STRAIN GAGE	± 1500/LBS	± 2%	160 Hz	X		
NO. 2 HINGE RADIAL LOAD	12	STRAIN GAGE	± 1500/LBS	± 2%	160 Hz	X		
NO. 3 HINGE RADIAL LOAD	13	STRAIN GAGE	± 1500/LBS	± 2%	160 Hz	X		

PRECEDING PAGE BLANK NOT FILMED

TABLE 2. INSTRUMENTATION DEFINITION AND LOCATION (CONT'D)

PARAMETER	MEASUREMENT NO.	TYPE	RANGE	ACCURACY	FREQ. RESP.	RECORDER TAPE	RECORDER OSCILL	AC-30 THRU AC-34 MEASUREMENT NO.
NO. 4 HINGE RADIAL LOAD	14	STRAIN GAGE	±1500/LBS	± 2%	160 Hz	X		
FAIRING JETTISON COMMAND	15	DIRECT	EVENT	± 1/2%	1 kHz	X	X	CC39X
PYRO RELAY BOX U3 OPERATION	16	DIRECT	EVENT	± 2%	790 Hz	X		CM210X
PYRO RELAY BOX U4 OPERATION	17	DIRECT	EVENT	± 2%	790 Hz	X		CM212X
PYRO RELAY BOX U5 OPERATION	18	DIRECT	EVENT	± 2%	790 Hz	X		CM214X
PYRO RELAY BOX U6 OPERATION	19	DIRECT	EVENT	± 2%	790 Hz	X		CM216X
PYRO BATTERY NO. 1 VOLTAGE	20	DIRECT	0-40 VDC	± 2%	10 kHz	X	X	
PYRO BATTERY NO. 1 VOLTAGE	21	PCM-OUTPUT	0-35 1/2 VDC	± 2%	50 Hz	X		
PYRO BATTERY NO. 1 RELAY CURRENT, BOX U3	22	50 MV SHUNT	0-100 AMP	± 2%	10 kHz	X	X	
PYRO BATTERY NO. 1 RELAY CURRENT, BOX U4	23	50 MV SHUNT	0-100 AMP	± 2%	10 kHz	X	X	
PYRO GROUND LOOP CURRENT, BATTERY NO. 1	24	50 MV SHUNT	0-50 AMP	± 2%	1 kHz	X	X	
PYRO BATTERY NO. 2 VOLTAGE	25	DIRECT	0-40 VDC	± 2%	10 kHz	X	X	

TABLE 2. INSTRUMENTATION DEFINITION AND LOCATION (CONT'D)

PARAMETER	MEASUREMENT NO.	TYPE	RANGE	ACCURACY	FREQ. RESP.	RECORDER		AC-30 THRU AC-34 MEASUREMENT NO.
						TAPE	OSCILL	
PYRO BATTERY NO. 2 VOLTAGE	26	PCM-OUTPUT	0-35 1/2 VDC	± 2%	50 Hz	X		
PYRO BATTERY NO. 2 RELAY CURRENT, BOX U5	27	50 MV SHUNT	0-100 AMP	± 2%	10 kHz	X	X	
PYRO BATTERY NO. 2 RELAY CURRENT, BOX U6	28	50 MV SHUNT	0-100 AMP	± 2%	10 kHz	X	X	
PYRO GROUND LOOP CURRENT, BATT. NO. 2	29	50 MV SHUNT	0-50 AMP	± 2%	1 kHz	X	X	
<u>FAIRING MOTION</u>								
QUAD I-IV NOSE	30	EXTENSOMETER	0-72 IN.	± 2%	450 Hz	Z		
QUAD II-III NOSE	31				450 Hz	X		
QUAD I KNEE	32				330 Hz	X		
QUAD II KNEE	33				330 Hz	X		
QUAD III KNEE	34				330 Hz	X		
QUAD IV KNEE	35		0-72 IN.		330 Hz	X		
QUAD IV BASE	36		0-15 IN.		220 Hz	X		
QUAD III BASE	37				220 Hz	X		
QUAD II BASE	38				160 Hz	X		
QUAD I BASE	39	EXTENSOMETER	0-15 IN.	± 2%	160 Hz	X		
QUAD II BASE	38V	ROTATIONAL VELOCITY	0-45°/SEC	± 2%	450 Hz	X	X	
QUAD I BASE	39V	ROTATIONAL VELOCITY	0-45°/SEC	± 2%	450 Hz	X	X	

TABLE 2. INSTRUMENTATION DEFINITION AND LOCATION (CONT'D)

PARAMETER	MEASURE-MENT NO.	TYPE	RANGE	ACCURACY	FREQ. RESP.	RECORDER TAPE	RECORDER OSCILL	AC-30 THRU AC-34 MEASUREMENT NO.
FAIRING BREATHING								
QUAD I SPLIT BARREL +X	40	LINEAR ACCEL-EROMETER	±7-1/2 G	±2%	50 Hz	X		
QUAD II SPLIT BARREL +X	41					X		
QUAD III SPLIT BARREL -X	42					X		
QUAD IV SPLIT BARREL -X	43					X		
QUAD I NOSE CYLINDER +X	44					X		
QUAD II NOSE CYLINDER +X	45					X		
QUAD III NOSE CYLINDER -X	46					X		
QUAD IV NOSE CYLINDER -X	47					X		
QUAD I NOSE CONE +X	48					X		
QUAD II NOSE CONE +X	49					X		
QUAD III NOSE CONE -X	50					X		
QUAD IV NOSE CONE -X	51	LINEAR ACCEL-EROMETER	±7-1/2G	±2%	50 Hz	X		

TABLE 2. INSTRUMENTATION DEFINITION AND LOCATION (CONT'D)

PARAMETER	MEASUREMENT NO.	TYPE	RANGE	ACCURACY	FREQ. RESP.	RECORDER TAPE	RECORDER OSCILL	AC-30 THRU AC-34 MEASUREMENT NO.
QUAD I-IV KNEE +Y	52	LINEAR ACCEL	±7 1/2 G	± 2%	50 Hz	X		
QUAD II-III KNEE -Y	53	LINEAR ACCEL	±7 1/2 G	± 2%	50 Hz	X		
MOTION PICTURE CORRELATION	54	0.1 SEC PULSE	EVENT	-	1 kHz	X	X	
IRIG "B" TIME	55	1 kHz & DC	-	-	-	X	X	
PYRO BATTERY NO. 1 TEMPERATURE	56	RESISTANCE BULB THERM.	0-100°F	± 2%	60 Hz	X	X	
PYRO BATTERY NO. 2 TEMPERATURE	57	RESISTANCE BULB THERM.	0-100°F	± 2%	60	X	X	
INSULATION PANEL CURRENT, BATTERY NO. 1	58	50 MV SHUNT	0-20 AMP	± 2%	80 Hz	X	X	
INSULATION PANEL CURRENT, BATTERY NO. 2	59	50 MV SHUNT	0-20 AMP	± 2%	80 Hz	X	X	

TABLE 3 - LIGHT HALF (QI/IV) FAIRING ROTATION SUMMARY

Event	Time (sec) Test 1	Test 3
Nose Fairing Jettison (NFJ) Command (Meas. 15)	0.000(1)	0.000(2)
Shock of Pyrotechnic Firing (Meas. 41)	0.03	0.03
B304P3 (Quad III/IV Vertical Split Line) Disconnects (3)	0.103	0.096
INTELSAT Payload Electrical Disconnects Separate		
Lower Card (Meas. 6)	0.109	N/A
Upper Card (Meas. 3)	0.112	N/A
8 Degrees Fairing Rotation		
Angular Displacement, QI Base (Meas. 36)	0.37	0.32
Angular Displacement, QI Knee (Meas. 32)	0.41	0.37
Angular Displacement, QIV Base (Meas. 39)	0.39	0.38
Angular Displacement, QIV Knee (Meas. 35)	0.43	0.40
Angular Displacement, QI/IV Backbone (Meas. 30)	0.41	0.37
45 Degree Fairing Rotation		
Breakwire (Meas. 4)	1.728	1.485
Hinge Separation (approximately 75 degree roation)		
Hinge Fitting 1 (4)	2.19	1.96
Hinge Fitting 4 (4)	2.17	1.97

Notes: (1) Nose Fairing Jettison command occurred at 1814:59.7734 EST

(2) Nose Fairing Jettison command occurred at 1736:36.7528 EST

(3) This event occurred at approximately 1 degree of fairing rotation

(4) Loss of hinge strain gauge loading

N/A - not applicable

TABLE 4 - HEAVY HALF (QII/III) FAIRING ROTATION SUMMARY

Event	Time (sec) Test 1	Test 3
Nose Fairing Jettison (NFJ) Command (Meas. 15)	0.000(1)	0.000(2)
Shock of Pyrotechnic Firing (Meas. 41)	0.03	0.03
8 Degree Fairing Rotation		
Angular Displacement, QII Base (Meas. 37)	0.41	0.38
Angular Displacement, QII Knee (Meas. 33)	0.43	0.38
Angular Displacement, QIII Base (Meas. 38)	0.42	0.39
Angular Displacement, QIII Knee (Meas. 34)	0.43	0.39
Angular Displacement, QII/III Backbone (Meas. 31)	0.43	0.38
Electrical Plub B100J16 Disconnects (21 degrees rotation)		
Buss Disconnect (Meas. 2)	1.037	0.911
Angular Displacement, QII Base (Meas. 37)	1.01	0.90
45 Degree Fairing Rotation		
Breakwire (Meas. 1)	1.781	1.588
Hinge Separation (approximately 75 degree rotation)		
Hinge Fitting 2 (3)	2.28	2.08
Hinge Fitting 3 (3)	2.26	2.07

Notes: (1) Nose Fairing Jettison command occurred at 1814:59.7734 EST

(2) Nose Fairing Jettison command occurred at 1736:36.7528 EST

(3) Loss of hinge strain loading

TABLE 5

Battery No. 1 System Data (1)

Data	Source Meas. No.	Units (2)	Value Test 1	Value Test 3
Pretest Battery Voltage	20	vdc	34.6	35.1
	21	vdc	34.6	35.0
Battery Temperature during Test	56	°F	71	70
Pyro Box U4 Activation	17	sec	0.0253	0.0253
Pyro Box U3 Activation	16	sec	0.0279	0.0277
Bolts 1-10 Squib #1 Voltage and Current Profile (10 KHz Freq. Response)				
Transient Load (Relay Contact Bounce)	23(4)	sec	0.0271	0.0264
	23	amp	12	13
	20	vdc	3	2
Hard Load Starts	23	sec	0.0272	0.0267
Maximum Current Conditions	23	sec	0.0280	0.0274
	23	amp	64	66
	20	vdc	17	18
Indicated Squib Blowoff	23	sec	0.0285	0.0278
	23	amp	5	3
Bolts 11-20 Squib #1 Voltage and Current Profile (10 KHz Freq. Response)				
Transient Load (Relay Contact Bounce)	22(4)	sec	0.0267	0.0264
	22	amp	17	25
	20	vdc	8	2
Hard Load Starts	22	sec	0.0268	0.0265
Maximum Current Conditions	22	sec	0.0269	0.0268
	22	amp	60	65
	20	vdc	15	9
Indicated Squib Blowoff	22	sec	0.0282	0.0278
	22	amp	0	0

TABLE 5 (CONTINUED)

Data	Source Meas. No.	Units(2)	Value Test 1	Value Test 3
Harness Fault Load Starts (3)	22	sec	N/A	0.154
Maximum Fault Load	22	sec	N/A	0.501
	22	amp	N/A	24
	21	vdc	N/A	14
Ground Path Current Leaves Zero	24	sec	0.0280	0.0274
Maximum Ground Path Current	24	sec	0.0288	0.0292
	24	amp	20.5	25.0
Maximum Battery Load Conditions				
Total Load	22 and 23	sec	0.0280	0.0271
	22 + 23	amp	114	102
	20	vdc	17	12.5
Minimum Observed Battery Volts				
10 KHz Data	20	sec	0.0271	0.0264
	20	vdc	3	2
600 Hz Data	21	sec	0.0285	0.0280
	21	vdc	11	11.9
Voltage at Squib Blowoff	20	sec	0.0286	0.0279
	20	vdc	27	28

NOTES:
(1) This system is contained in the Quad I/IV (light) fairing half.
(2) Units of Function or Time in Seconds from Fairing Jettison Command
(3) This was the only relay current measurement with sustained fault loads.
(4) Measurement 22 is the current at Relay U3 and measurement 23 is the current at Relay U4.

N/A - not applicable

TABLE 6

Battery No. 2 System Data (1)

Data	Source Meas. No.	Units (2)	Value Test 1	Value Test 3
Pretest Battery Voltage	25	vdc	34.5	35.0
	26	vdc	34.5	35.6
Battery Temp During Test	57	^{o}F	70	77
Pyro Relay U6 Activation	19	sec	0.0258	0.0244
Pyro Relay U5 Activation	18	sec	0.0287	0.0282
Bolts 1-10 Squib # 2 Voltage and Current Profile (10 KHz Freq. Response)				
Transient Load (Relay Contact Bounce)	28(4)	sec	0.0279	0.0270
	28	amp	30	26
	25	vdc	14	9
Hard Load Starts	28	sec	0.0280	0.0271
Maximum Current Conditions	28	sec	0.0281	0.0273
	28	amp	52	62
	25	vdc	16.5	13
Indicated Squib Blowoff	28	sec	0.0298	0.0283
	28	amp	4	1
Harness Fault Load Starts (3)	28	sec	0.043	N/A
Maximum Fault Load	28	sec	0.096	N/A
	28	amp	55	N/A
	25	vdc	20	N/A
Bolts 11-20 Squib # 2 Voltage and Current Profile (10 KHz Freq. Response)				
Transient Load (Relay Contact Bounce)	27(4)	sec	0.0277	0.0271
	27	amp	20	30
	25	vdc	9.5	9
Hard Load Starts	27	sec	0.0279	0.0274

TABLE 6 (CONTINUED)

Data	Source Meas. No.	Units (2)	Value Test 1	Value Test 3
Maximum Current Conditions	27	sec	0.0288	0.0279
	27	amp	50	60
	25	vdc	13	15
Indicated Squib Blowoff	27	sec	0.0296	0.0285
	27	amp	2	2
Ground Path Current Starts	29	sec	0.0294	0.0282
Maximum Ground Path Current	29	sec	0.0299	0.0298
	29	amp	17.2	23.0
Maximum Battery Load Conditions				
Total Load	27 and 28	sec	0.0288	0.0278
	27 + 28	amp	99	116
	25	vdc	12.5	14.5
Minimum Observed Battery Volts				
10 KHz Data	25	sec	0.0283	0.0272
	25	vdc	8.5	8.5
600 HZ Data	26	sec	0.0297	0.0291
	26	vdc	11.9	11.7
Voltage at Squib Blowoff	25	sec	0.0298	0.0285
	25	vdc	25	27

NOTES:
(1) This system is contained in the Quad II/III (domed) fairing half.
(2) Units of function or time in seconds from fairing jettison command.
(3) This harness was the only relay current with sustained fault loads.
(4) Measurement 27 is the current at Relay U5 and measurement 28 is the current at Relay U6.

N/A - not applicable

TABLE 7. MAXIMUM NOSE FAIRING HINGE LOADS

Load Condition	Maximum Hinge Load (lb.) Hinge 1 Test 1	Hinge 1 Test 3	Hinge 4 Test 1	Hinge 4 Test 3	Hinge 2 Test 1	Hinge 2 Test 3	Hinge 3 Test 1	Hinge 3 Test 3
Axial Compression Load Time (1)	1540 0.20	1250 1.10	1600 0.09	1400 0.10	1250 0.40	1050 0.74	1120 0.09	950 0.06
Tension Load Time (1)	(2)	125 (3)	40 0.03	(2)	(2)	175 (3)	460 0.59	75 0.03
Radial Inboard Load Time (1)	300 0.71	190 0.78	490 0.40	240 1.28	240 0.27	180 1.47	100 0.03	190 0.53 & 1.59
Outboard Load Time (1)	410 0.63	580 0.45	430 0.76	420 0.71	590 0.37	480 0.46	570 0.33	490 0.46

NOTES: (1) Time in seconds from Nose Fairing Jettison Command.

(2) Tension loading did not occur.

(3) Hinge was preloaded in tension.

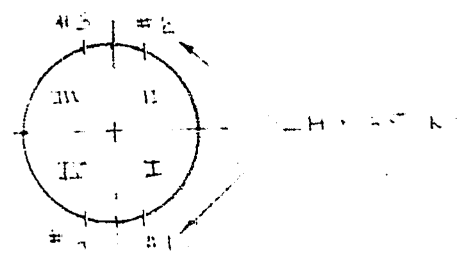

VIEW LOOKING AFT

TABLE 8 FAIRING SPLIT LINE BREATHING

AC-31 Configuration - Test No. 1

Meas. No.	Location	Deflection(1) Outboard Inches (o-p)	Outboard Time (sec)	Inboard Inches (o-p)	Inboard Time (sec)
40	Quad I VSL, 41.25 in. above HSL	0.5	0.29	0.4	0.35
43	Quad IV VSL, 41.25 in. above HSL	0.45	0.11	0.55	0.24
44	Quad I VSL, 173.8 in. above HSL	0.7	0.29	0.7	0.20
47	Quad IV VSL, 173.8 in. above HSL	0.65	0.18 & 0.47	0.8	0.25
48	Quad I VSL, 234.7 in. above HSL	0.5	0.44	0.45	0.37
51	Quad IV VSL, 234.7 in. above HSL	0.85	0.16	0.55	0.22
41	Quad II VSL, 41.25 in. above HSL	0.33	0.16	0.4	0.22
42	Quad III VSL, 41.25 in. above HSL	0.35	0.28	0.35	0.38
45	Quad II VSL, 173.8 in. above HSL	0.55	0.14	0.6	0.37
46	Quad III VSL, 173.8 in. above HSL	0.55	0.35	0.45	0.26
49	Quad II VSL, 234.7 in. above HSL	0.7	0.14	0.5	0.21
50	Quad III VSL, 234.7 in. above HSL	0.5	0.16	0.5	0.24

Notes: HSL - Horizontal split line, split barrel and fixed adapter interface.
VSL - Vertical split line, QI/IV and QII/III fairing halves interface.
(1) - Slide rule calculations from filtered raw accelerometer data.

TABLE 9. FAIRING SPLIT LINE BREATHING

MVM Configuration - Test No. 3

Meas. No.	Location	Deflection (1) Outboard Inches (o-p)	Outboard Time (sec.)	Inboard Inches (o-p)	Inboard Time (sec.)
40	Quad I VSL, 41.25 in. above HSL	(2)		(2)	
43	Quad IV VSL, 41.25 in. above HSL	(2)		(2)	
44	Quad I VSL, 173.8 in. above HSL	0.9	0.25	0.8	0.32
47	Quad IV VSL, 173.8 in. above HSL	0.9	0.25	0.9	0.16
48	Quad I VSL, 234.7 in. above HSL	0.6	0.12	0.8	0.18
51	Quad IV VSL, 234.7 in. above HSL	0.8	0.26	0.8	0.19
41	Quad II VSL, 41.25 in. above HSL	(2)		(2)	
42	Quad III VSL, 41.25 in. above HSL	(2)		(2)	
45	Quad II VSL, 173.8 in. above HSL	0.6	0.25	0.7	0.33
46	Quad III VSL, 173.8 in. above HSL	0.7	0.12 & 0.25	0.7	0.18
49	Quad II VSL, 234.7 in. above HSL	0.9	0.12	0.6	0.19
50	Quad III VSL, 234.7 in. above HSL	0.7	0.12	0.7	0.19

NOTES:
- HSL - Horizontal split line, split barrel and fixed adapter interface.
- VSL - Vertical split line, QI/IV and QII/III fairing halves interface.
- (1) - Slide rule calculations from filtered raw accelerometer data.
- (2) - Negligible deflection.

TABLE 10 INSULATION PANEL JETTISON SIMULATION

AC-31 Configuration - Test No. 1

Event	Battery 1 System	Battery 2 System
Insulation Panel Jettison Command	0.000(1)	0.000(1)
Voltage Prior to Load (vdc)	34.5	34.8
Time of First Load Indication (sec)		
In Voltage Data	0.023	0.024
In Current Data	0.024	0.024
Initial Peak Value @ Time		
In Voltage Data (vdc @ sec)	20.0 @ 0.025	20.7 @ 0.025
In Current Data (amp @ sec)	16.1 @ 0.025	19.1 @ 0.025
Value at Load Removal		
In Voltage Data (vdc @ sec)	24.8 @ 0.043	25.1 @ 0.043
In Current Data (amp @ sec)	18.1 @ 0.043	20.2 @ 0.043
Voltage After Load Removal		
At +0.010 sec	29.7 (2)	30.2 (2)
At +0.056 sec (IPJ Cmnd Deactivate)	28.6 (2)	29.2 (2)
At +0.156 sec	30.3	31.2
At +1.156 sec	32.9	33.3
At +3.156 sec	33.9	34.1
At +5.156 sec	34.1	34.3

Notes: (1) The Insulation Panel Jettison (IPJ) command (Measurement 61) was energized at 1813:49.560 EST and deactivated at 1813:49.658 EST.

(2) A small residual load of 0.8 to 1.3 amperes was present during this interval.

TABLE 11 INSULATION PANEL JETTISON SIMULATION

MVM Configuration - Test No. 3

Event	Battery 1 System	Battery 2 System
Insulation Panel Jettison Command	0.000(1)	0.000(1)
Voltage Prior to Load (vdc)	35.1	35.2
Time of First Load Indication (sec.)		
In Voltage Data	0.023	0.024
In Current Data	0.022	0.024
Initial Peak Value @ Time		
In Voltage Data (vdc @ sec.)	20.7 @ 0.024	22.6 @ 0.025
In Current Data (amp @ sec.)	17.8 @ 0.026	21.2 @ 0.026
Value at Load Removal		
In Voltage Data (vdc @ sec.)	24.9 @ 0.043	25.9 @ 0.044
In Current Data (amp @ sec.)	17.9 @ 0.043	21.1 @ 0.044
Voltage After Load Removal		
At +0.010 sec.	30.6(2)	31.0(2)
At +0.056 sec. (IPJ Cmnd Deact.)	30.0(2)	31.4(2)
At +0.156 sec.	33.0	34.0
At +1.156 sec.	35.0	35.1
At +3.156 sec.	35.1	35.2
At +5.156 sec.	35.1	35.2

NOTES: (1) The Insulation Panel Jettison (IPJ) command (Measurement [illegible]) was energized at 1735:26.334 EST and deactivated at 1735:26.433.

(2) A small residual load of 1.0 to 1.5 amperes was present during this interval.

Table 12 BATTERY POWER COMPARISON

Parameter	Initial Activation S/N-053 System 1	Initial Activation S/N-054 System 2	Recharged S/N-053 System 1	Recharged S/N-054 System 2
Battery Load Data				
Initial Voltage, vdc	34	34	35.1	35.2
Current Delivered, amps	51	51	53	53
Current Duration, sec	2	2	2.57	2.58
Voltage at 0.1 sec, vdc	23.5	23.6	25	24.5
Voltage at 2.0 sec, vdc	23.6	23.8	25.2	25
Peak Current and Squib Blowoff Times (milliseconds/amperes)				
Relay Box U3	1.4/60	--	1.3/65	--
Relay Box U4	1.3/64	--	1.1/66	--
Relay Box U5	--	1.6/50	--	1.1/60
Relay Box U6	--	1.8/52	--	1.2/62

TABLE 13

MVM ROTATION TEST

Quad 1-4 Half

Rotation Angles Used For Instrumentation Checks	Special Events Recorded
0^{o}-00'	A/C Inlet to FPA Released Before 1^{o}-00' of Rotation
1^{o}-54'	
2^{o}-57'	Seal Started To Release Near Umbilical Island
3^{o}-27'	
3^{o}-44'	
4^{o}-02'	
4^{o}-32'	
4^{o}-52'	
5^{o}-42'	Complete Seal Release (+Y)
6^{o}-12'	
7^{o}-17'	
8^{o}-29'	
10^{o}-32'	
11^{o}-50'	Lower Quad I N/F Disconnect Released
12^{o}-37'	
13^{o}-37'	Helper Spring Dropped Free
14^{o}-24'	Upper Quad 4 N/F Disconnect Released
15^{o}-46'	Upper Quad 1 N/F Disconnect Released
17^{o}-02'	
18^{o}-49'	
20^{o}-35'	Instrumentation N/F Disconnect Released
22^{o}-26'	
24^{o}-17'	
27^{o}-07'	
29^{o}-02'	
30^{o}-02'	
31^{o}-52'	Maximum Rotation

TABLE 14

MVM ROTATION TEST

Quad 2-3 Half

Rotation Angles Used For Instrument Checks	Special Events Recorded
1^{o}-50'	
3^{o}-03'	
3^{o}-36'	
5^{o}-35'	Complete Seal Release (-Y)
7^{o}-55'	
9^{o}-53'	
11^{o}-22'	Fwd N/F Disconnect Released
13^{o}-41'	Helper Spring Dropped Free
15^{o}-15'	Middle N/F Disconnect Released
15^{o}-56'	
19^{o}-39'	
21^{o}-20'	Aft N/F Disconnect Released
23^{o}-59'	
27^{o}-22'	
30^{o}-22'	
37^{o}-01'	
39^{o}-14'	Maximum Rotation

Table 15

45 Degree Rotation Event Time Comparison with Flight Data

Event	(1), (4) Test No. 1	(1), (4) AC-31 Flight	(3), (4) Test No. 3	(3), (4) D-1A Flights AC-30	AC-32	AC-34	AC-35	(5) AC-36	(5) AC-37
	Elapsed Time From N/F Jettison Command (Seconds)								
45° Breakwire (2) QI-IV	1.7	1.6	1.5	1.4	1.4	1.5	1.5	1.5	1.7
45° Breakwire (2) QII-III	1.8	1.6	1.6	1.4	1.4	1.6	1.5	1.6	1.7

(1) Forward actuators only; no aft helper springs

(2)

QI-IV
QII-III

(3) Forward actuators and aft helper springs used

(4) 1-g gravity gield during tests; approximately 0.75-g acceleration field at flight nose fairing jettison

(5) 35-inch-long split fairing added to nose fairing configuration

ATLAS/CENTAUR D-IA

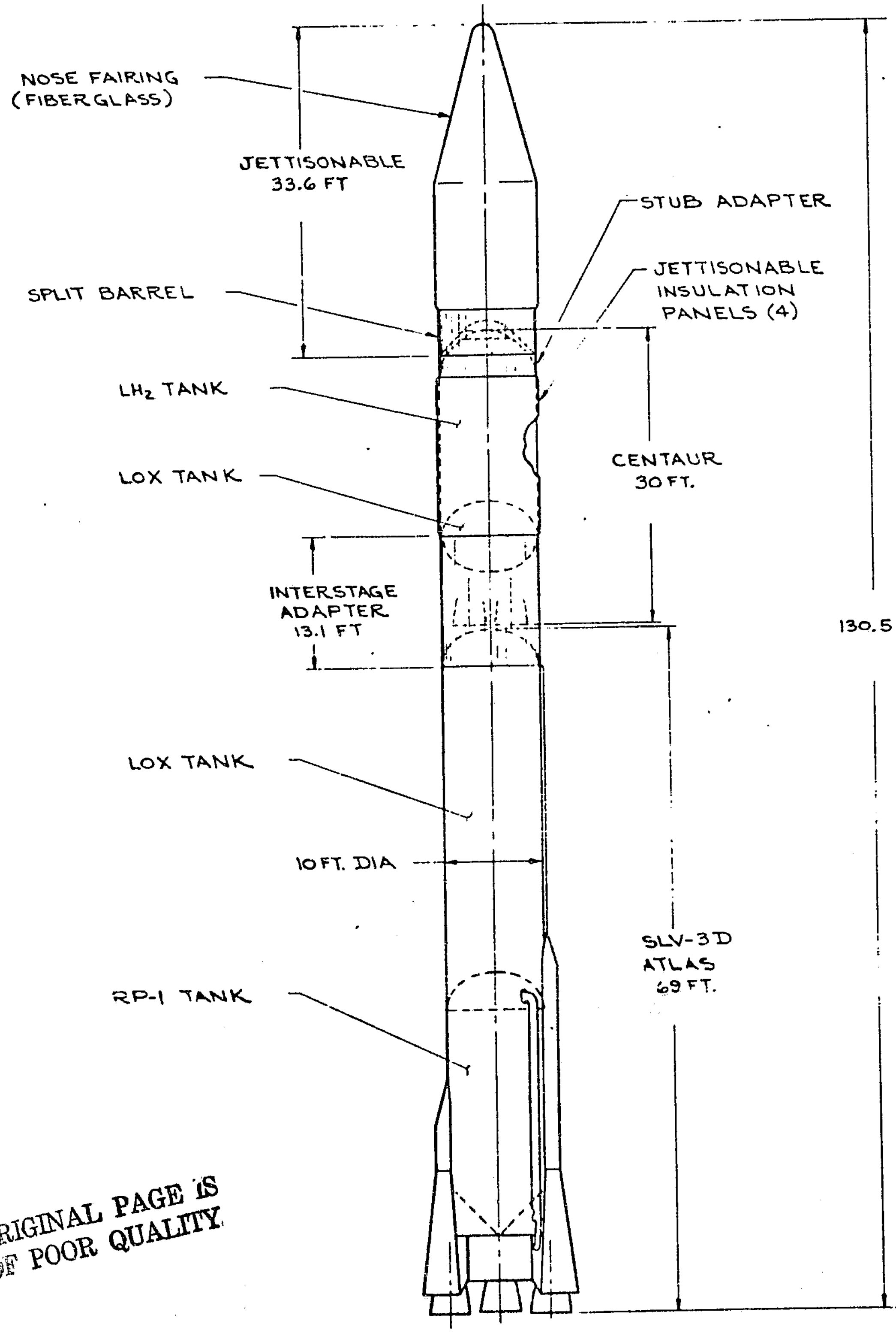

FIGURE 1 ATLAS/CENTAUR D-1A LAUNCH VEHICLE

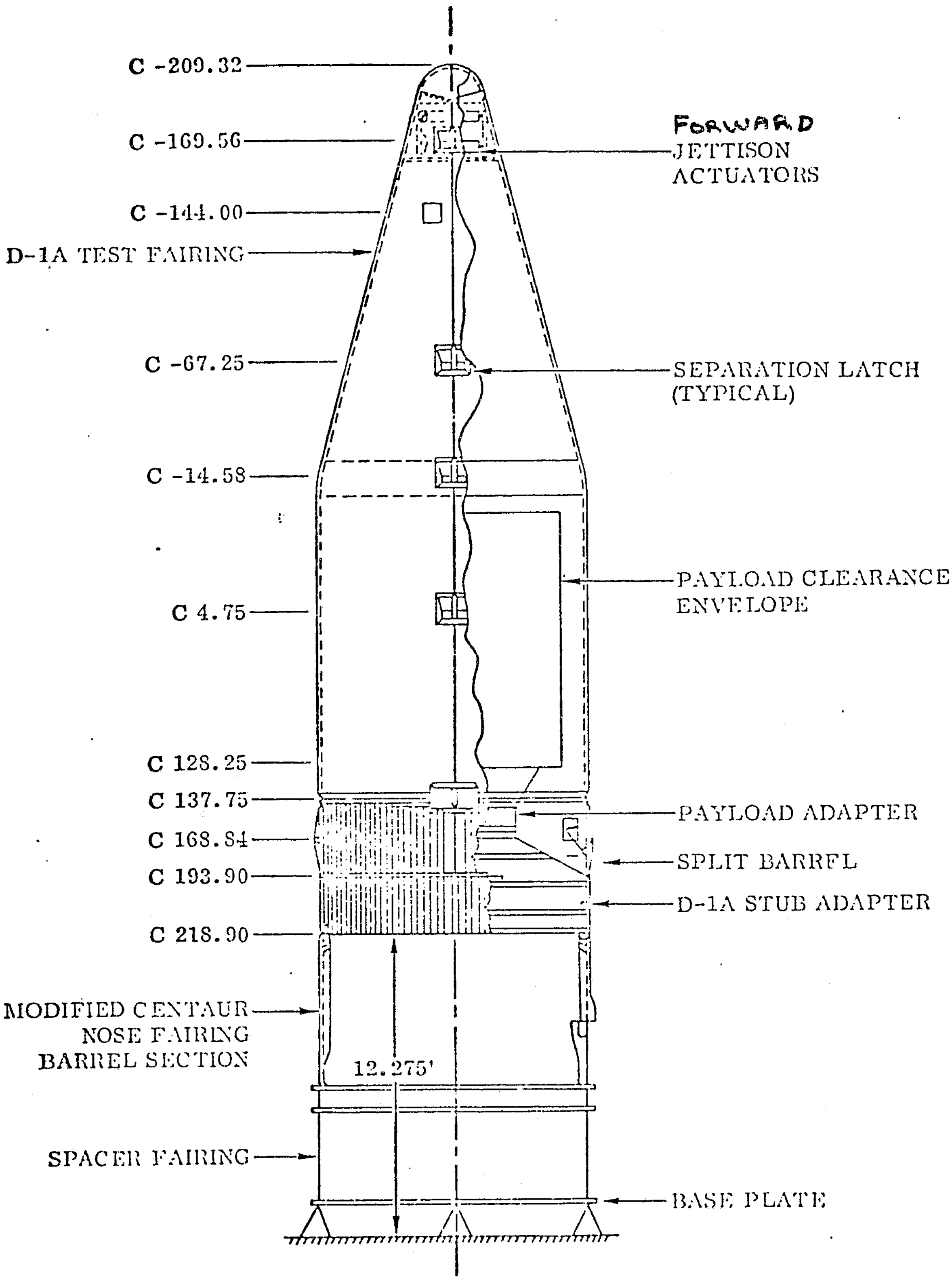

Figure 2 CENTAUR/D-1A NOSE FAIRING JETTISON TEST CONFIGURATION

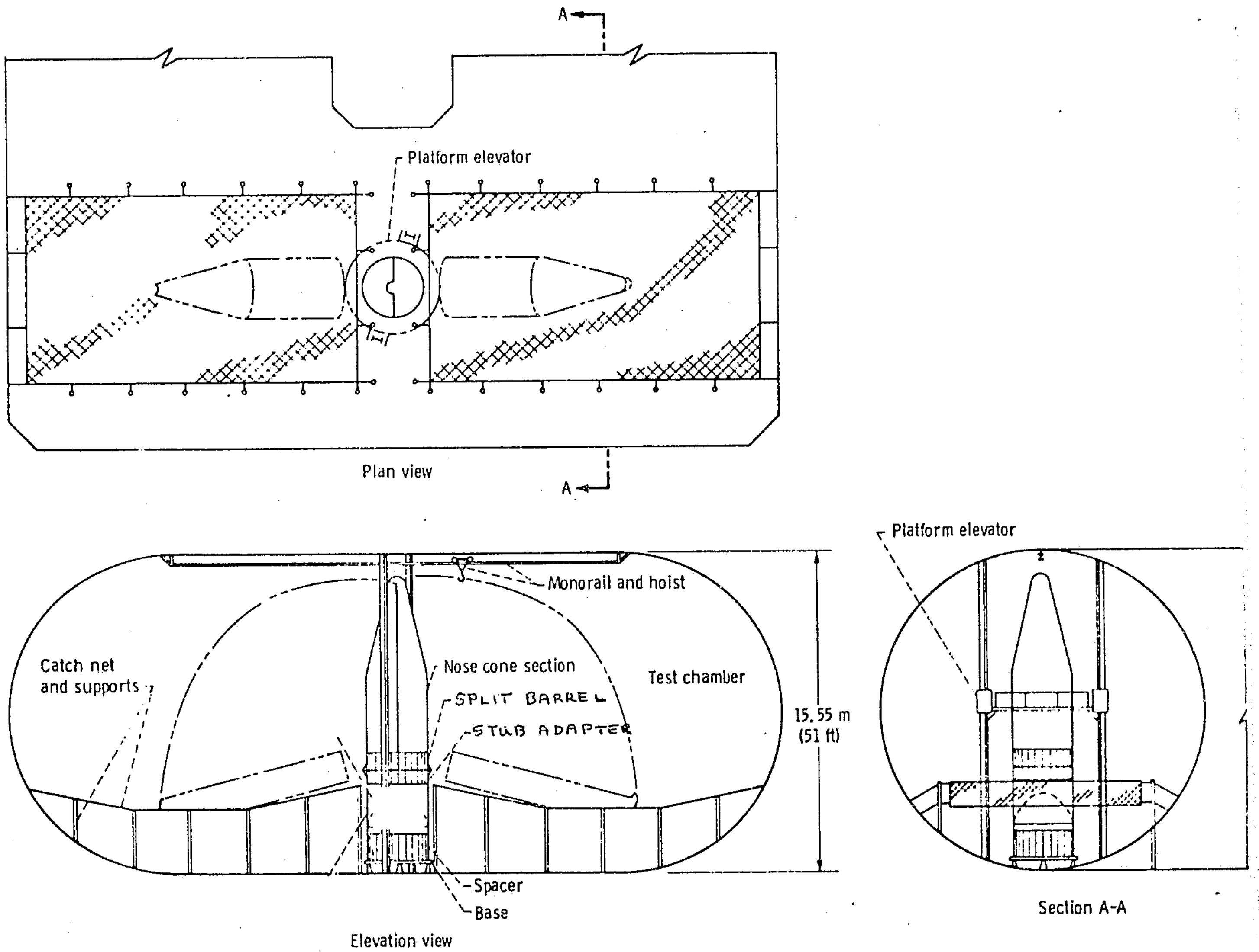

FIGURE 3 TEST SPECIMEN ARRANGEMENT IN TEST CHAMBER

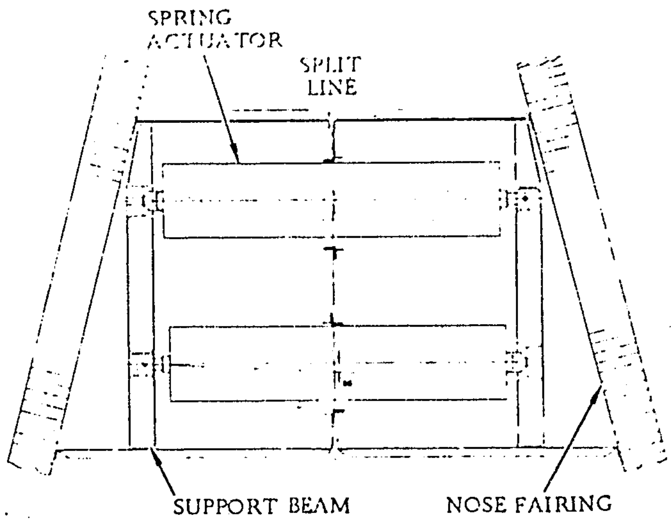

FORWARD Jettison actuator
installation.

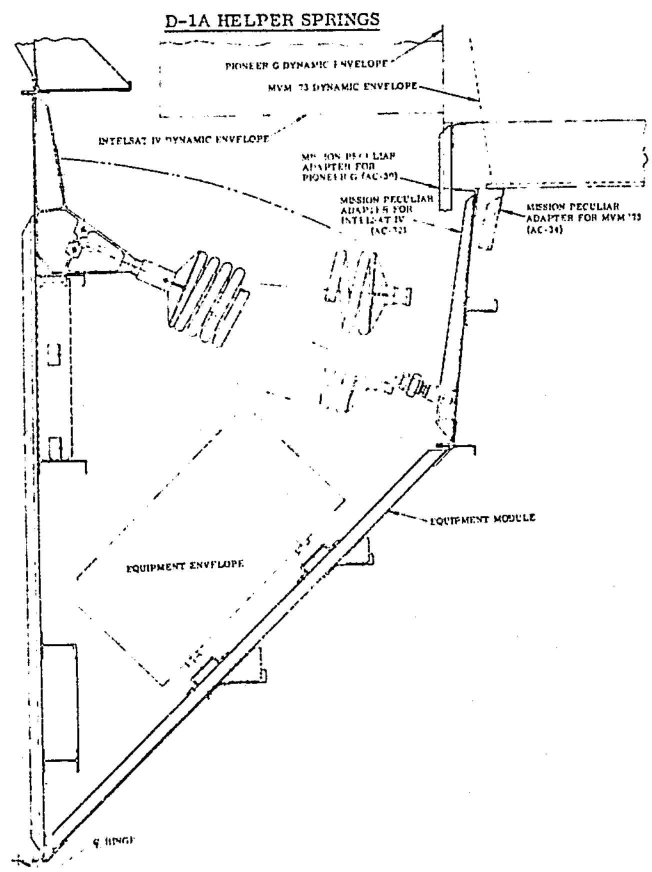

FIGURE 4 JETTISON SPRING CONFIGURATION

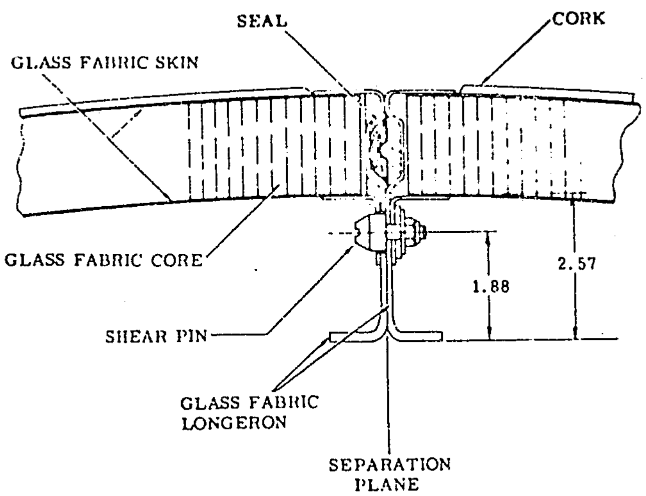

Typical vertical split line.

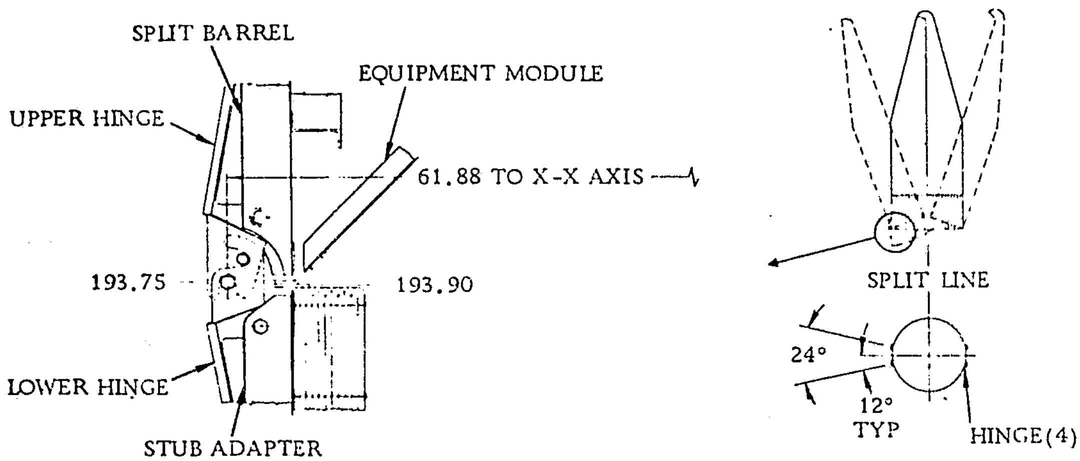

Hinge installation.

FIGURE 5 FIBERGLASS VERTICAL SPLIT LINE CONFIGURATION AND HINGE INSTALLATION

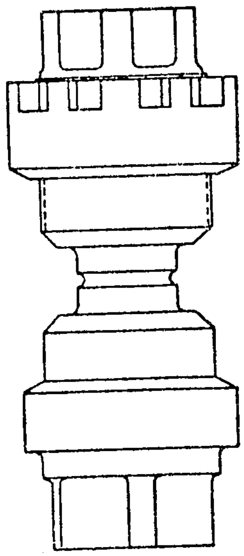

Explosive bolt.

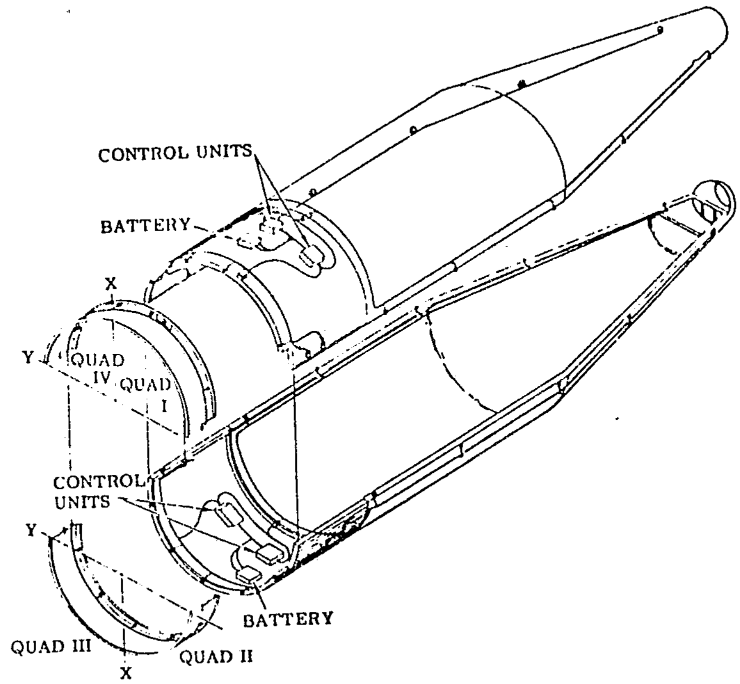

Nose fairing electrical pyrotechnic system.

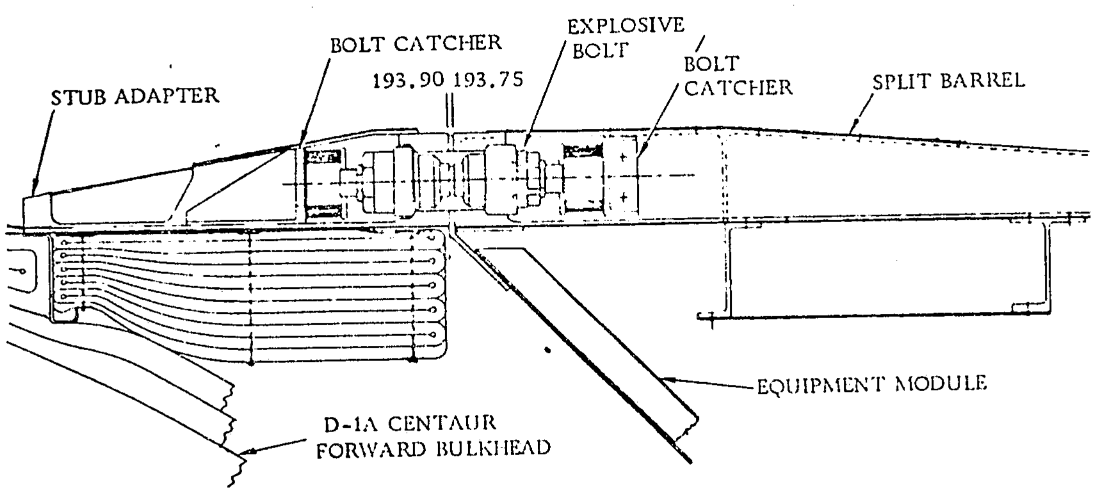

Typical explosive bolt installation.

FIGURE 6 TYPICAL EXPLOSIVE BOLT INSTALLATION AND PYROTECHNIC ELECTRICAL SYSTEM

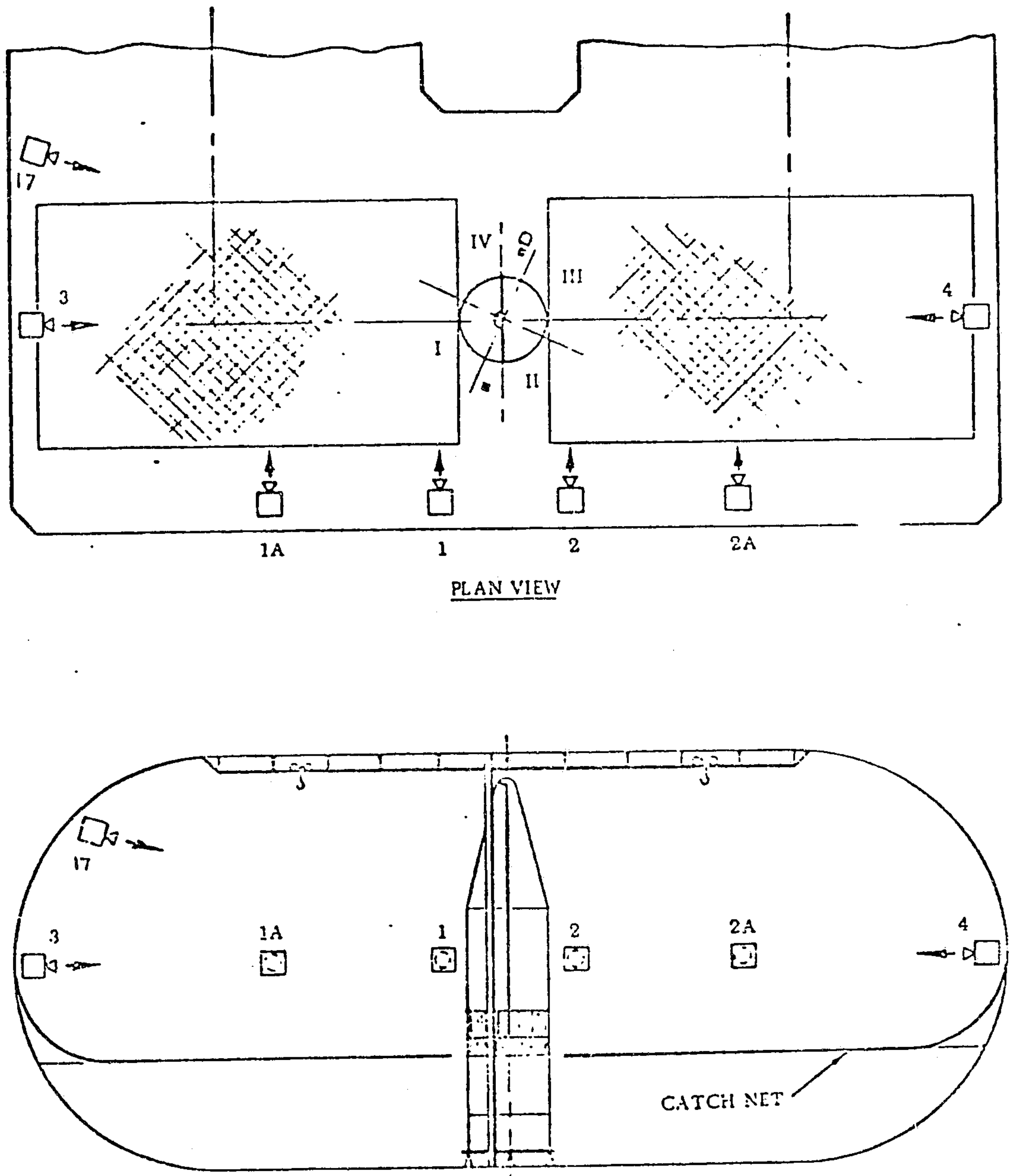

Figure 7 Centaur/OAO Separation Test Movie Camera Locations in Test Chamber

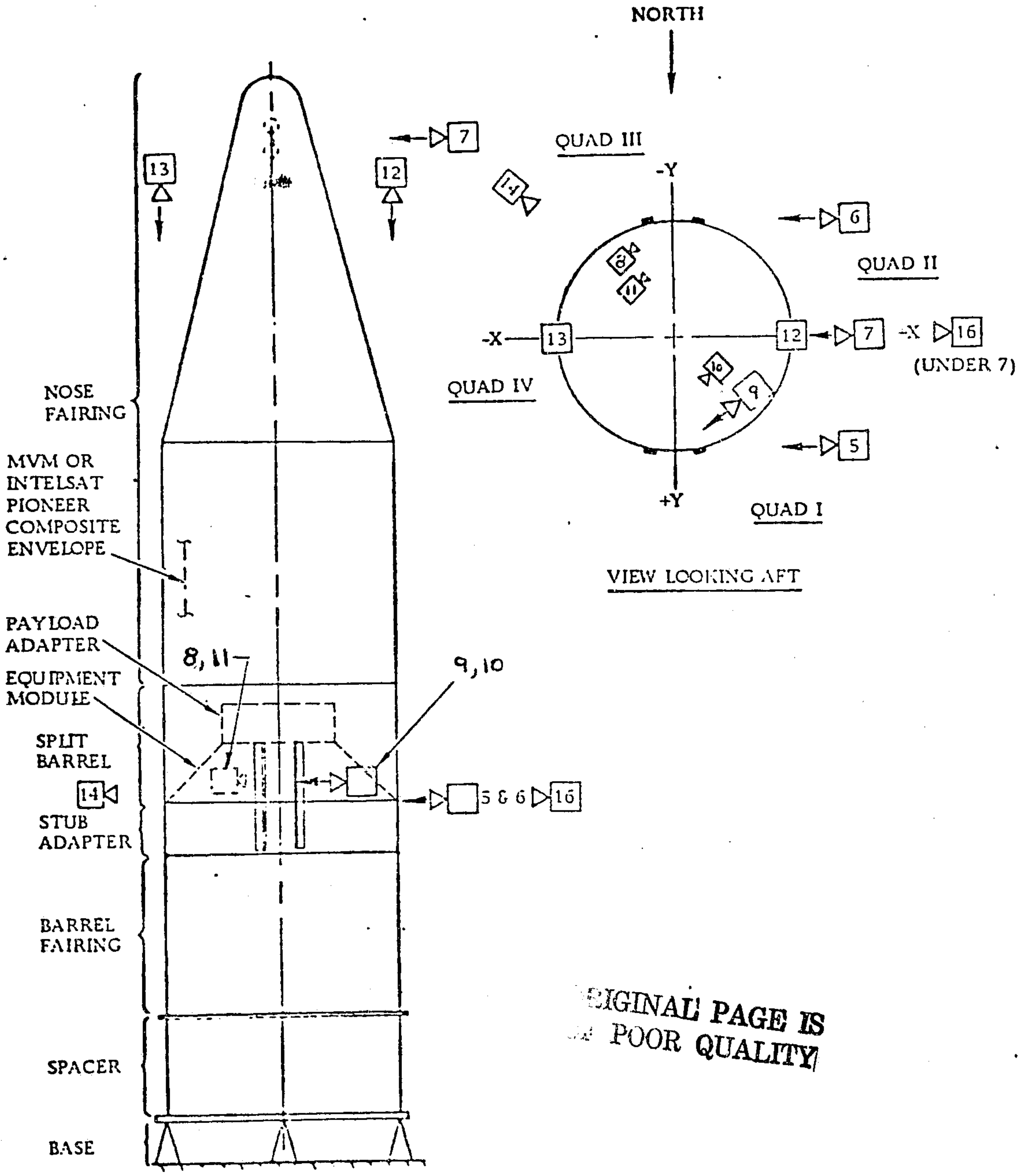

Figure 8 Centaur D-1A Separation Test Movie Camera Locations in Test Chamber

Camera No.	Frame Speed	Target
1	400 fps	Trajectory of QI - IV Fairing Half
1A	400 fps	
2	400 fps	Trajectory of QII - III Fairing Half
2A	400 fps	
3	400 fps	Fairing Half Rocking Motion QI - IV
4	400 fps	Fairing Half Rocking Motion QII - III
5	400 fps	Hinge Operation QI-IV
6	400 fps	Hinge Operation QII - III
7	5000 fps	Separation Spring Actuator and Separation Latch Operation
8	400 fps	Electrical Disconnect and LH_2 Vend Disconnect QII-III
9	400 fps	Electrical Disconnect and LH_2 Vent Disconnect QI-IV
10	400 fps	HELPER SPRING +Y AXIS
11	400 fps	HELPER SPRING -Y AXIS
12	400 fps	Split Line +X Axis
13	400 fps	Split Line -X Axis
14	5000 fps	Separation Bolt
15		Deleted
16	400 fps	Horizontal, Vertical Split Line Intersection
17	400 fps	Fairing Jettison Overview
18		Deleted

Figure 9. Centaur D-1A Separation Test Movie Camera Description

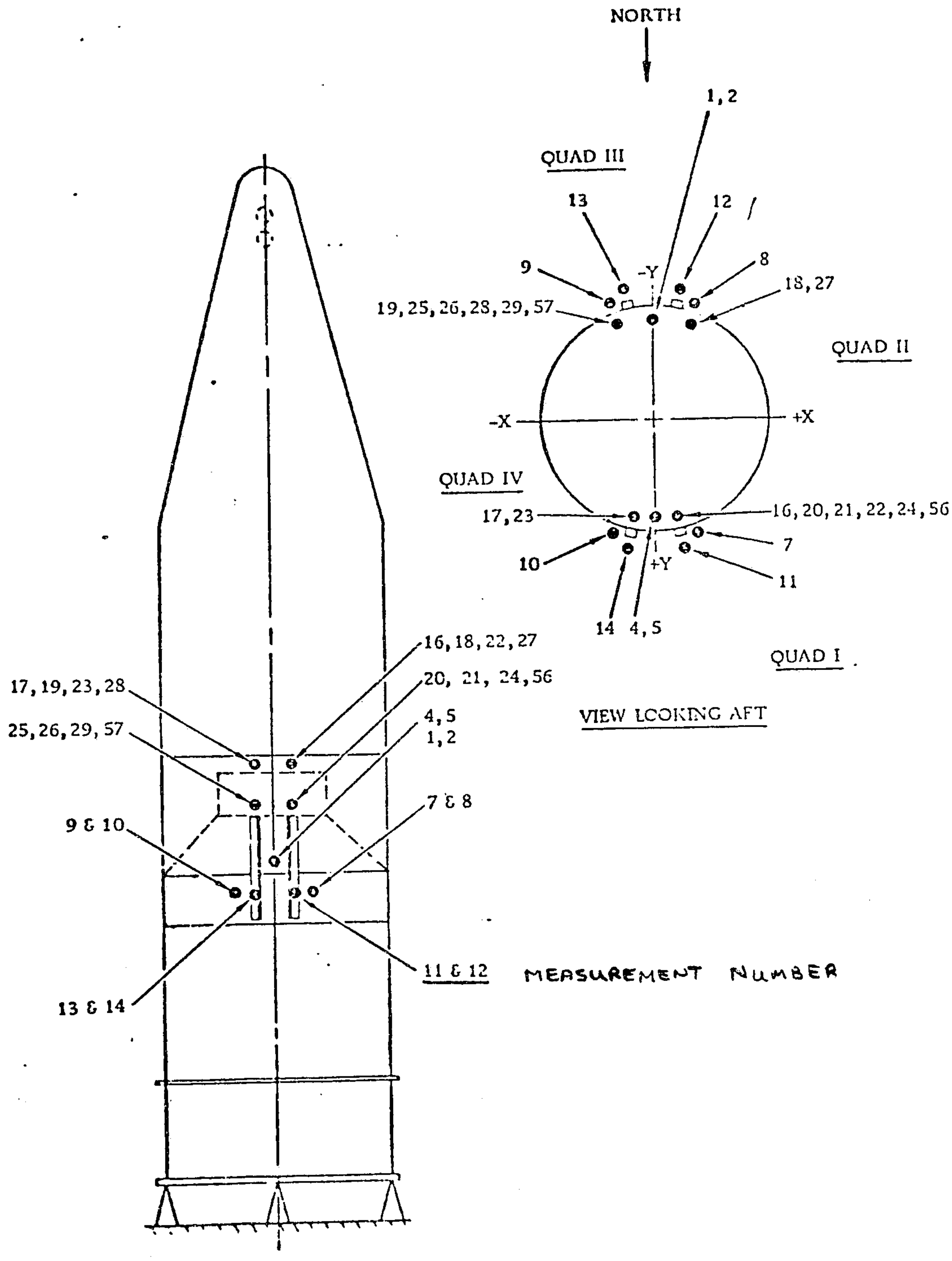

Figure 10 Centaur D-1A Separation Test Transducer Locations on Test Specimen

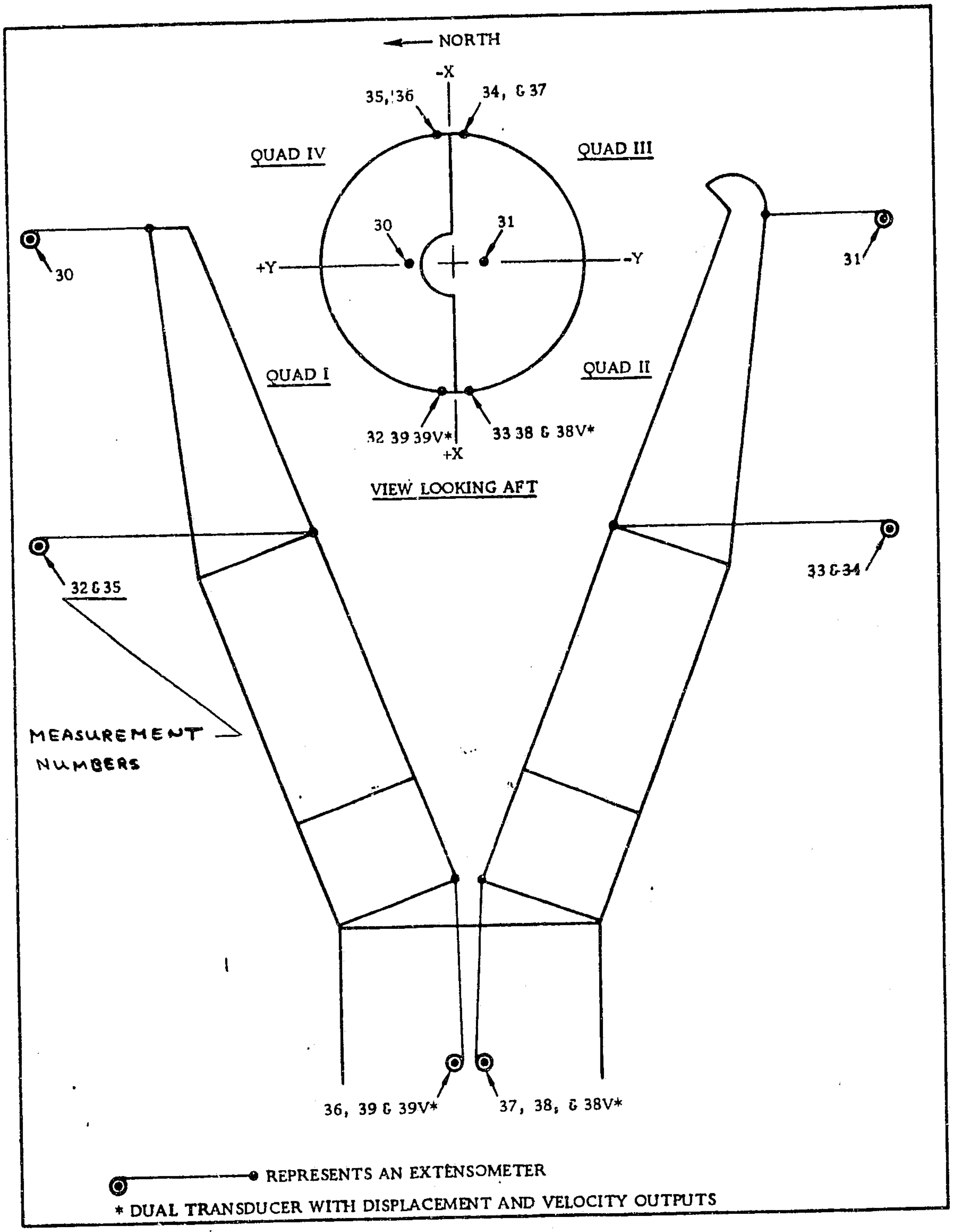

FIGURE 11 LINEAR MOTION TRANSDUCER LOCATION

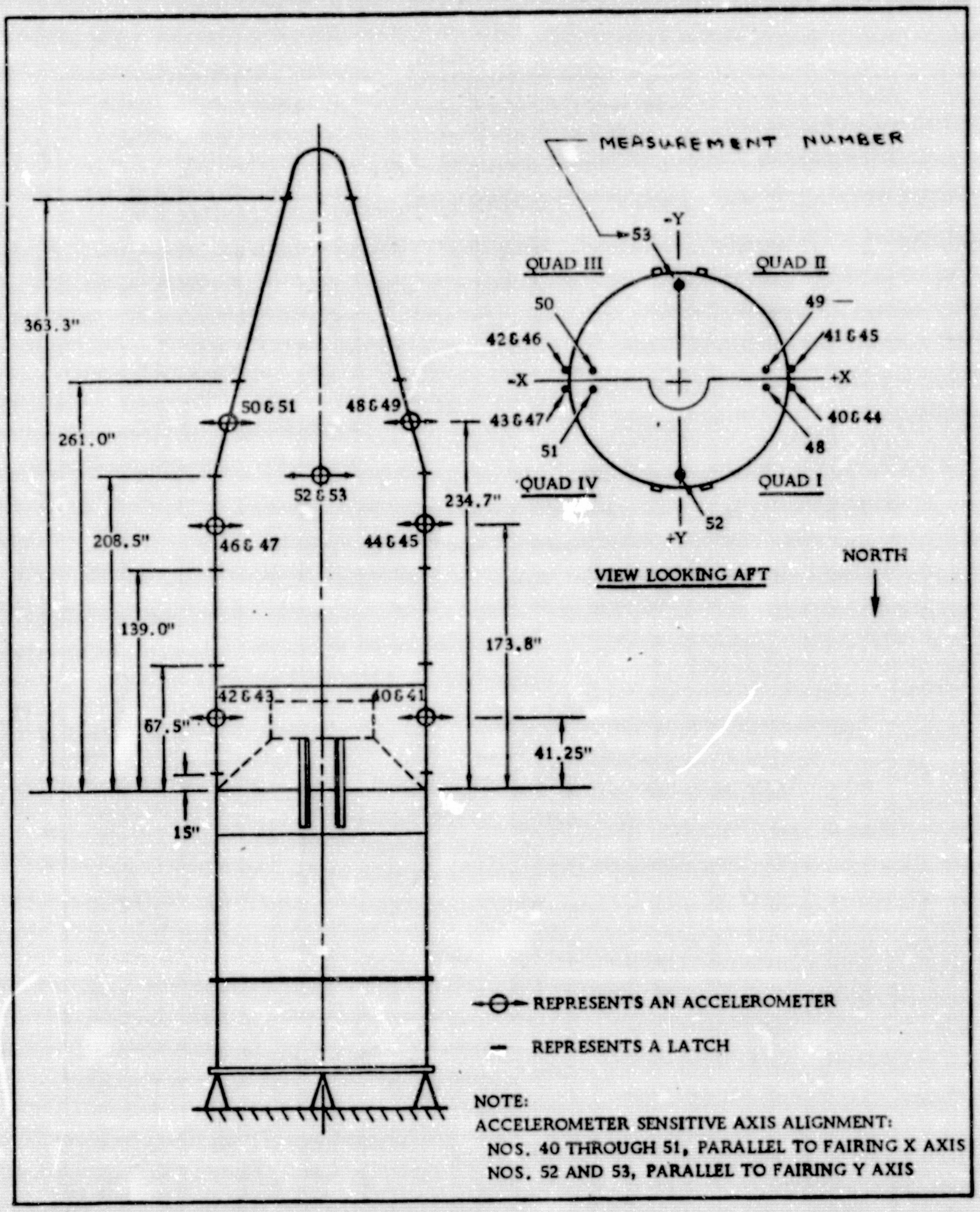

FIGURE 12 ACCELEROMETER LOCATIONS

ORIGINAL PAGE IS
OF POOR QUALITY

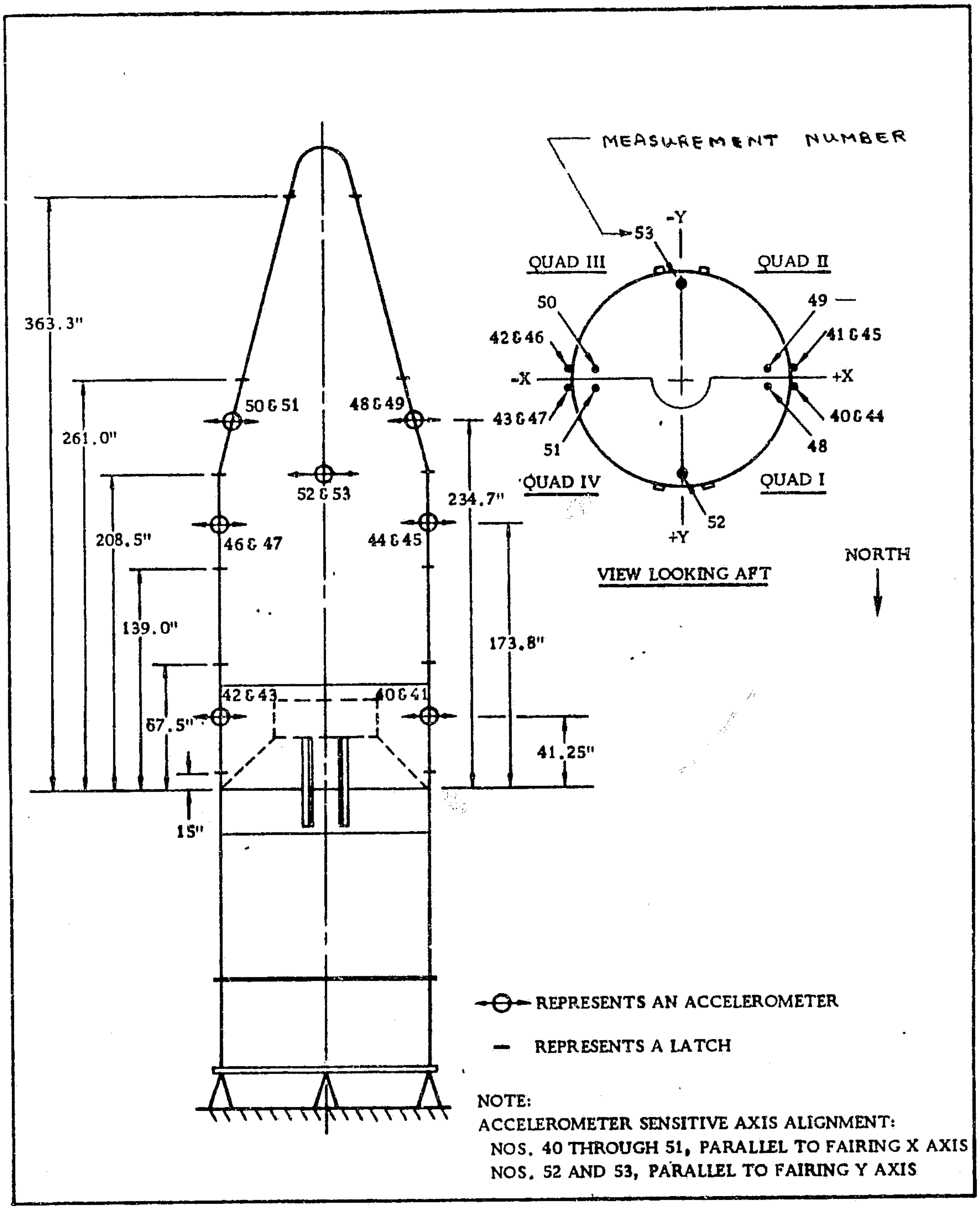

FIGURE 12 ACCELEROMETER LOCATIONS

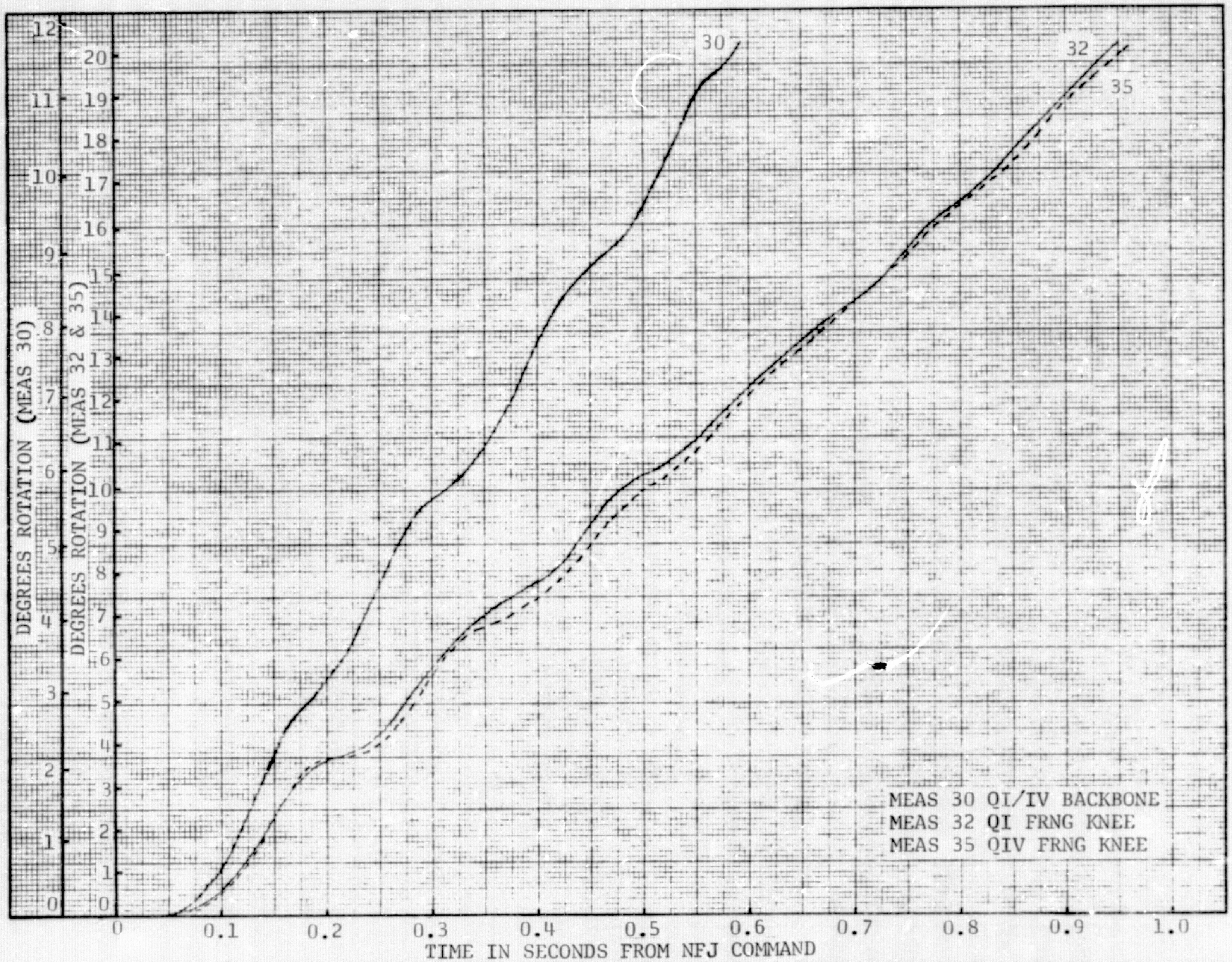

FIGURE 13 QUAD I/IV FAIRING ROTATION - TEST 1

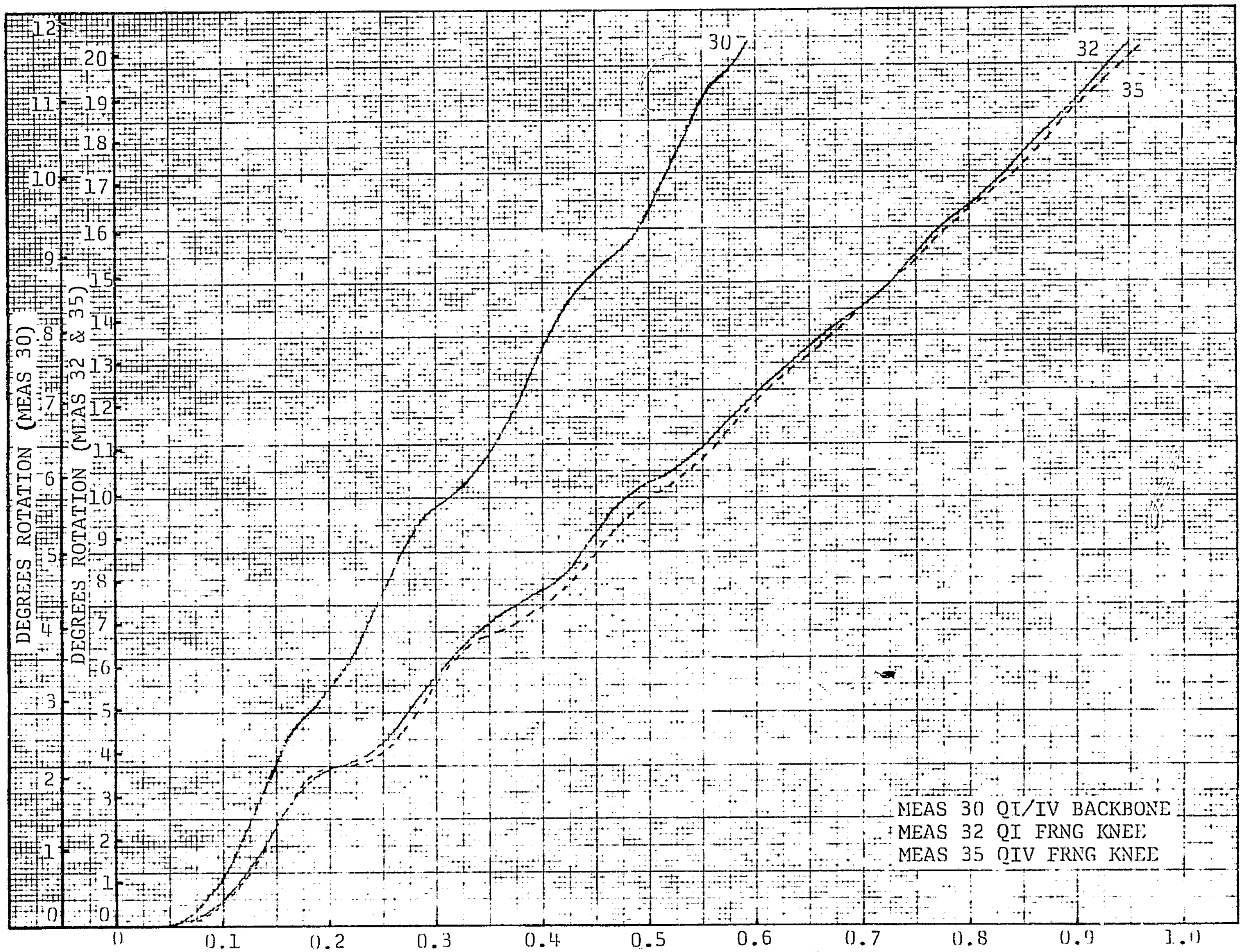

FIGURE 13 QUAD I/IV FAIRING ROTATION - TEST 1

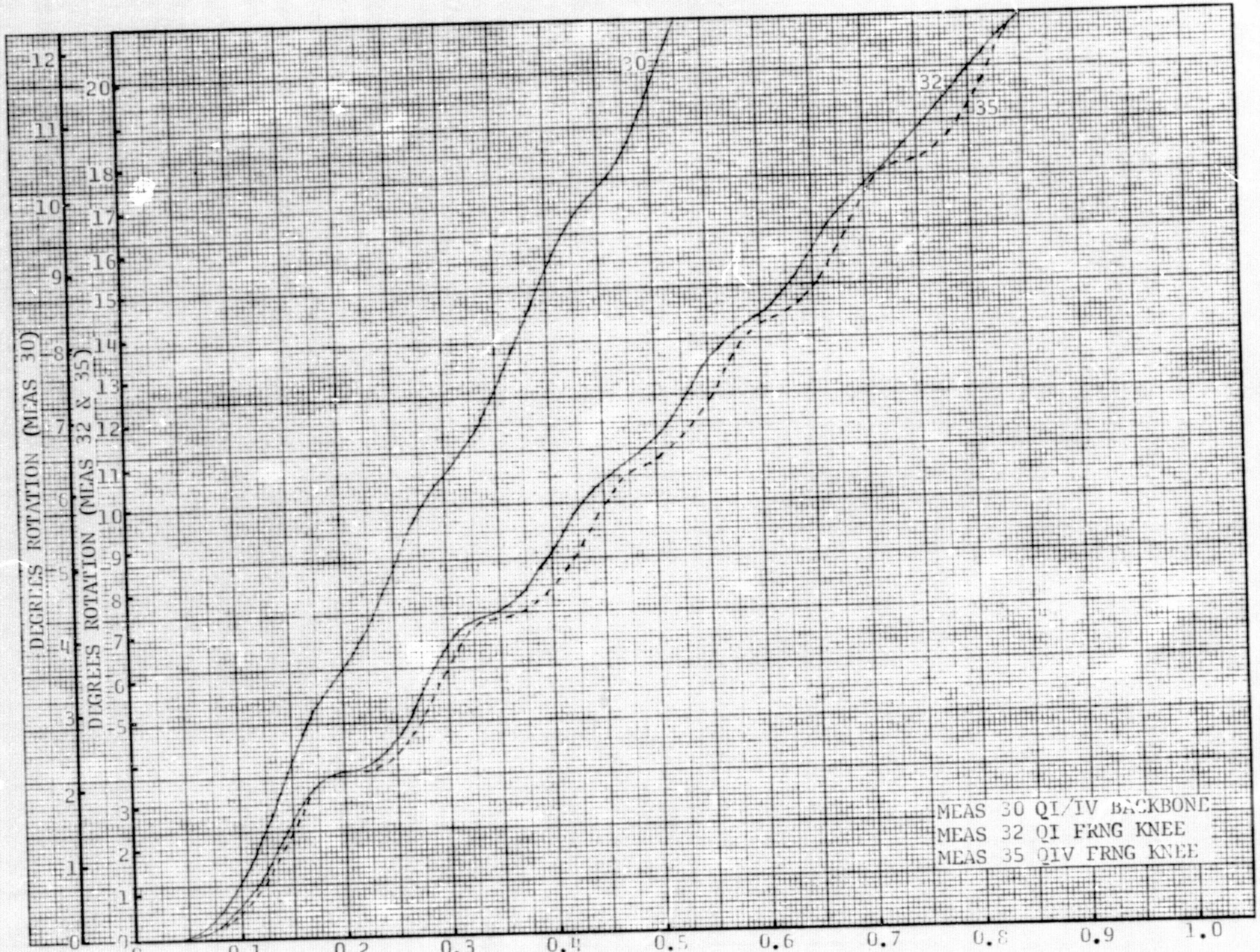

FIGURE 14 QUAD I/IV FAIRING ROTATION - TEST 3

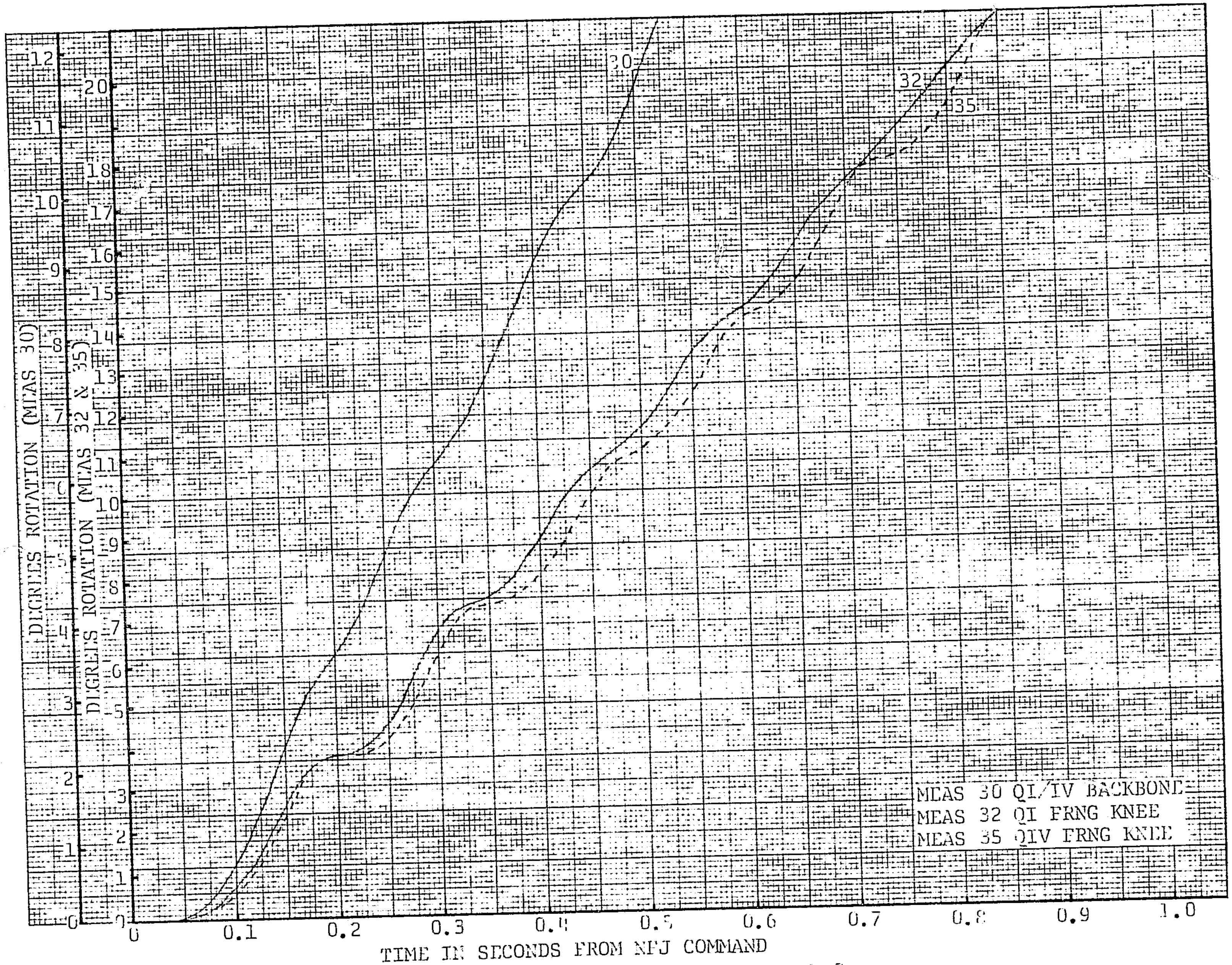

FIGURE 14 QUAD I/IV FAIRING ROTATION - TEST 3

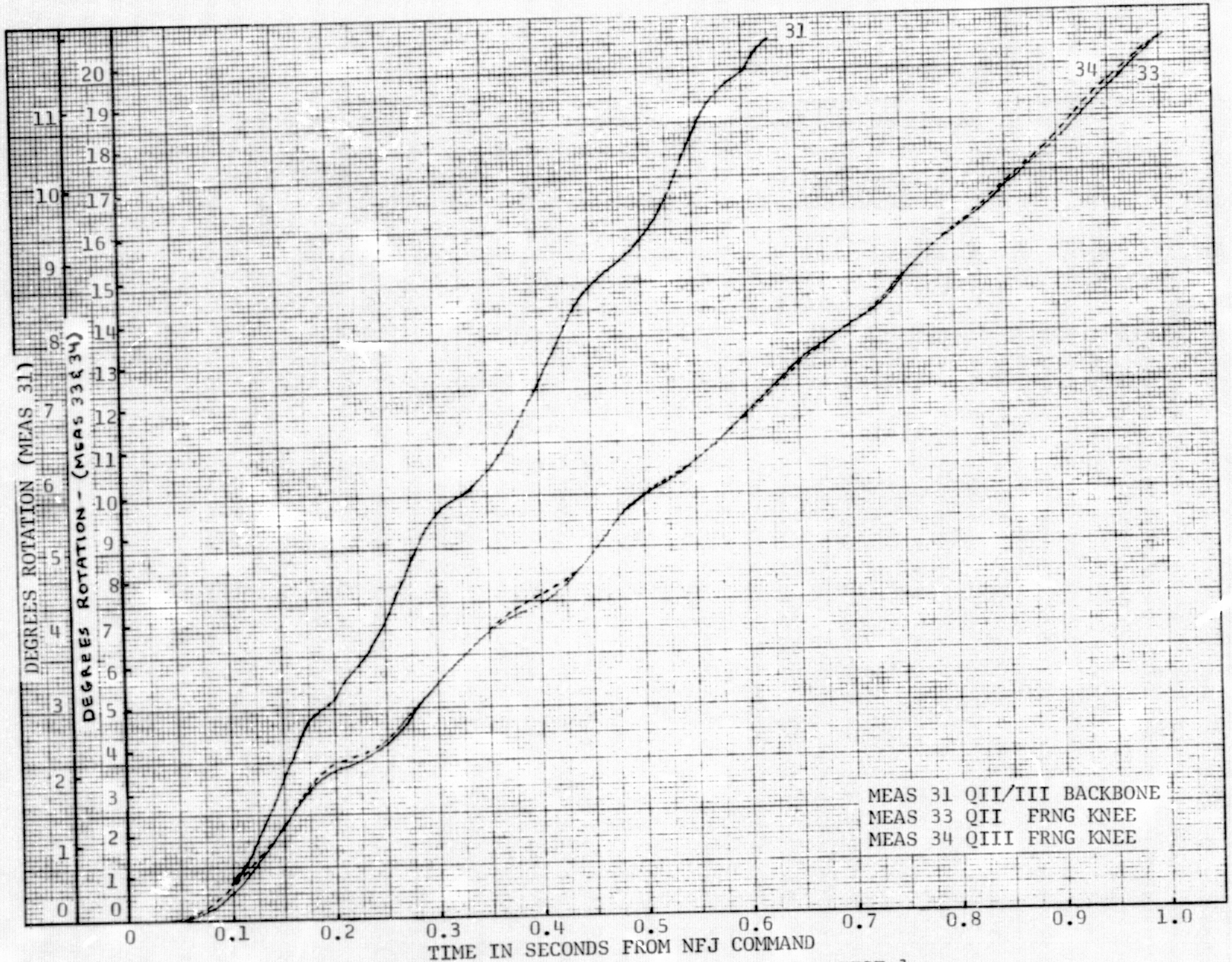

FIGURE 15 QUAD II/III FAIRING ROTATION - TEST 1

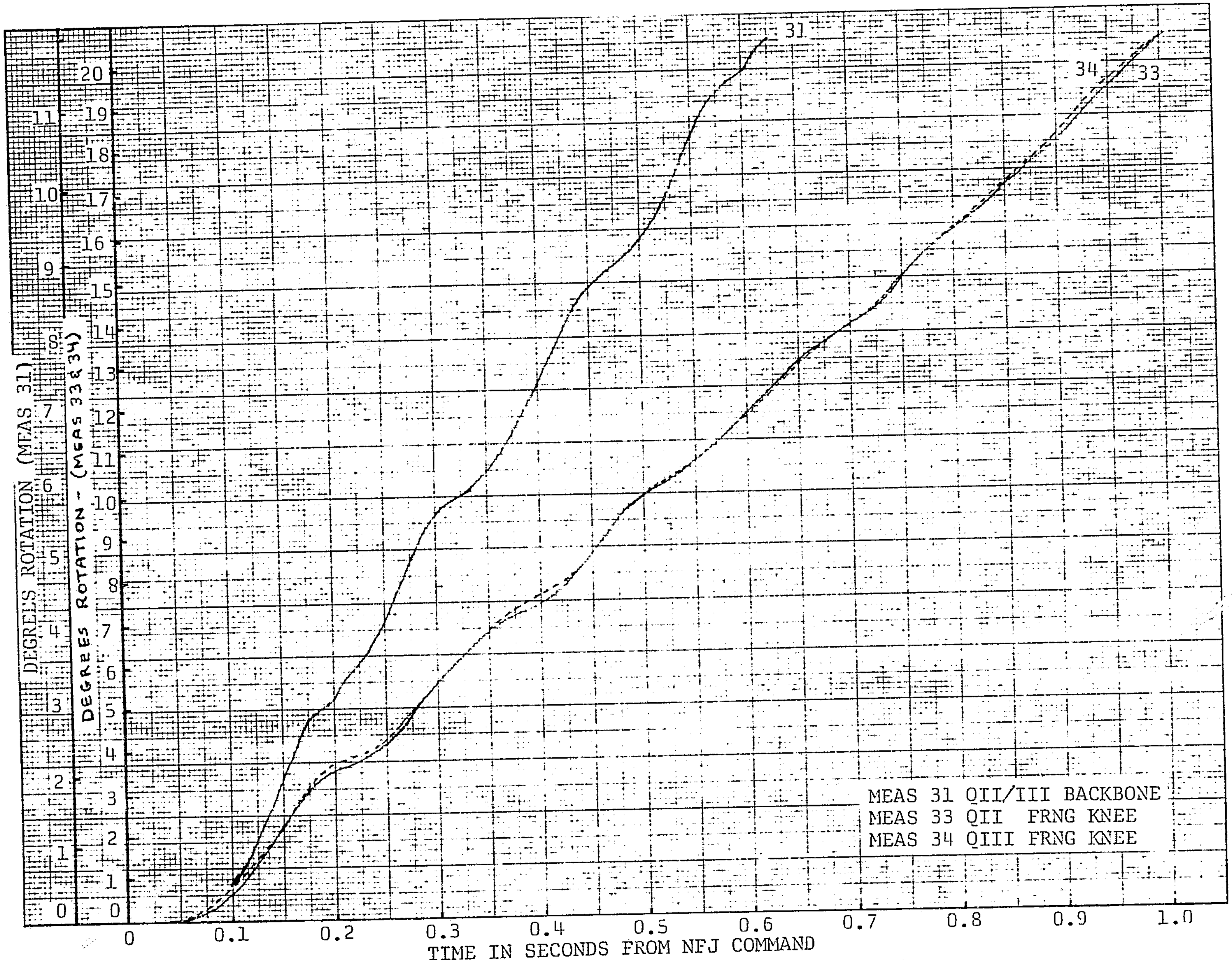

FIGURE 15 QUAD II/III FAIRING ROTATION - TEST 1

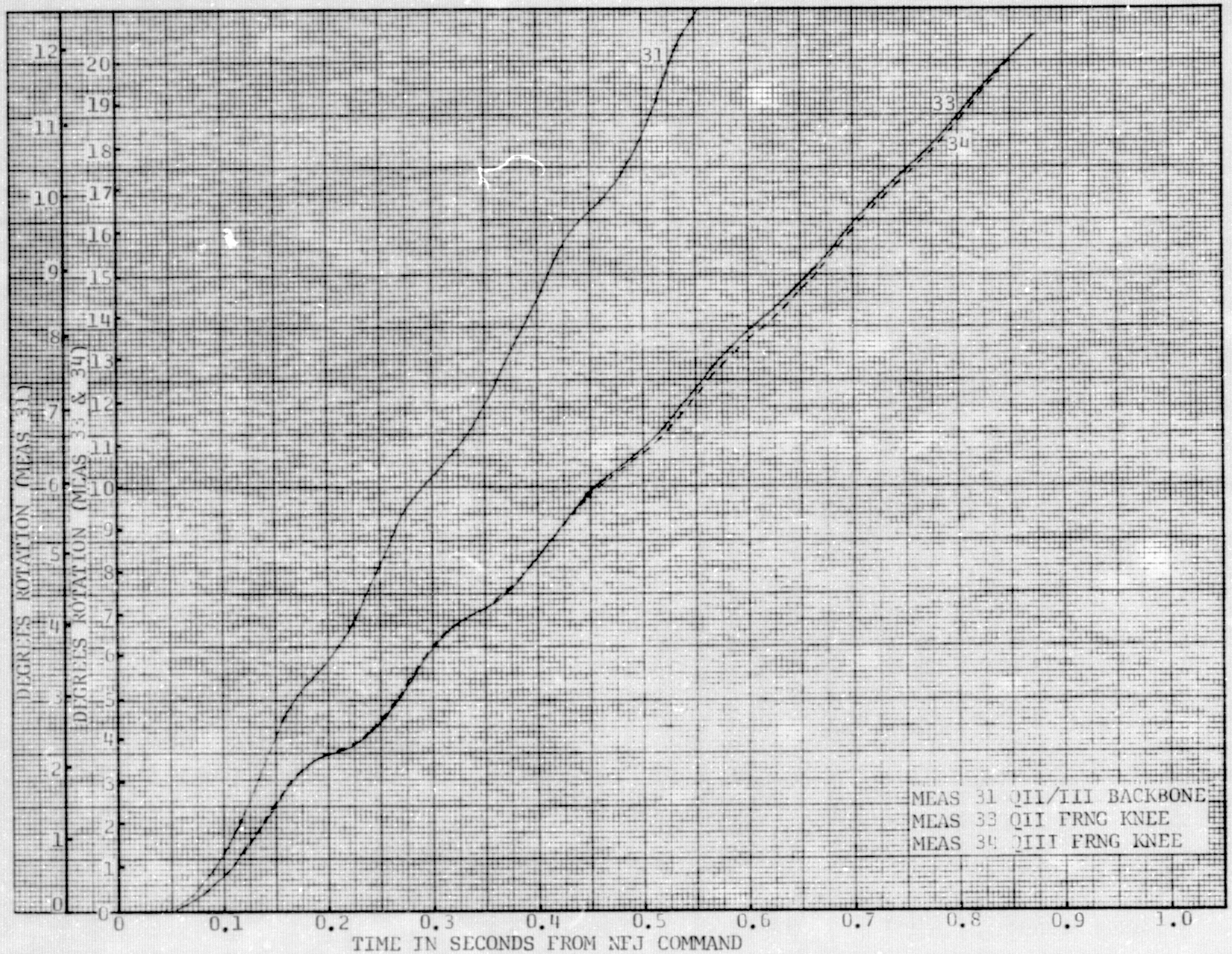

FIGURE 16 QUAD II/III FAIRING ROTATION - TEST 3

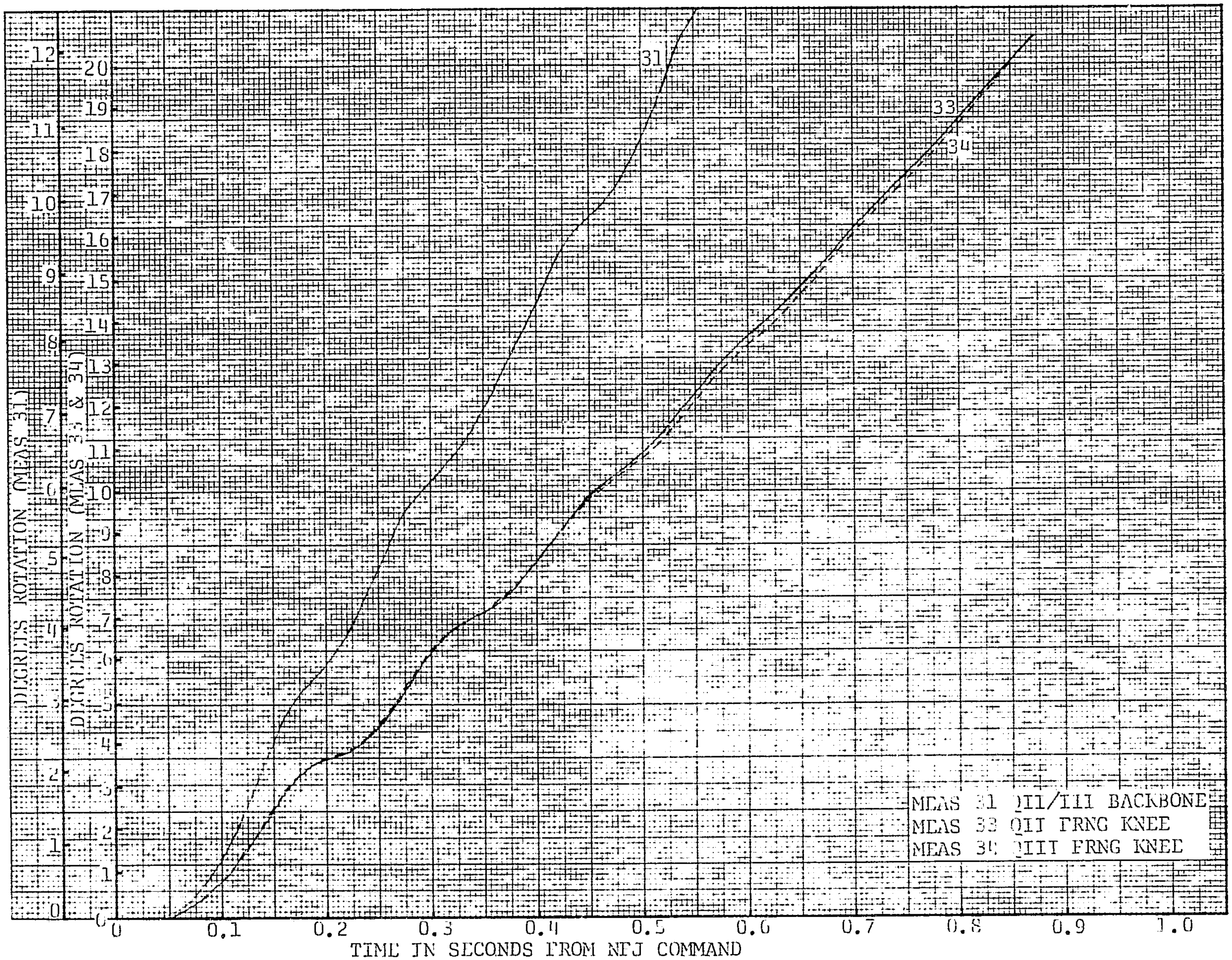

FIGURE 16 QUAD II/III FAIRING ROTATION - TEST 3

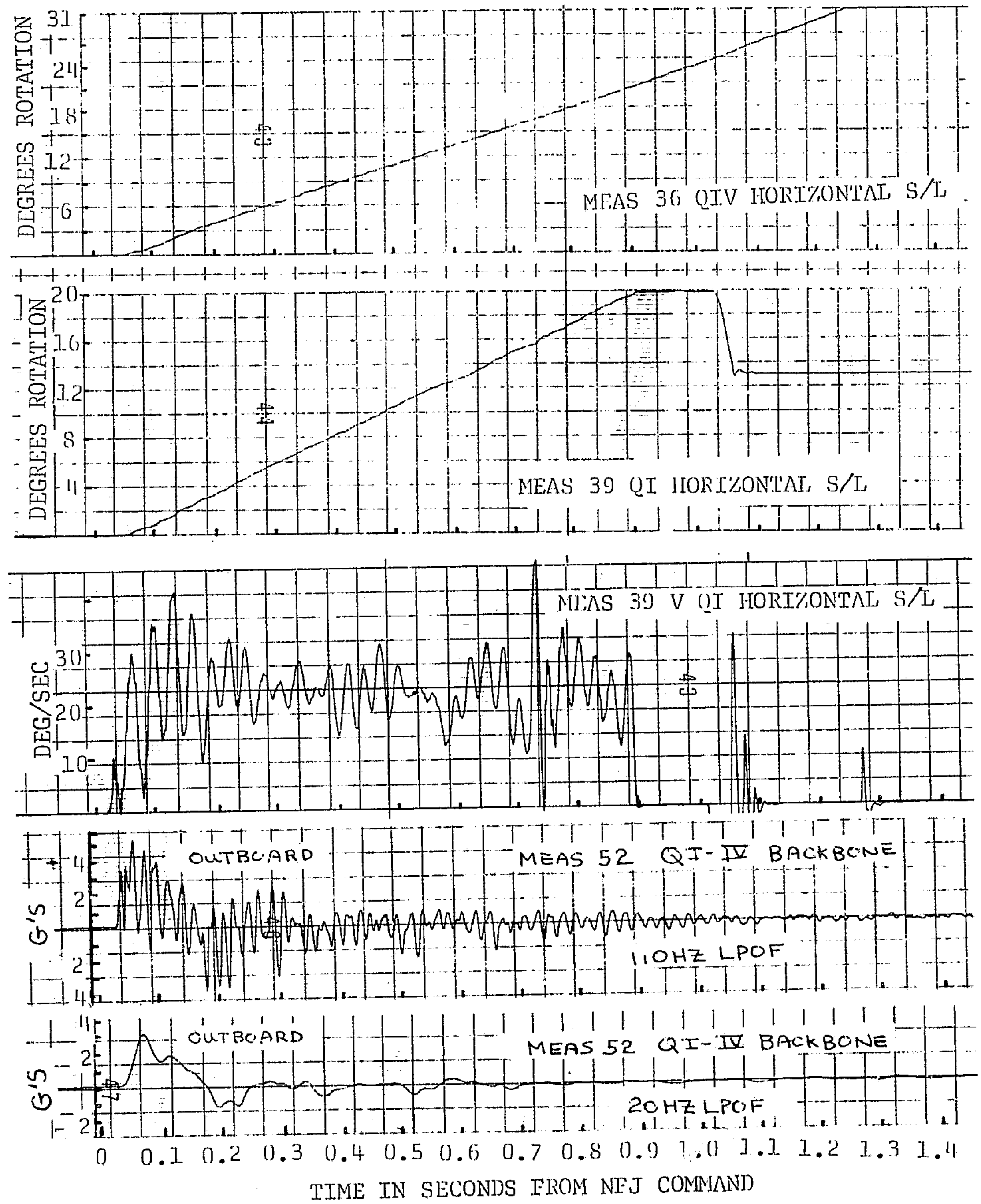

FIGURE 17 QUAD I/IV FAIRING ROTATION AND VELOCITY - TEST 1

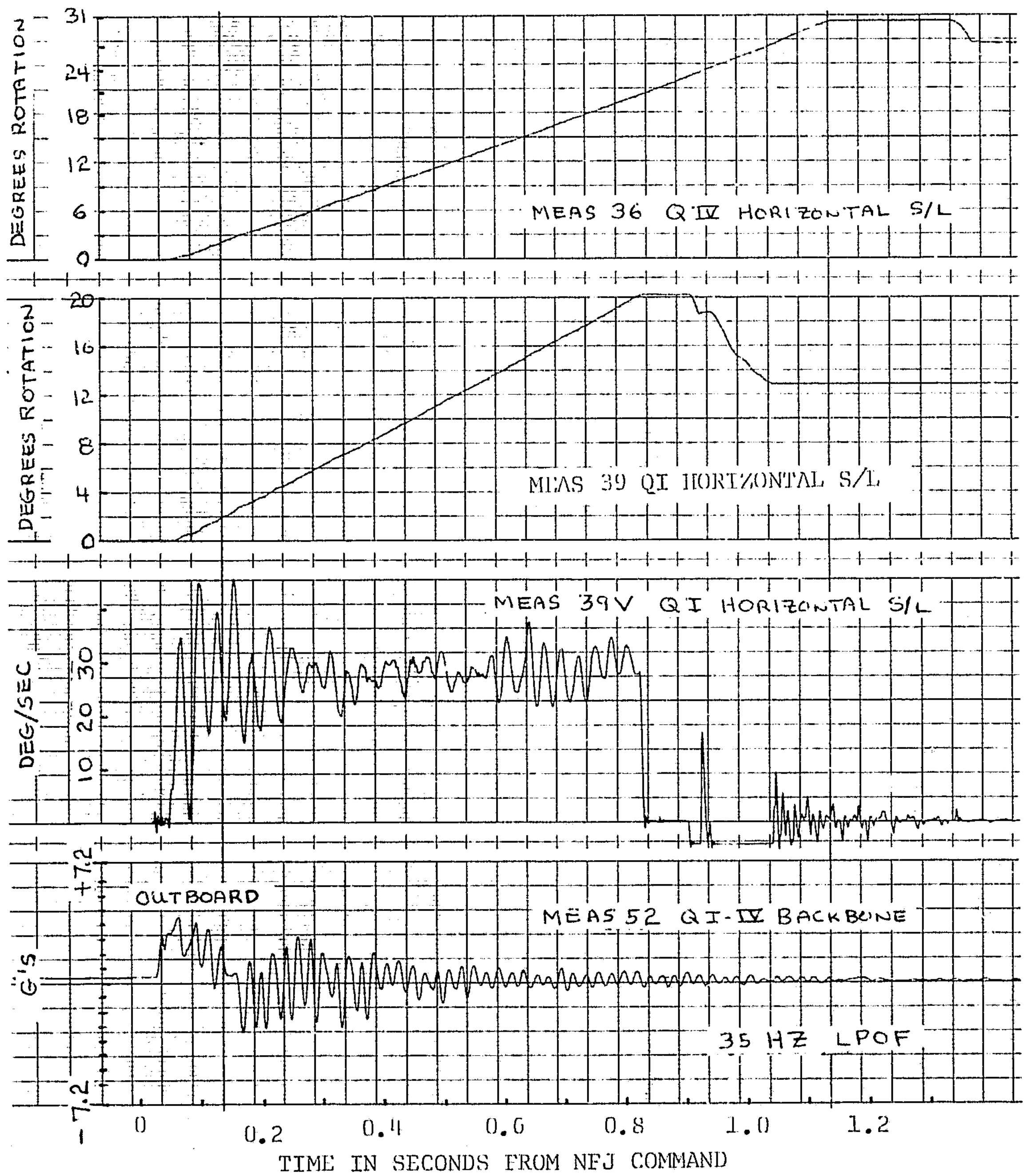

FIGURE 18 QUAD I/IV FAIRING ROTATION AND VELOCITY - TEST 3

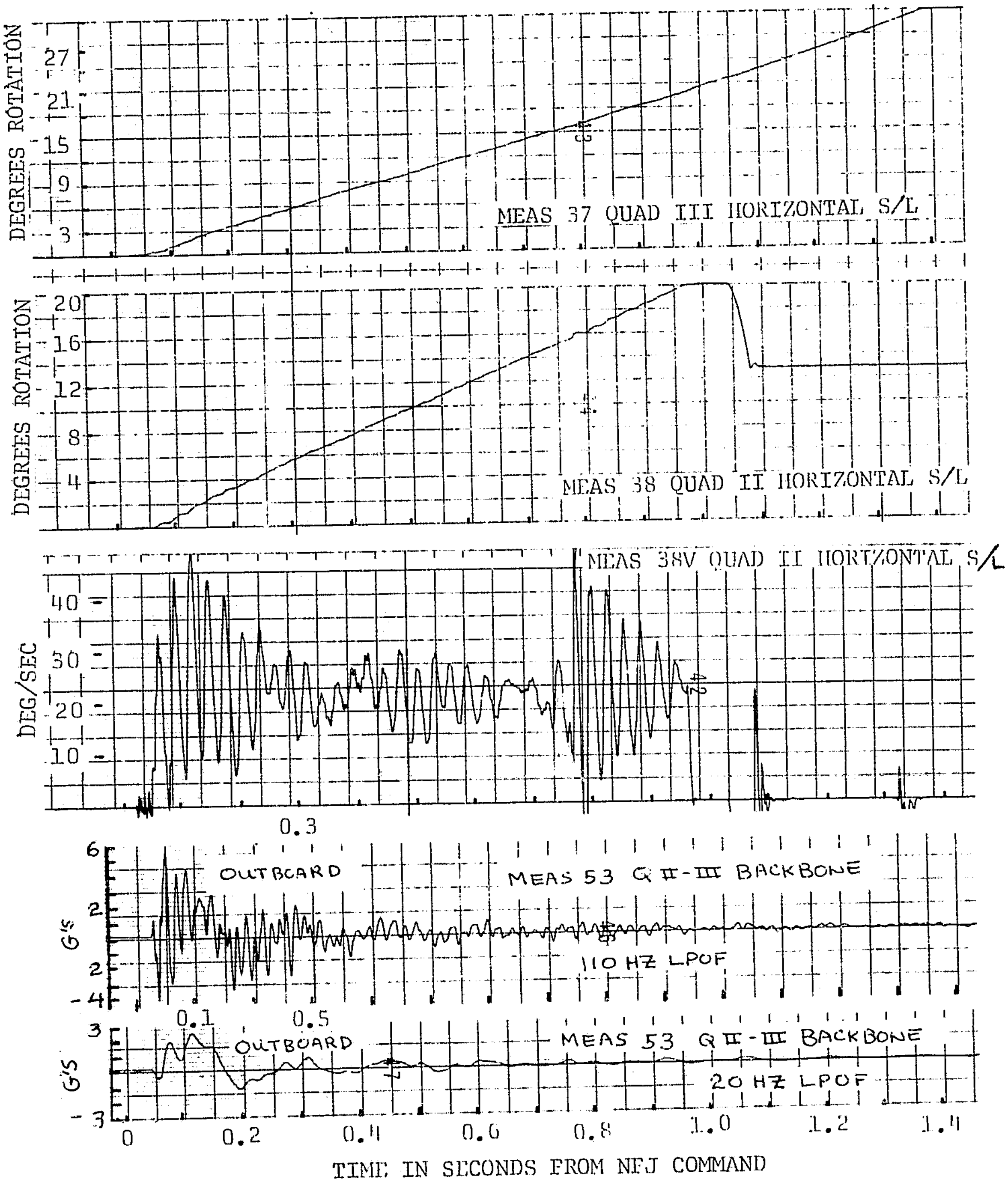

FIGURE 19 QUAD II/III FAIRING ROTATION AND VELOCITY - TEST 1

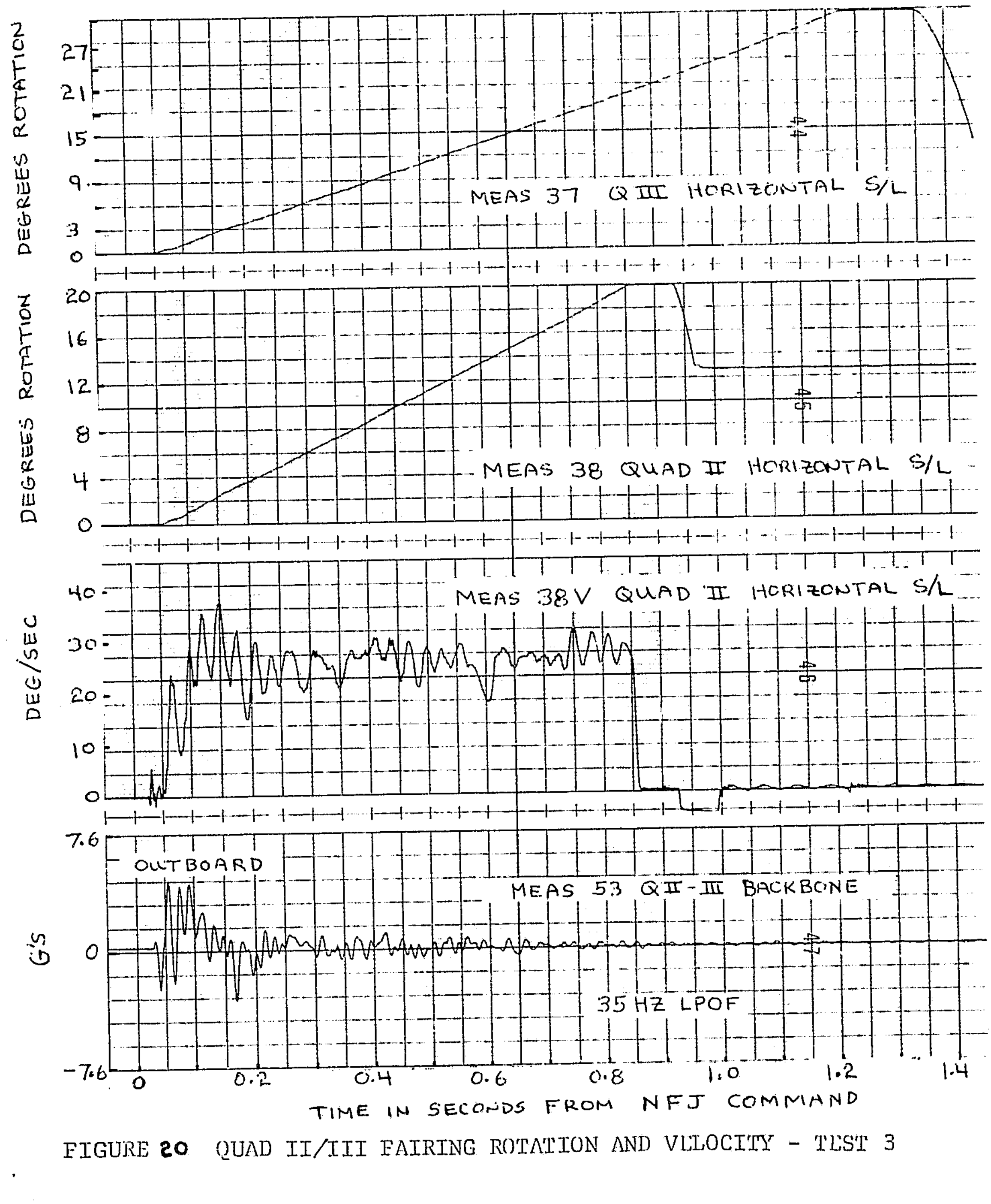

FIGURE 20 QUAD II/III FAIRING ROTATION AND VELOCITY - TEST 3

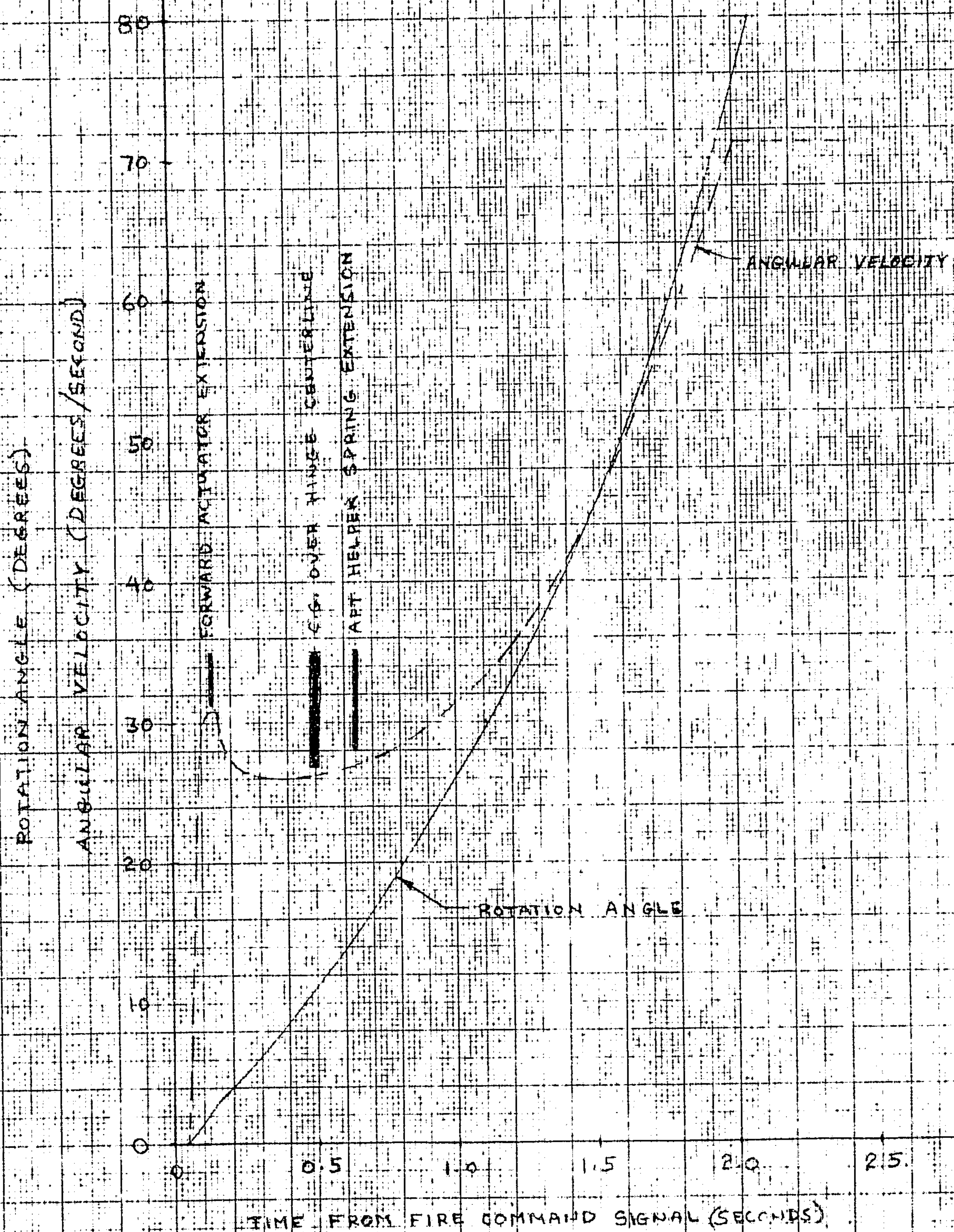

FIGURE 21 Q I/IV FAIRING ROTATION ANGLE/VELOCITY VS TIME - TEST 3 (MVM)

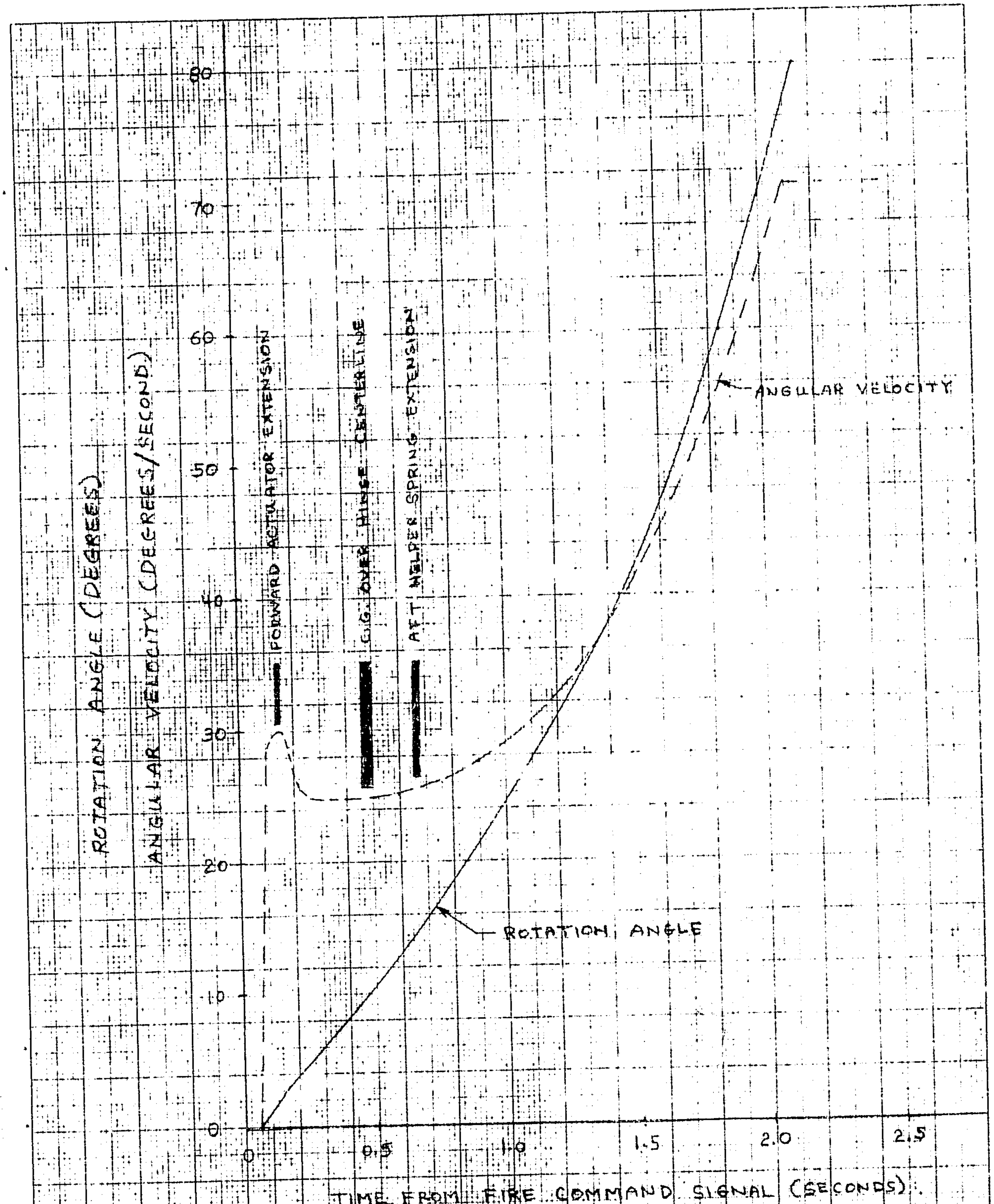

FIGURE 22 QII-III FAIRING ROTATION ANGLE/VELOCITY VS TIME — TEST 3 (MVM)

ORIGINAL PAGE IS
OF POOR QUALITY

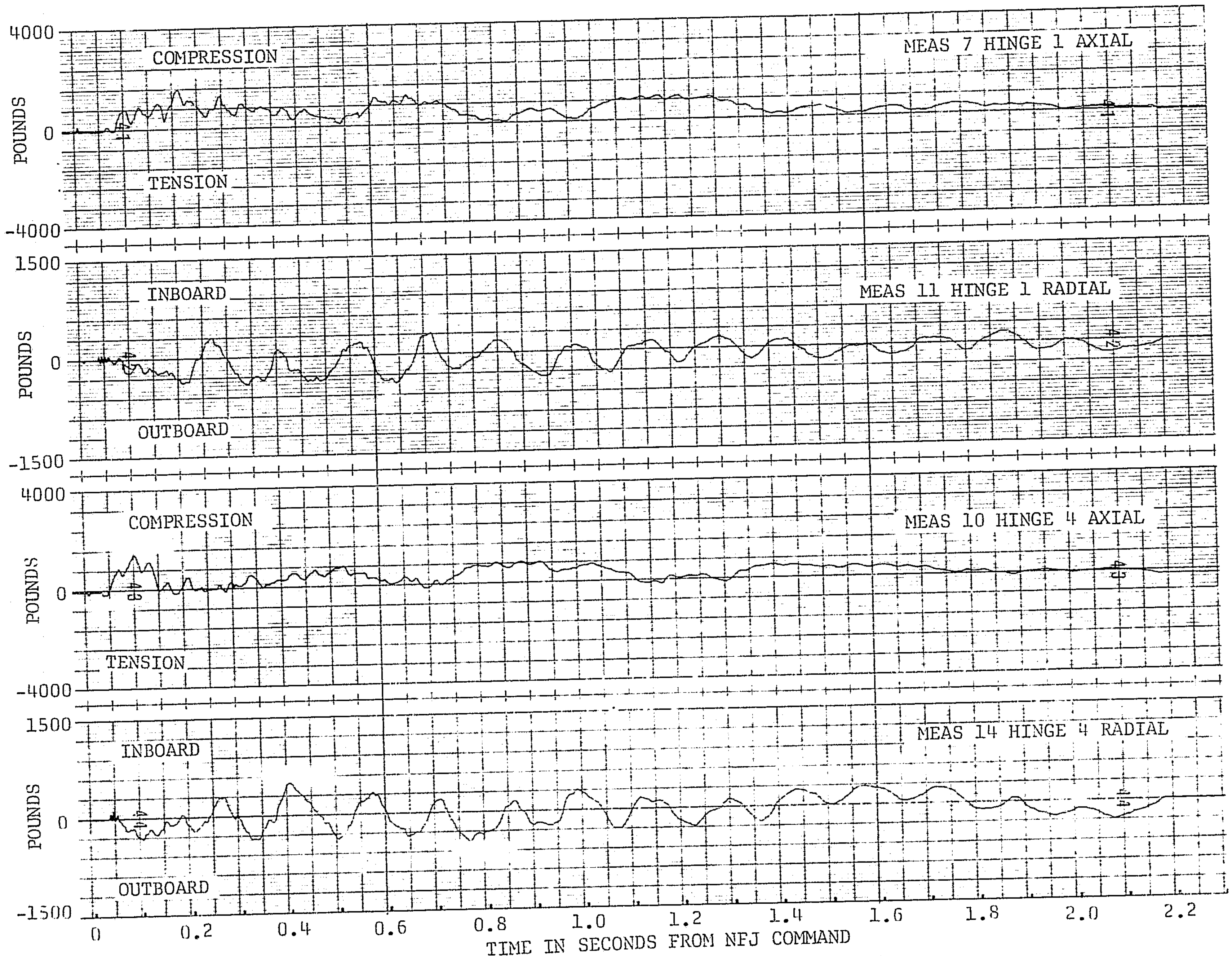

FIGURE 23 QUAD I/IV HINGE LOADS - TEST 1

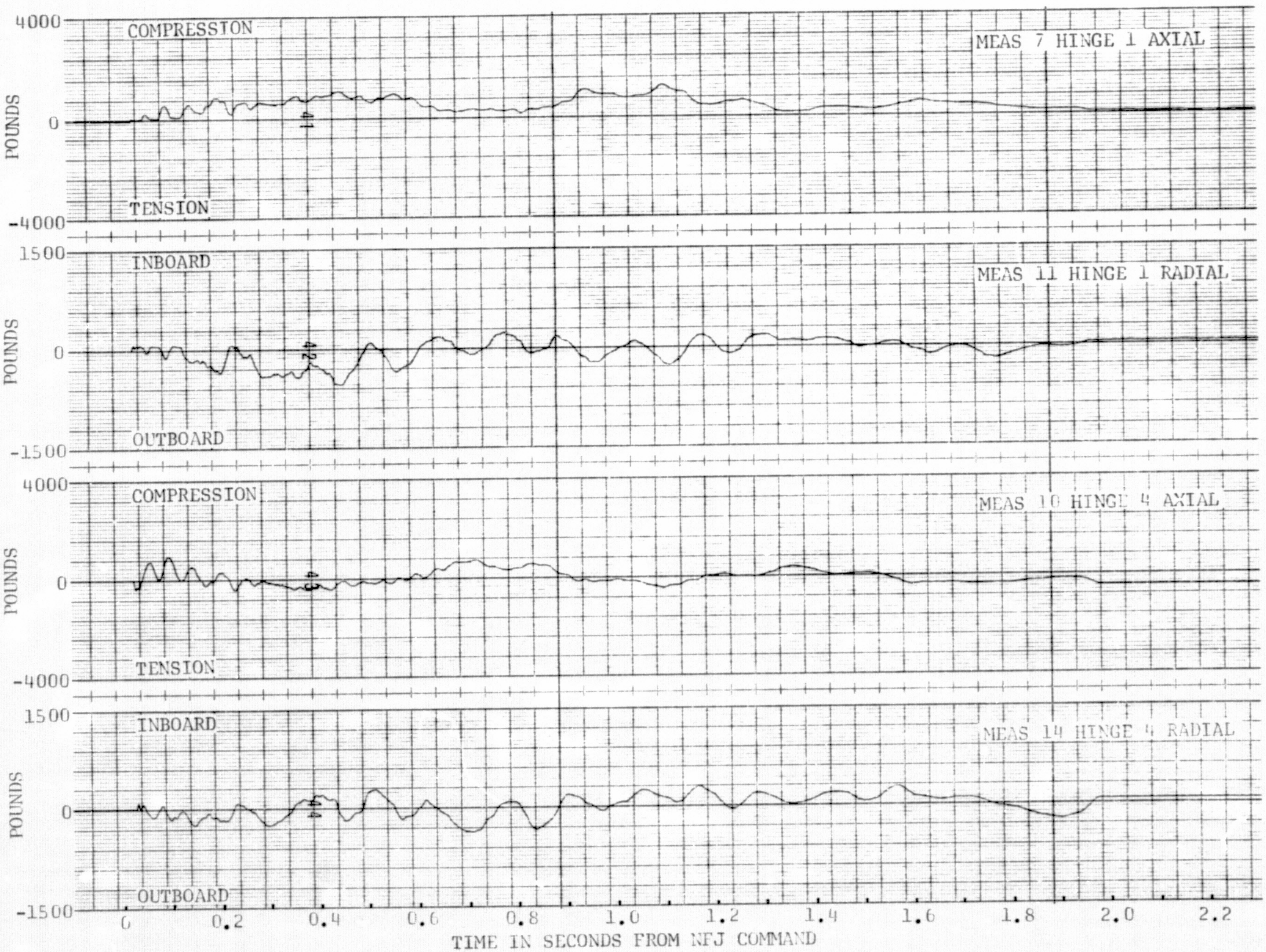

FIGURE 24 QUAD I/IV HINGE LOADS - TEST 3

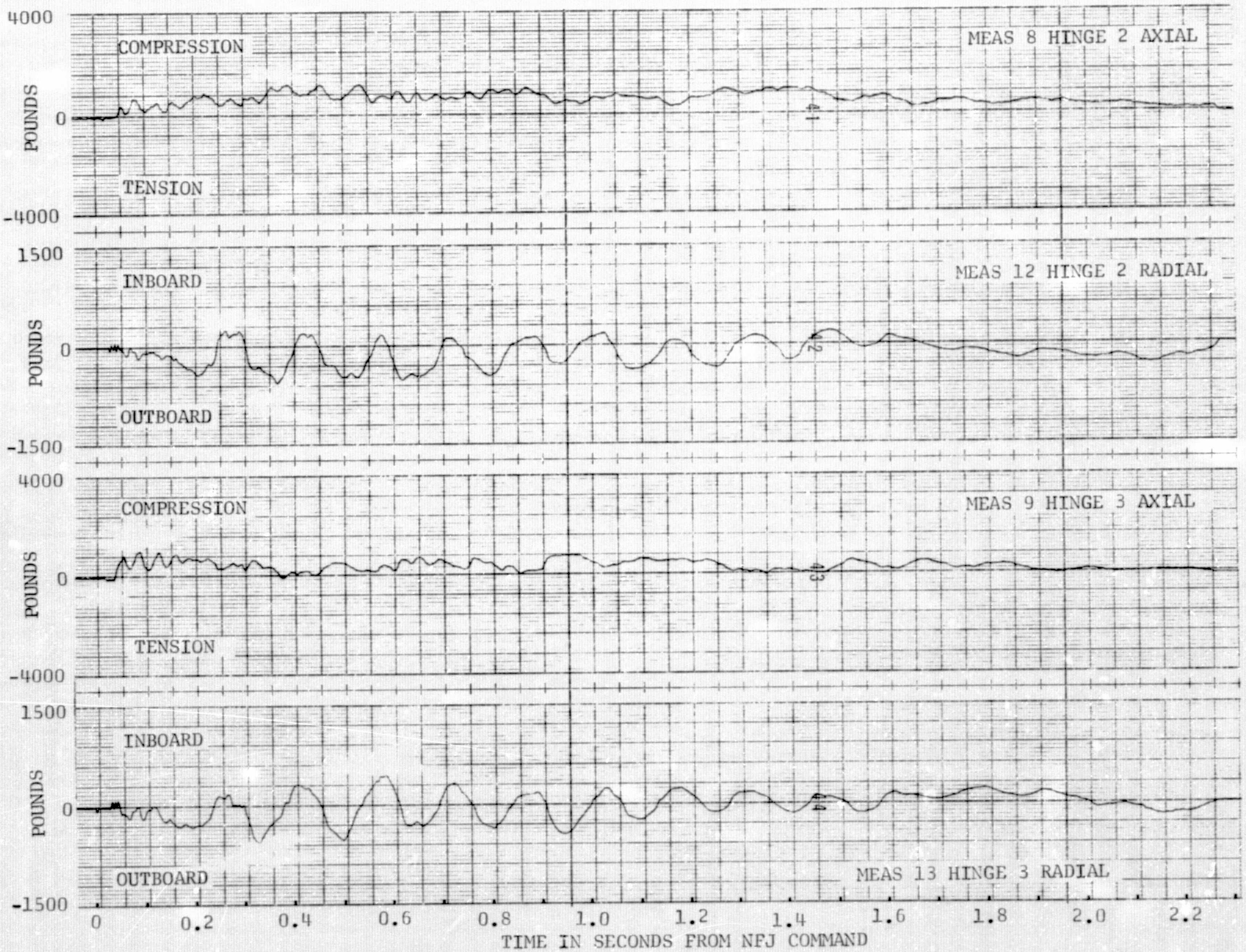

FIGURE 25. QUAD II/III HINGE LOADS - TEST 1

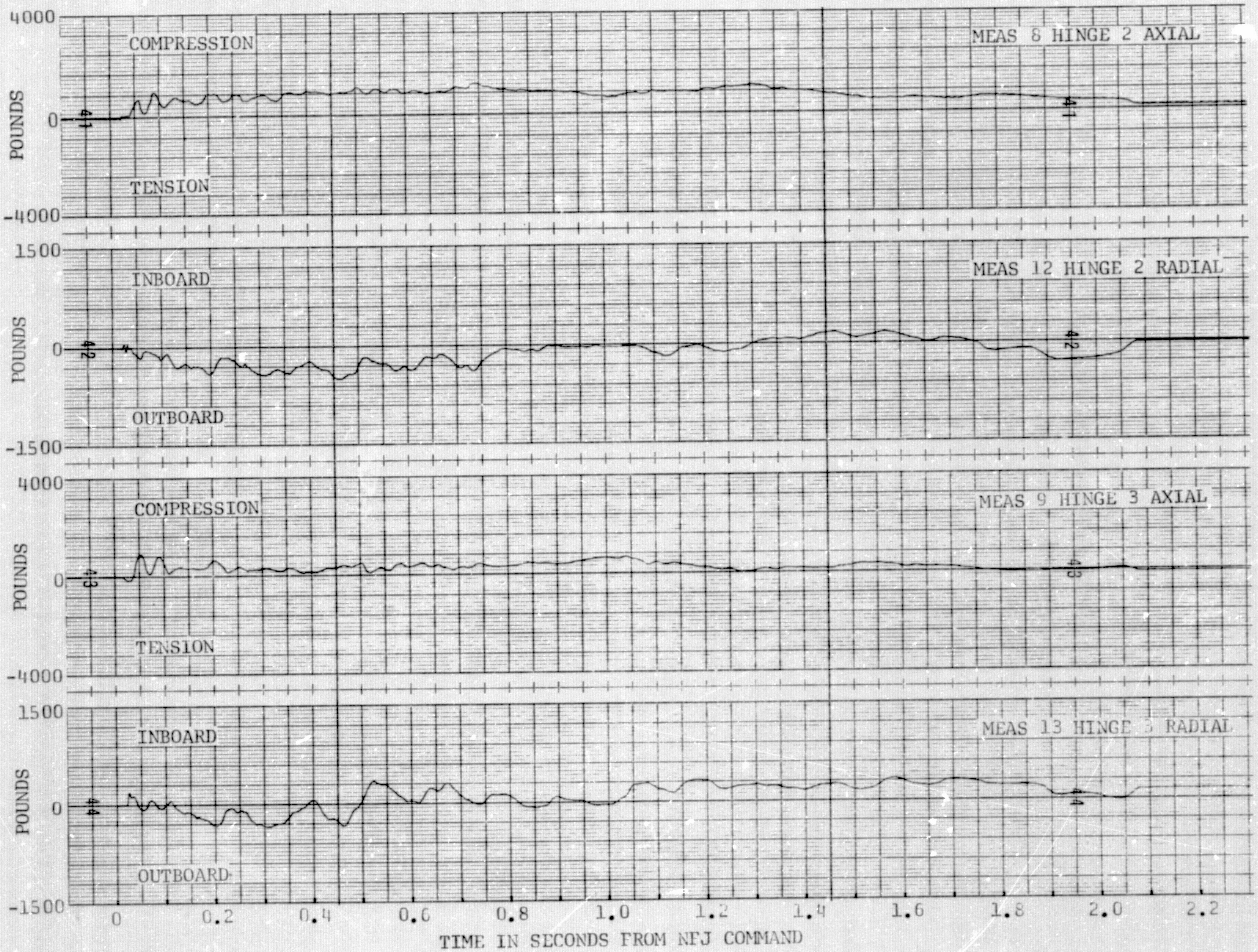

FIGURE 26 QUAD II/III HINGE LOADS - TEST 3

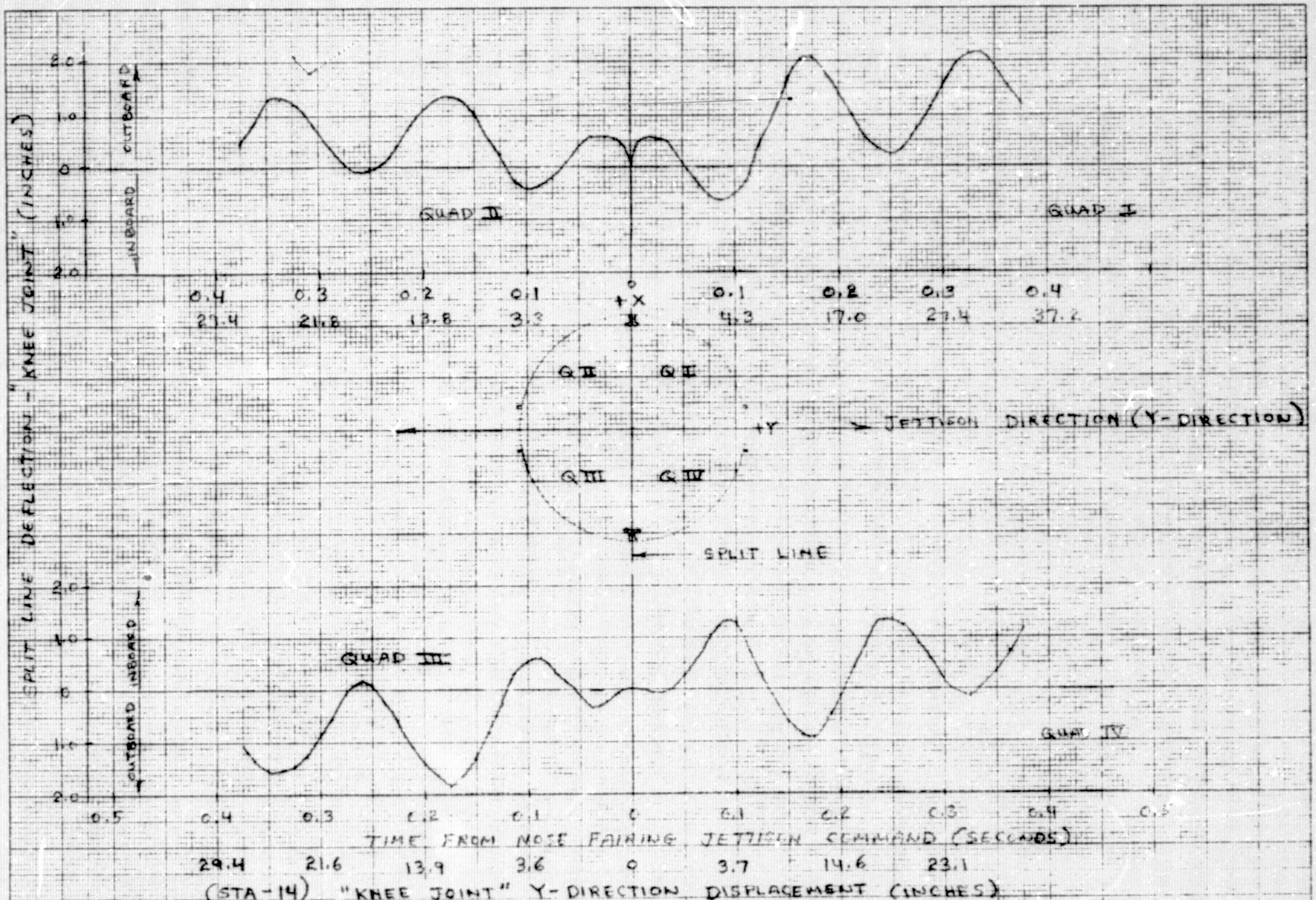

FIGURE 27 NOSE FAIRING SPLIT LINE "BREATHING" DEFLECTION – TEST #1

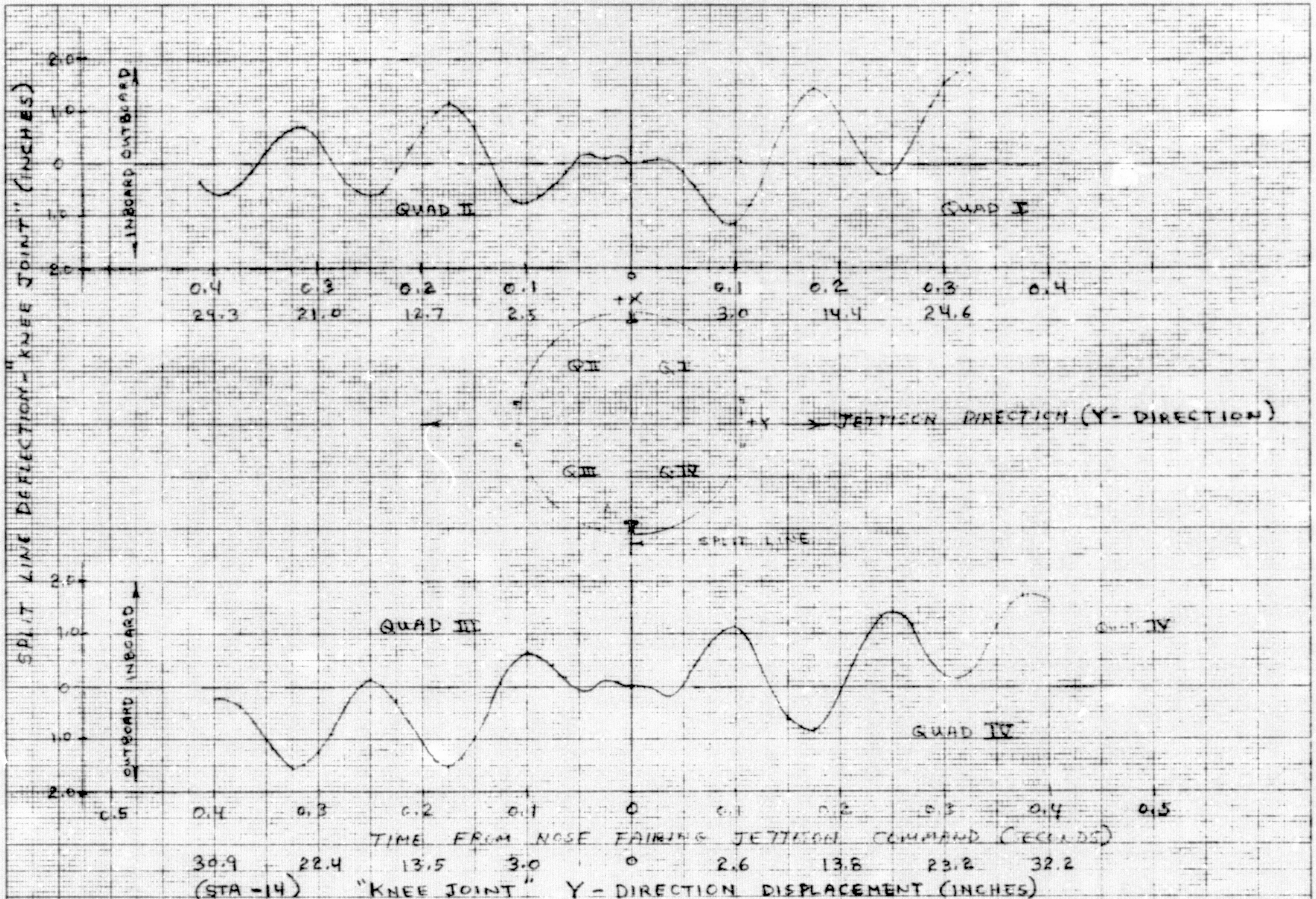

FIGURE 28 NOSE FAIRING SPLIT LINE "BREATHING" DEFLECTION - TEST # 3 (MVM)

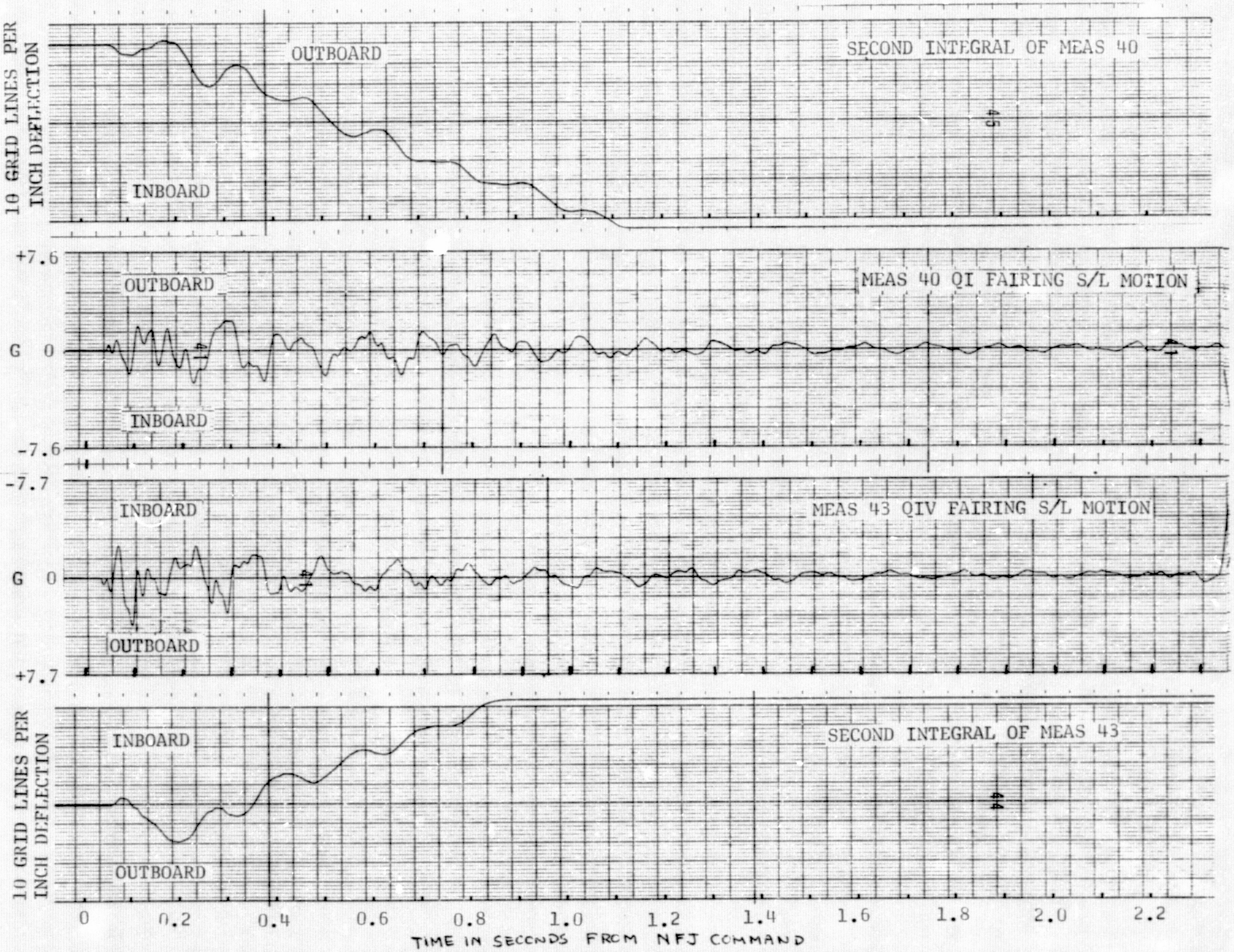

FIGURE 29 QUAD I/IV FAIRING MOTION - TEST 1

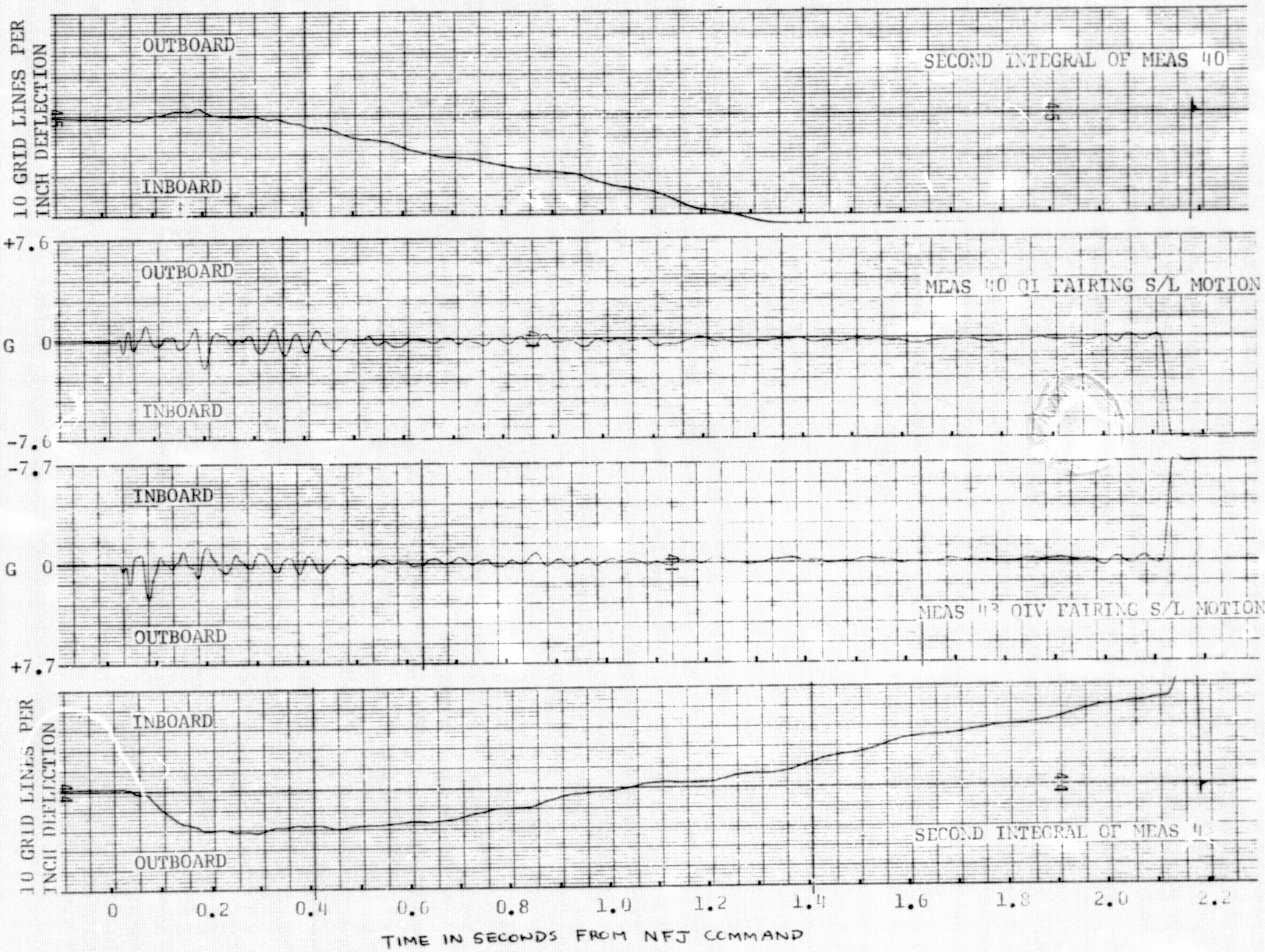

FIGURE 30 QUAD I/IV FAIRING MOTION - TEST 3

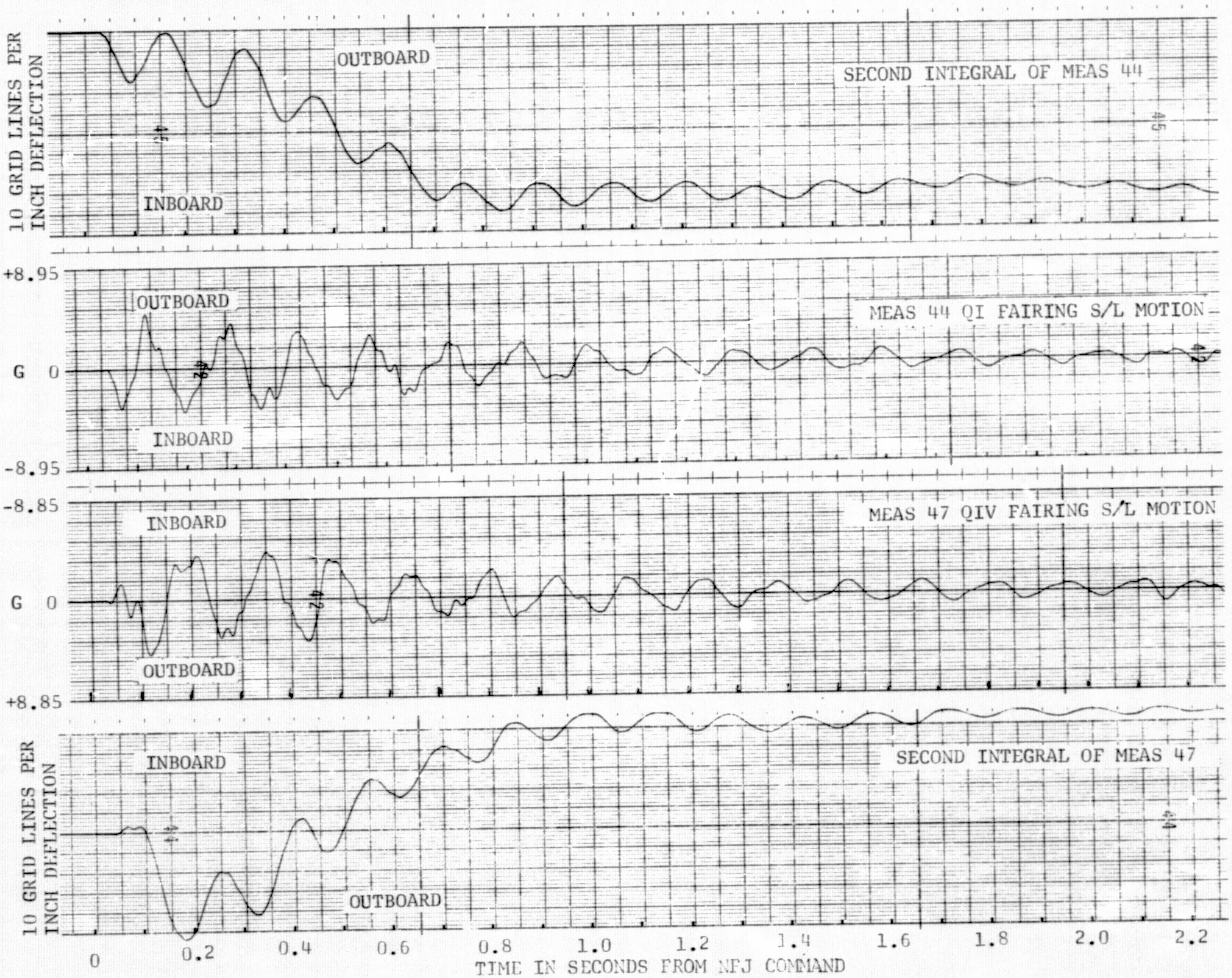

FIGURE 31 . QUAD I/IV FAIRING MOTION - TEST 1

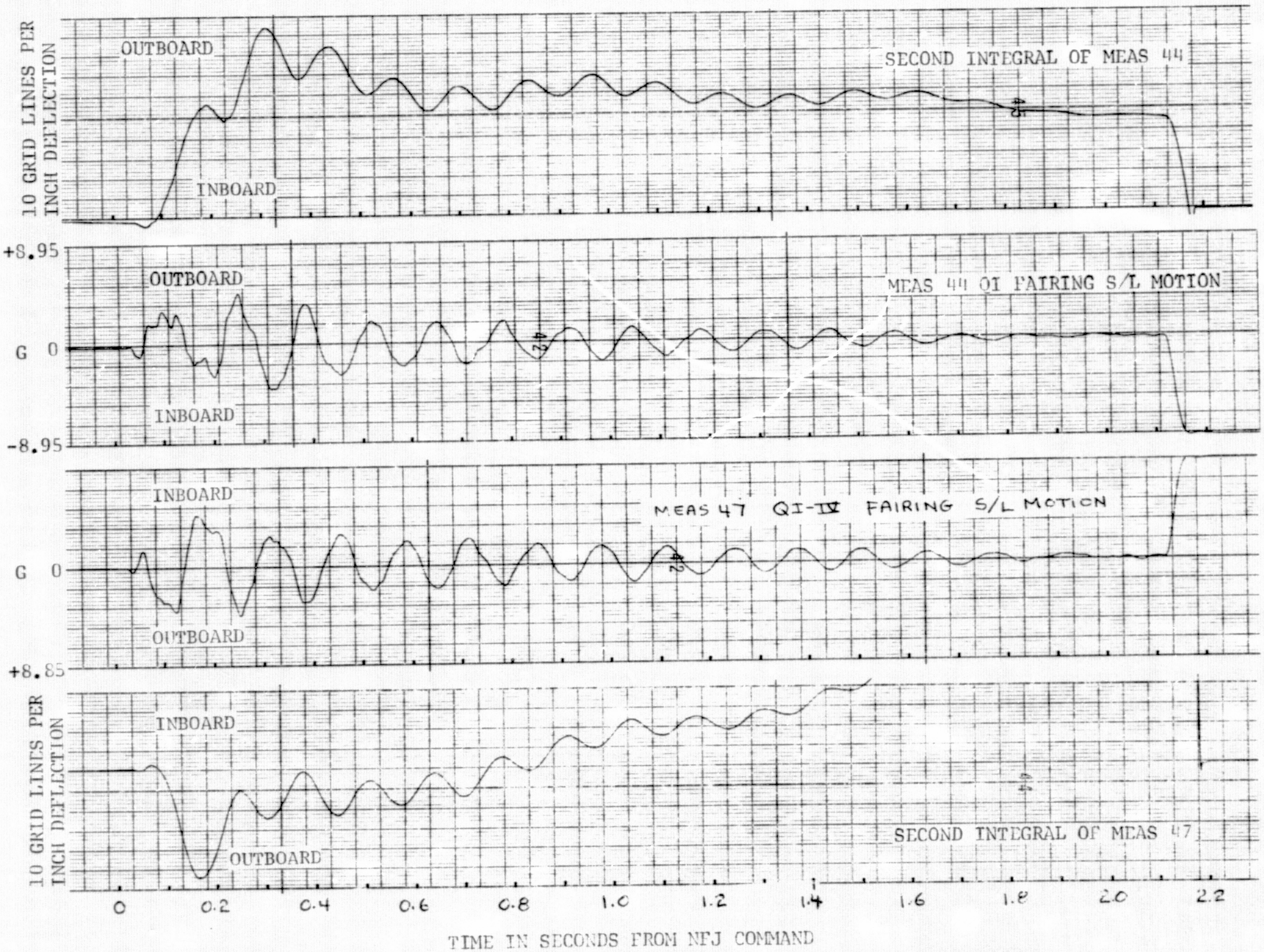

FIGURE 32 QUAD I/IV FAIRING MOTION - TEST 3

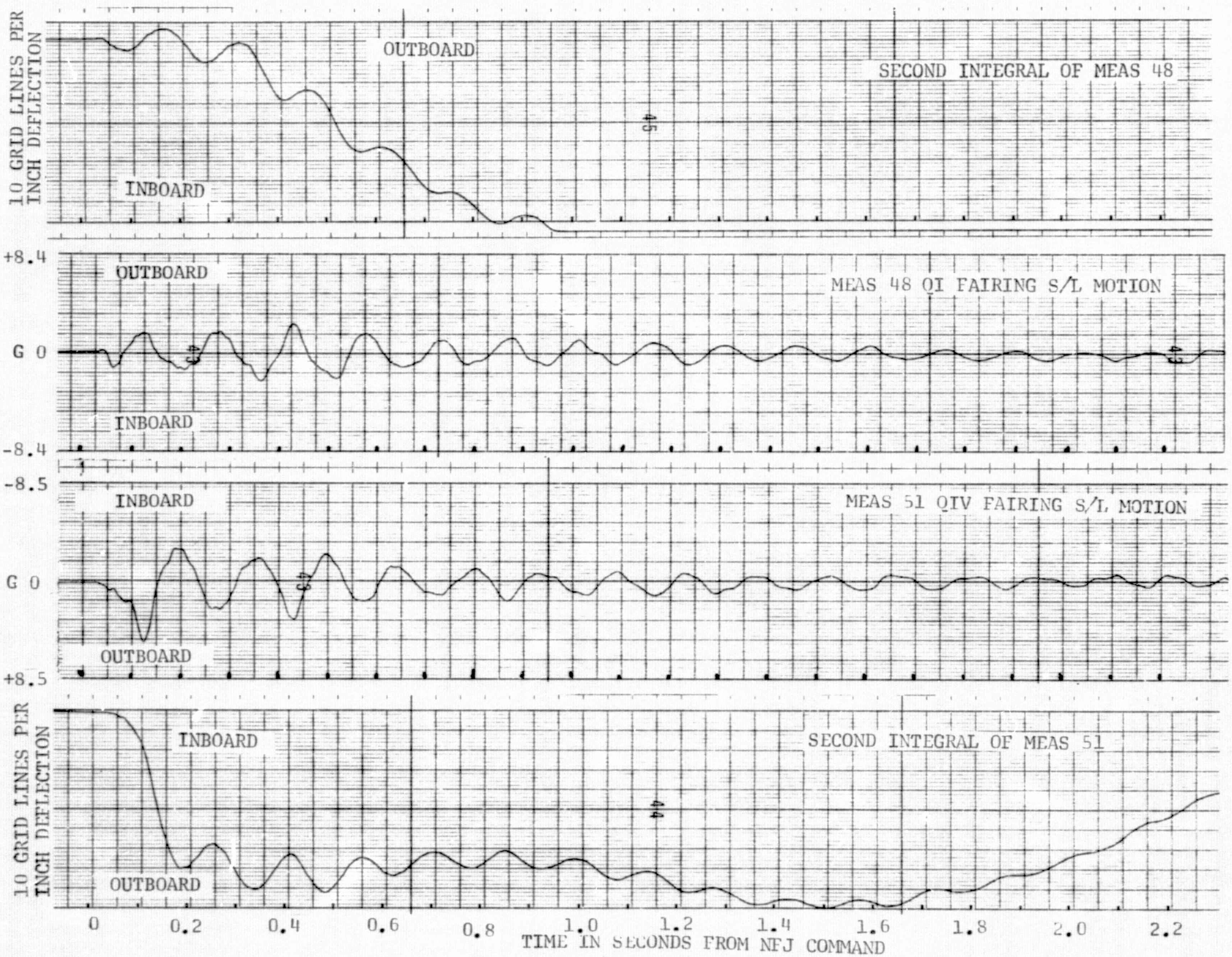

FIGURE 33 QUAD I/IV FAIRING MOTION - TEST 1

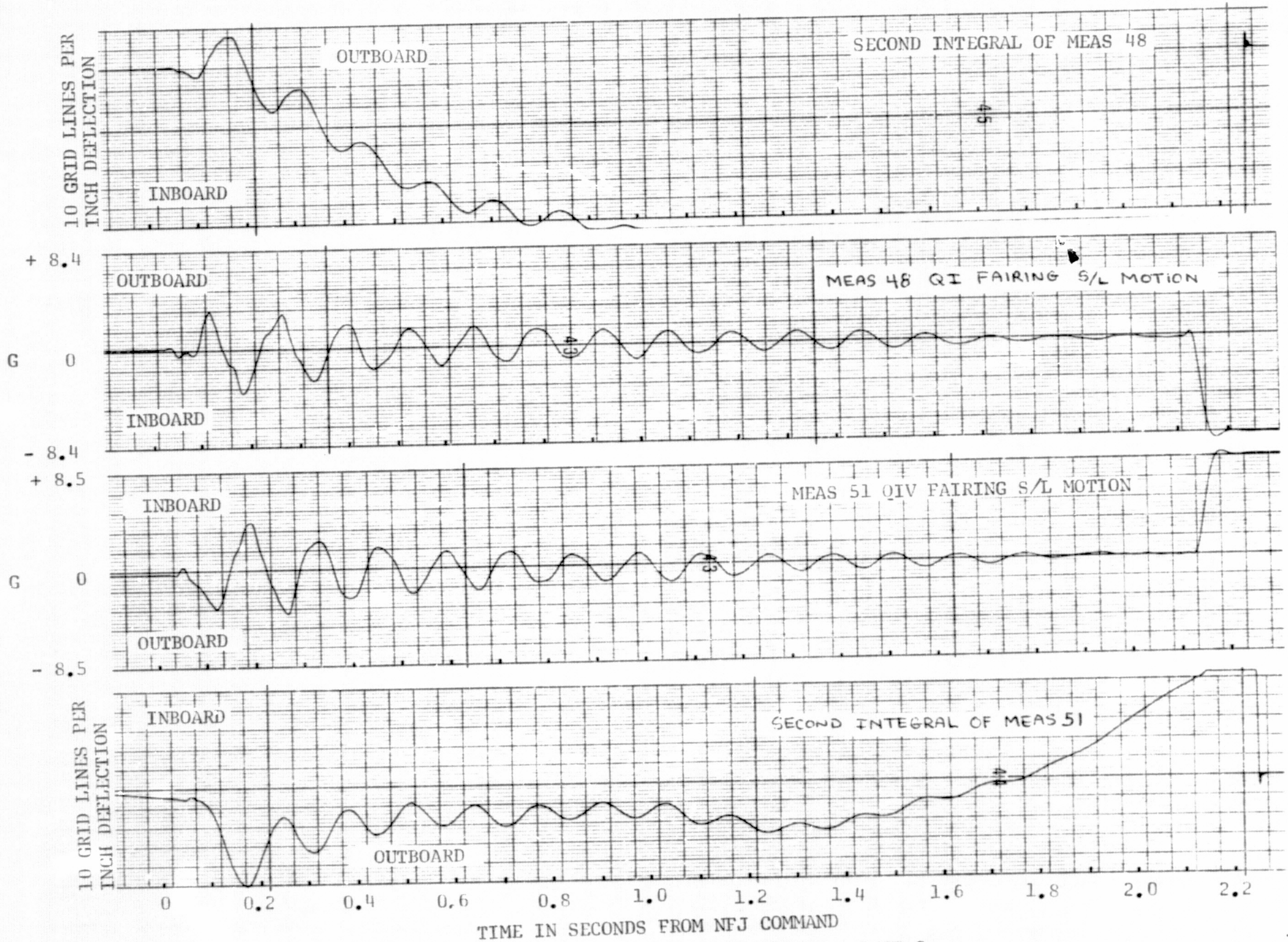

FIGURE 34. QUAD I/IV FAIRING MOTION - TEST 3

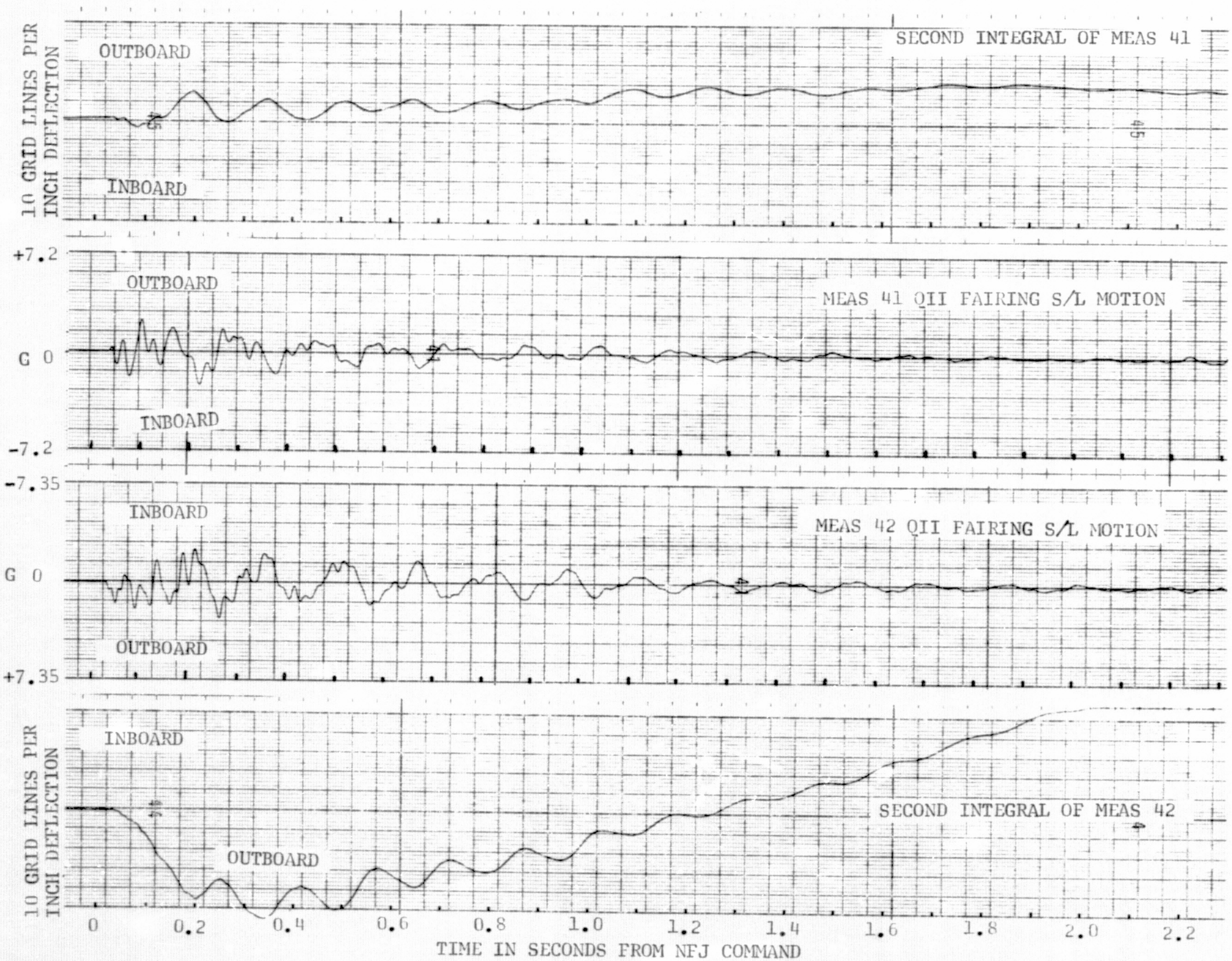

FIGURE 35 QUAD II/III FAIRING MOTION - TEST 1

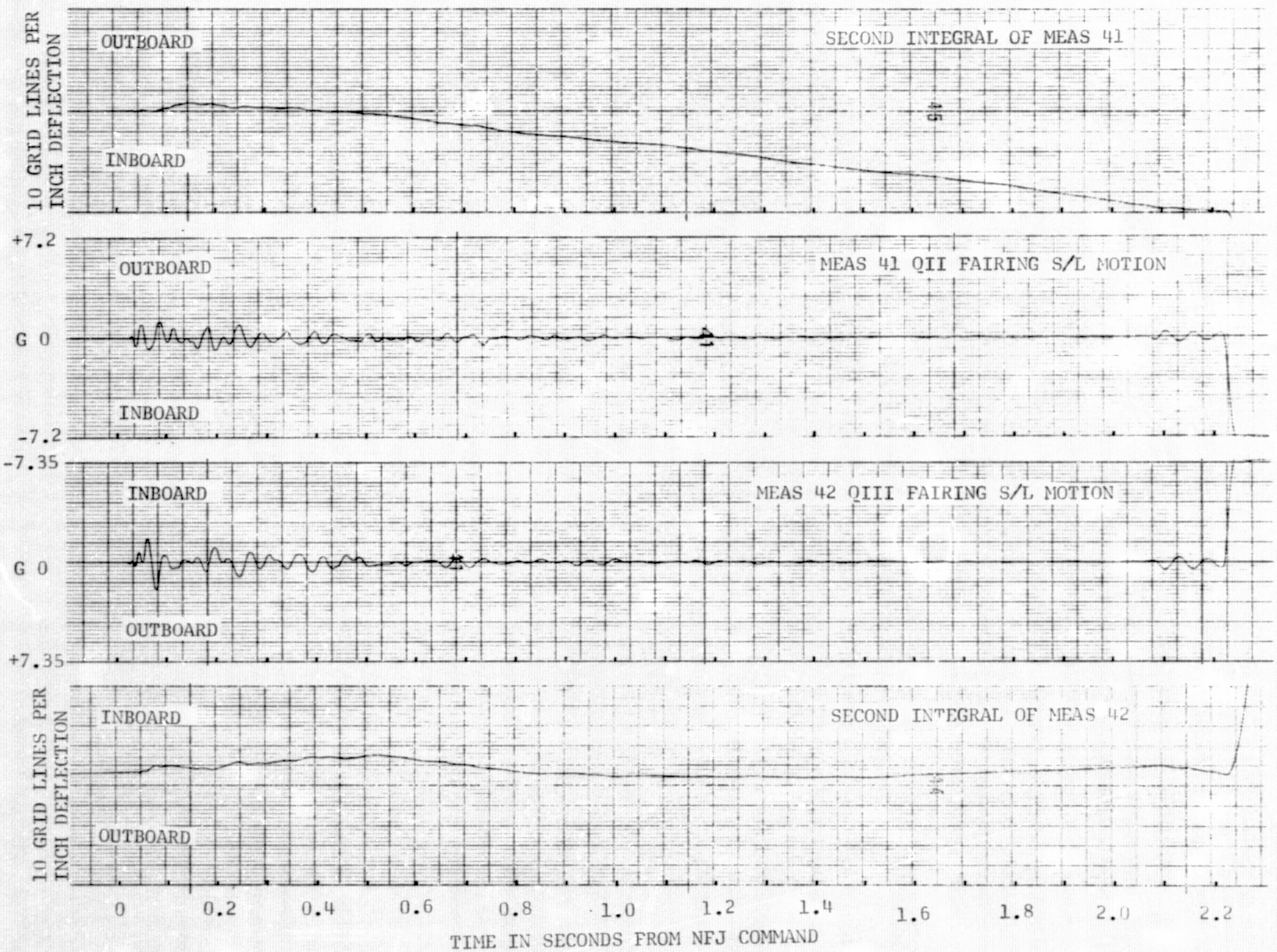

FIGURE 36 QUAD II/III FAIRING MOTION - TEST 3

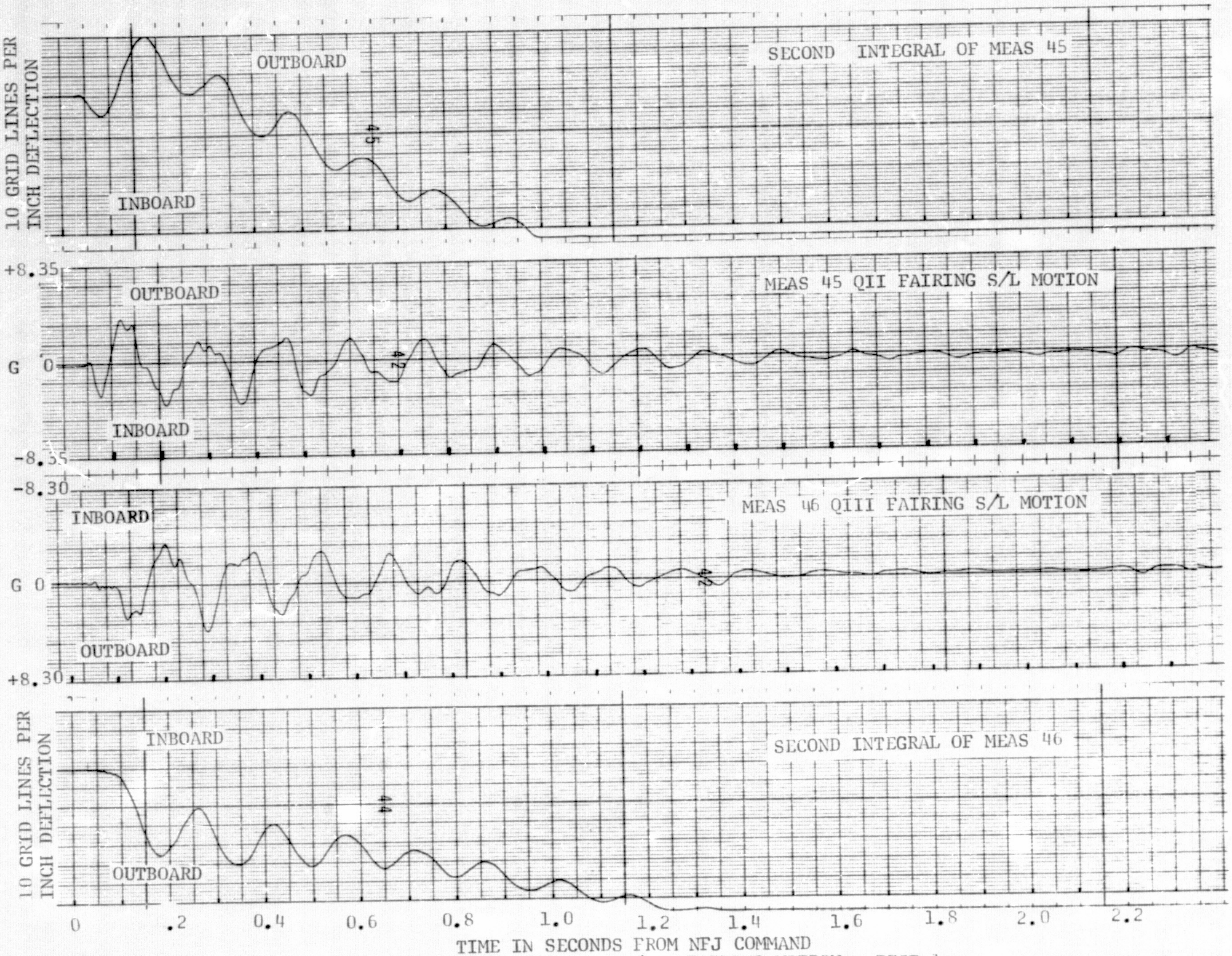

FIGURE 37 QUAD II/III FAIRING MOTION - TEST 1

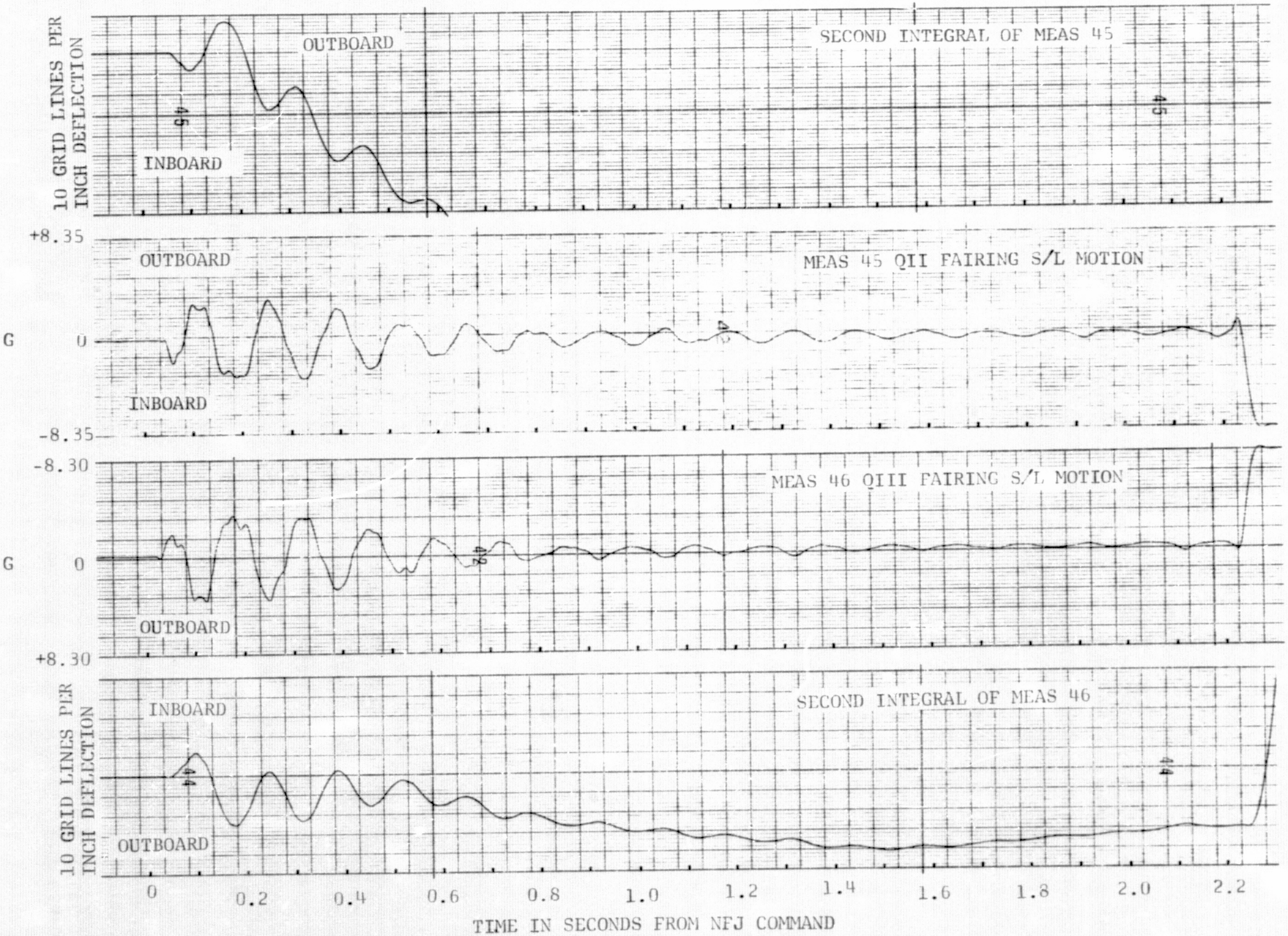

FIGURE 38 QUAD II/III FAIRING MOTION - TEST 3

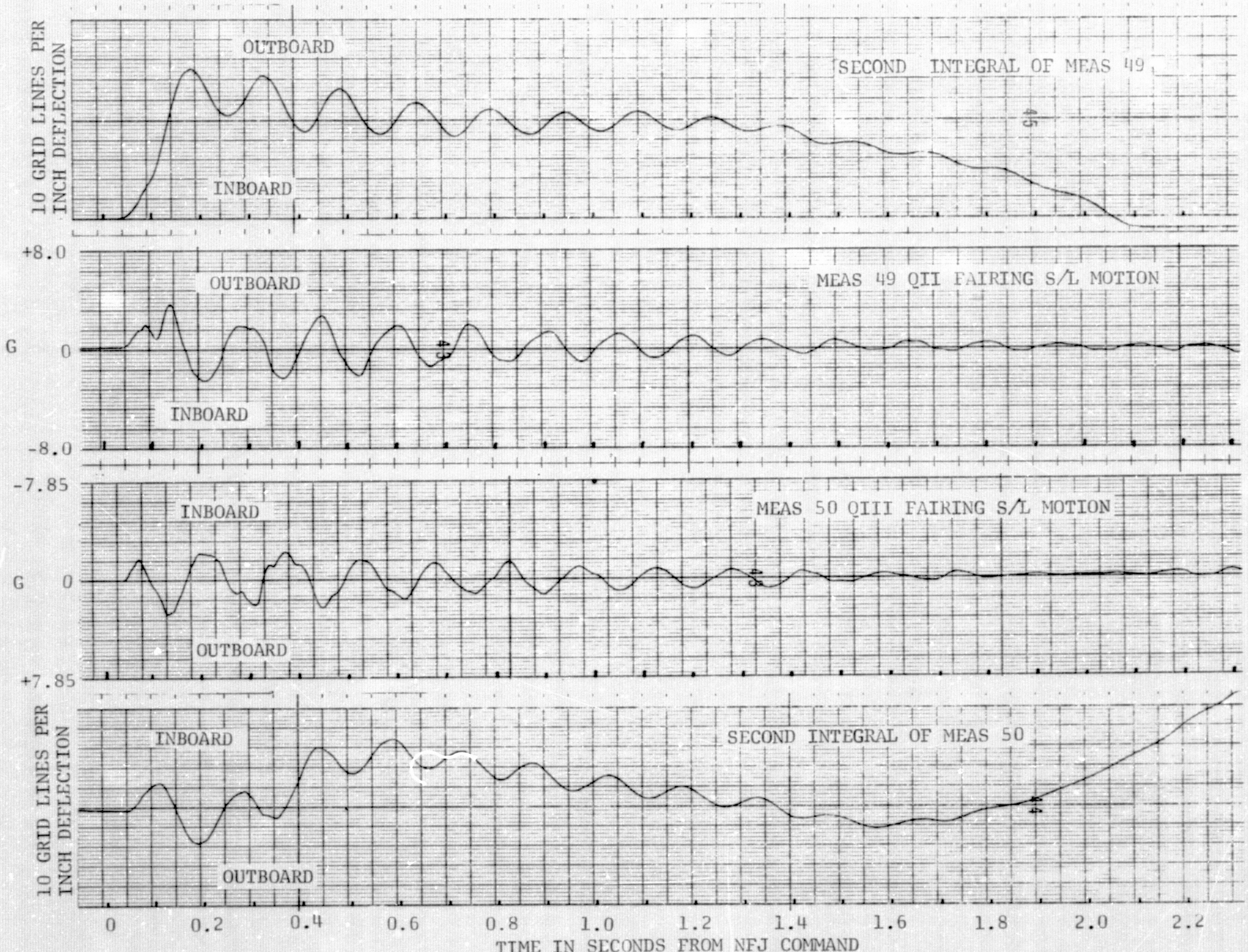

FIGURE 39 QUAD II/III FAIRING MOTION - TEST 1

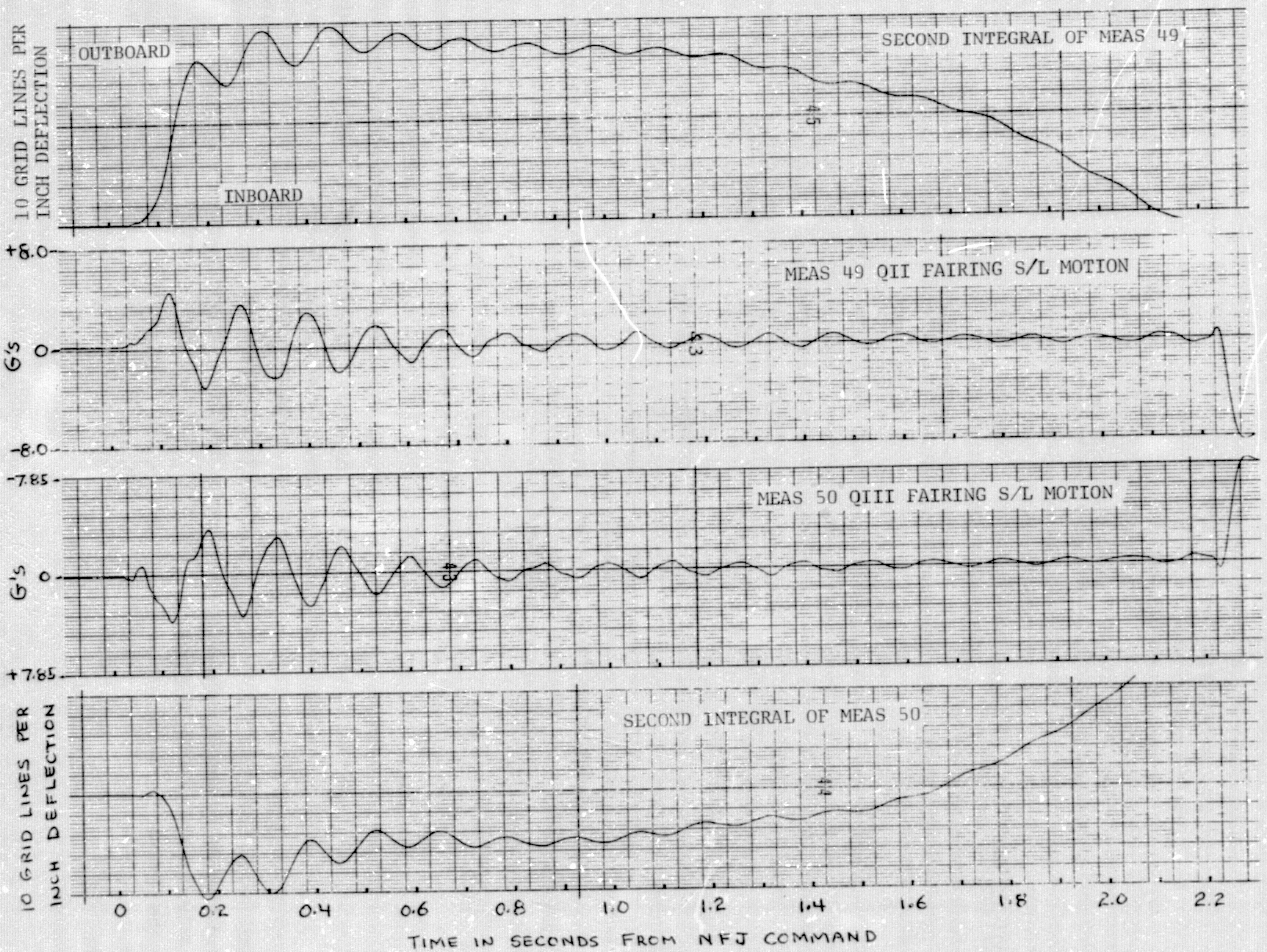

FIGURE 40 QUAD II/III FAIRING MOTION - TEST 3

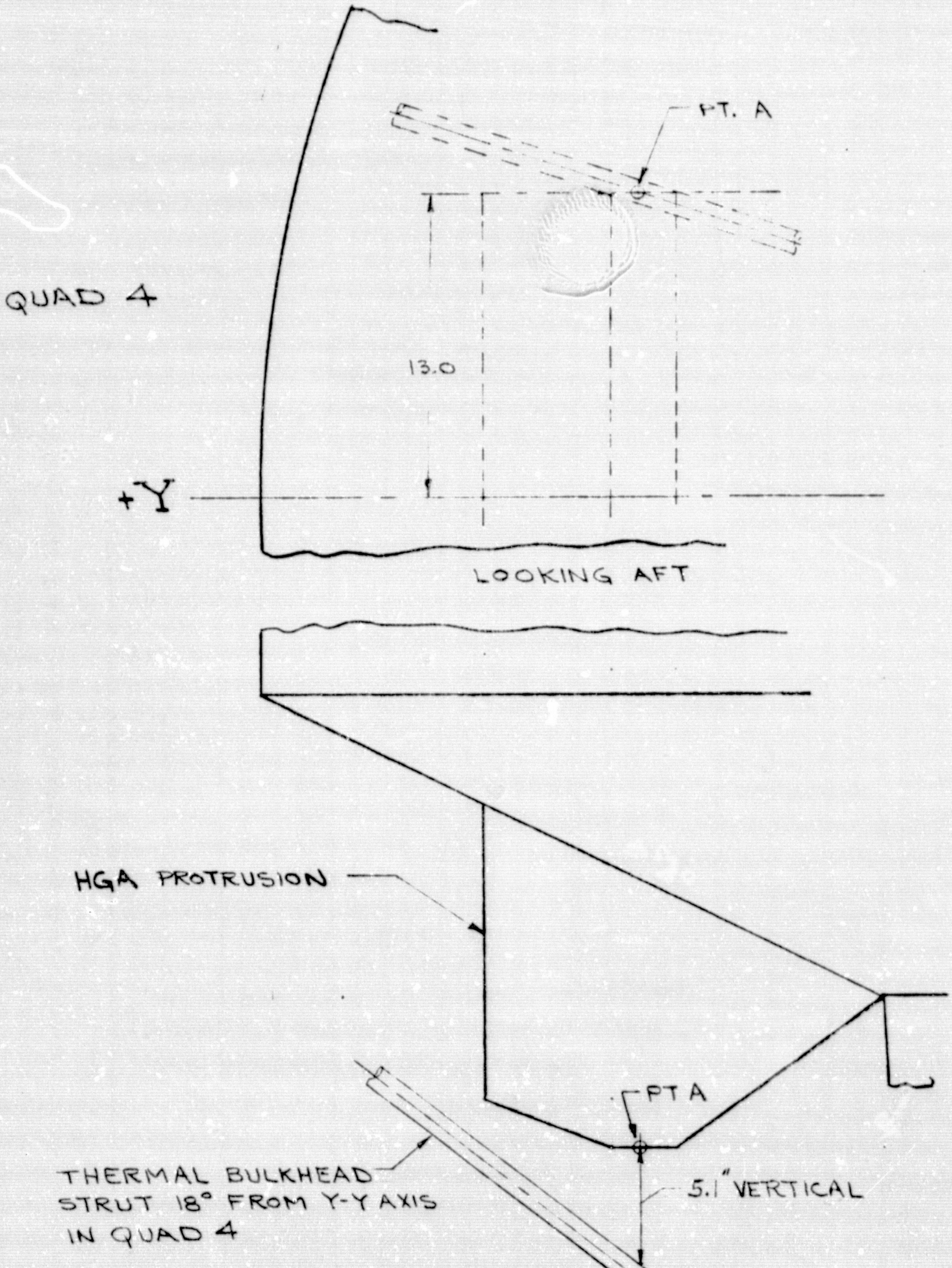

STATIC CLEARANCE (MVM)

FIGURE 41

QUAD 1 (AS SHOWN)

ROTATION ANGLE	HORIZONTAL MEASUREMENTS
0°-00'	5.25" (PT. A)
8°-29'	5.44" (PT. B)

QUAD 4 (SAME AS QUAD 1 EXCEPT OPPOSITE HAND)

ROTATION ANGLE	HORIZONTAL MEASUREMENTS
0°-00'	5.0" (PT. A)
8°-29'	4.8" (PT. B)

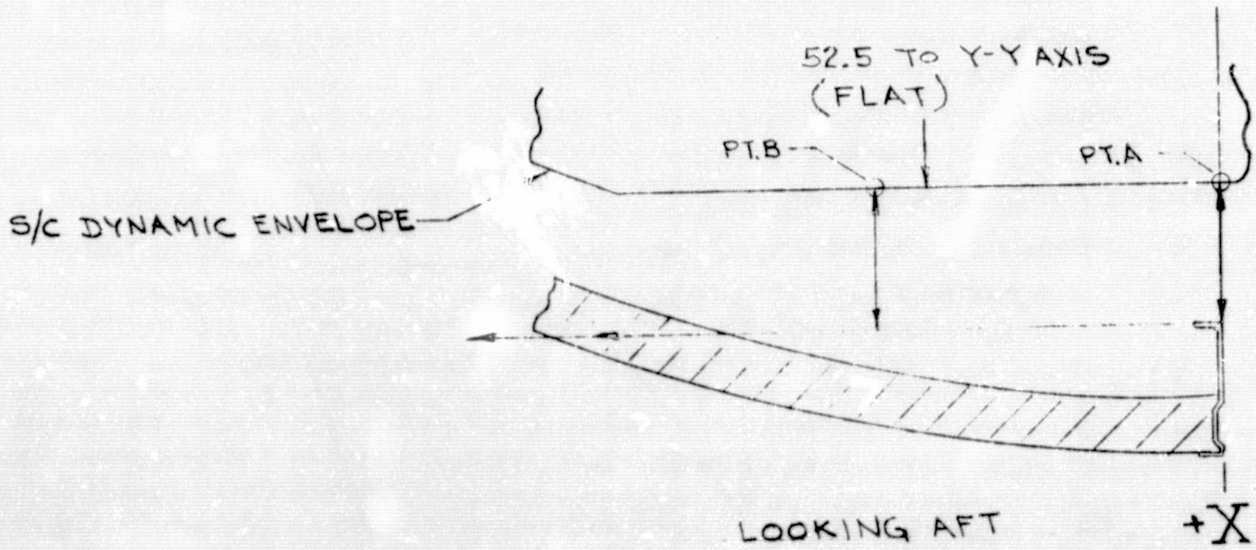

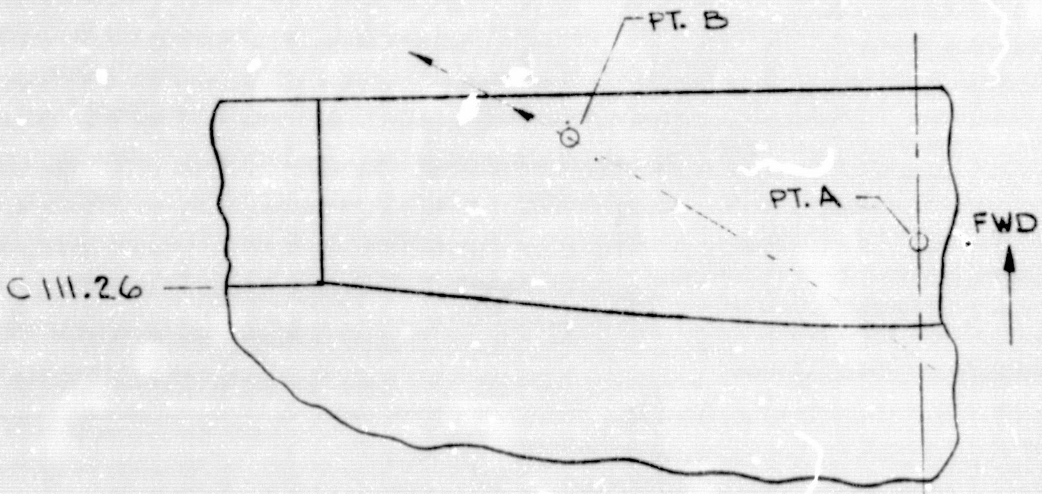

N/F LONGERON CLEARANCE WITH AFT FLAT OF DYNAMIC ENVELOPE

MVM STATIC ROTATION TEST

FIGURE 42

QUAD 1 (AS SHOWN)

ROTATION ANGLE	HORIZONTAL MEASUREMENT
0°-00'	5.4" (PT.A)
2°-57'	5.4" (PT.B)

QUAD 4 (SAME AS QUAD 1 EXCEPT OPPOSITE HAND)

ROTATION ANGLE	HORIZONTAL MEASUREMENT
0°-00'	5.0" (PT.A)
2°-57'	4.6" (PT.B)

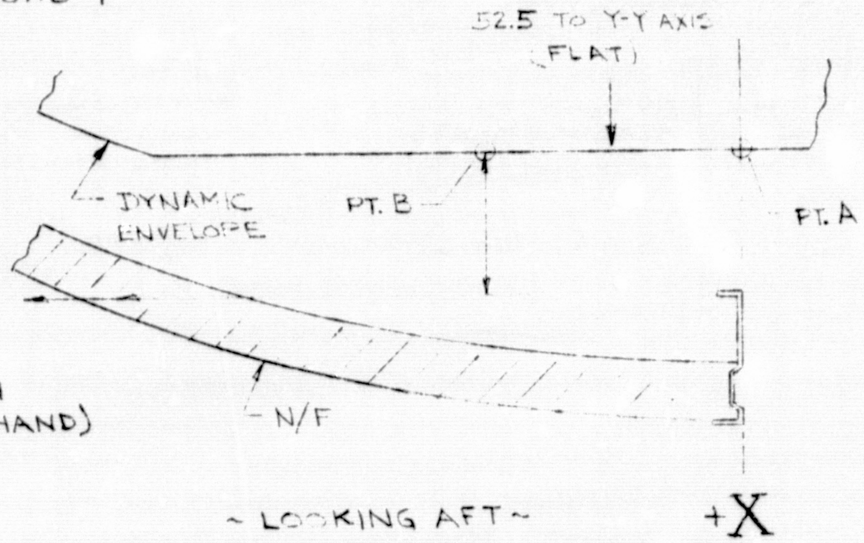

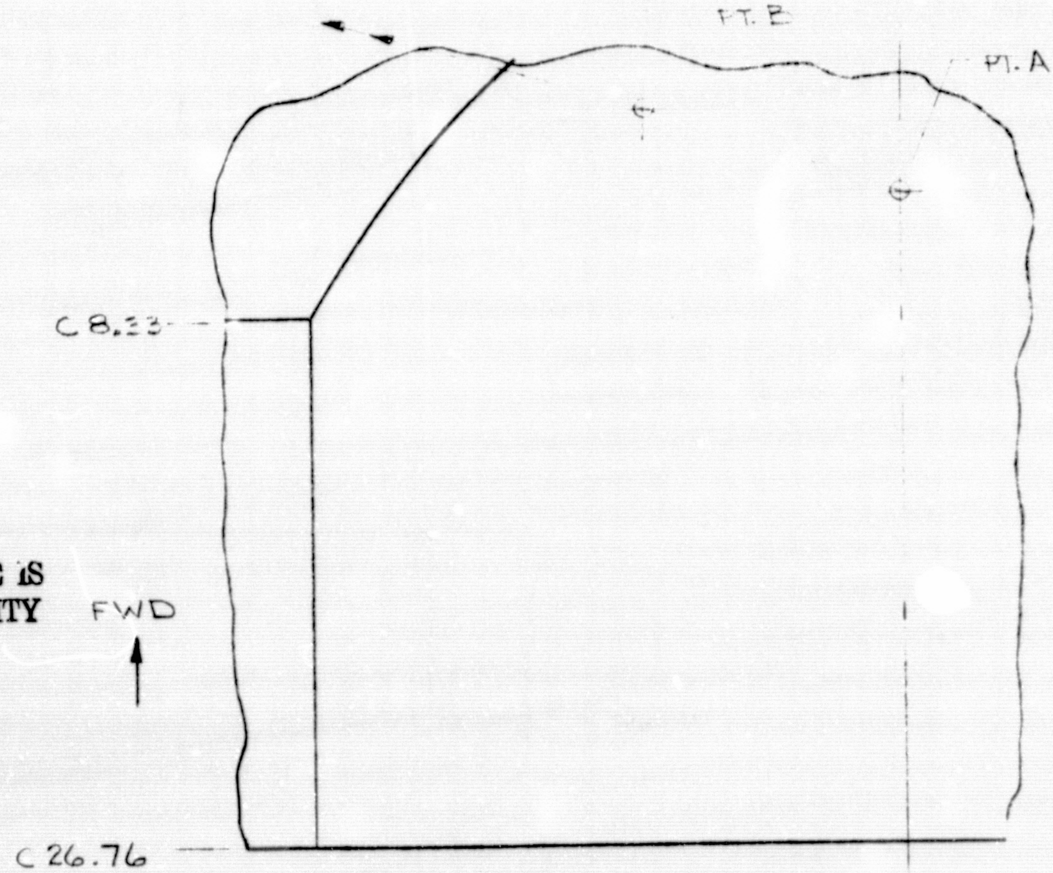

N/F LONGERON CLEARANCE WITH FORWARD FLAT OF DYNAMIC ENVELOPE

MVM STATIC ROTATION TEST

FIGURE 43 (MVM)

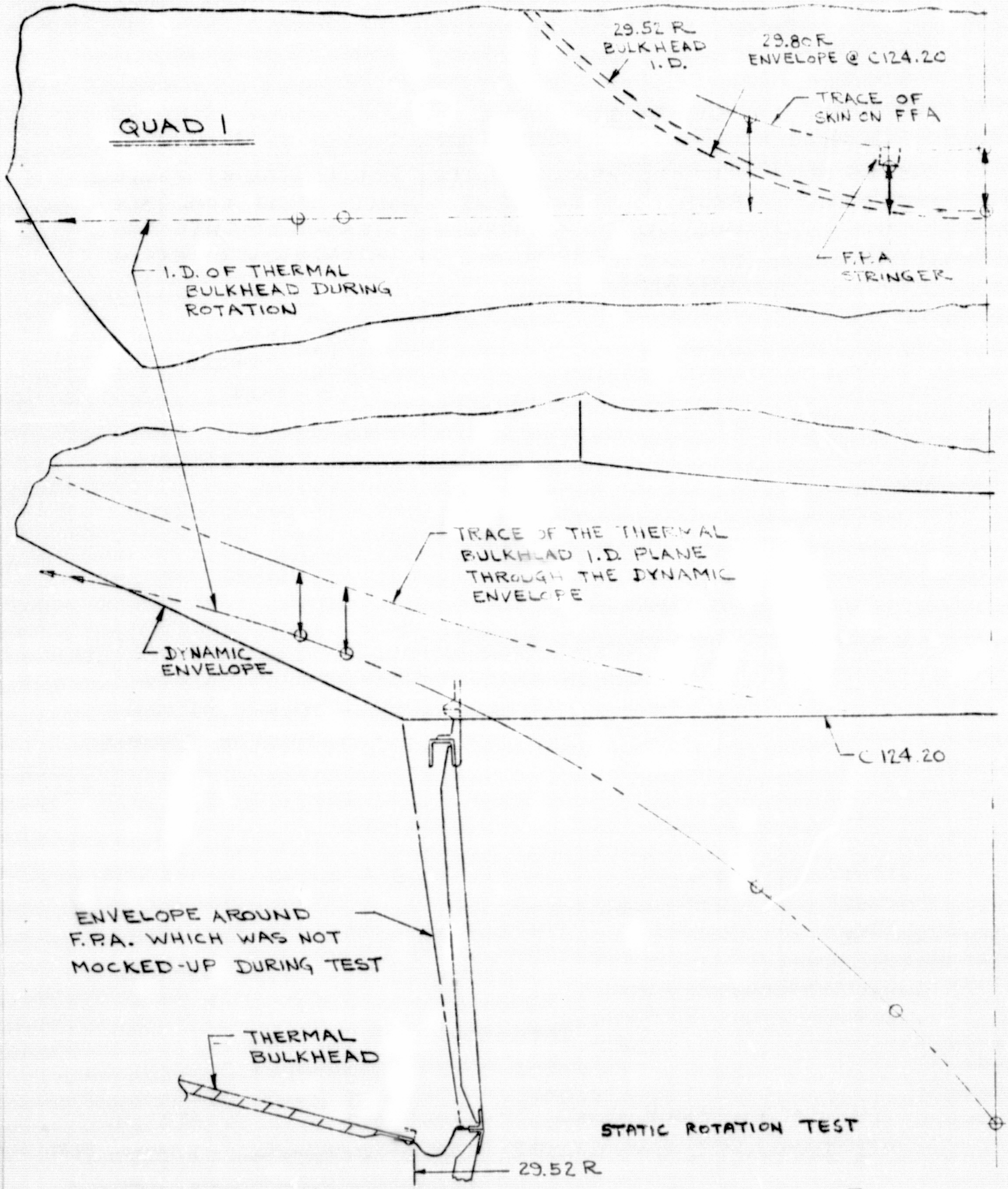

THERMAL BULKHEAD SPLIT LINE I.D. TO ENVELOPE

FIGURE 44 (MVM)

QUAD 1

ANGLES OF ROTATION	VERTICAL MEASUREMENTS FROM BULKHEAD SPLIT LINE I.D. TO CONICAL SECTION OF DYNAMIC ENVELOPE	HORIZONTAL & PARALLEL WITH SPLIT LINE (X-X AXIS) MEASUREMENTS TO F.P.A. SKIN OR STRINGER
0°-00'		3.3" SKIN
5°-42'		2.6" STRINGER
13°-37'		5.9" SKIN
29°-02'	3.5"	

QUAD 4

ANGLES OF ROTATION	VERTICAL MEASUREMENTS FROM BULKHEAD SPLIT LINE I.D. TO CONICAL SECTION OF DYNAMIC ENVELOPE	HORIZONTAL & PARALLEL WITH SPLIT LINE (X-X AXIS) MEASUREMENTS TO F.P.A. SKIN OR STRINGER
0°-00'		3.24" SKIN
5°-42'		2.4" STRINGER
12°-37'		5.5" SKIN
29°-02'	3.0"	
31°-52'	3.0"	

THERMAL BULKHEAD SPLIT LINE I.D. TO DYNAMIC ENVELOPE CLEARANCES — STATIC ROTATION TEST

FIGURE 45 (MVM) SEE FIGURE 44

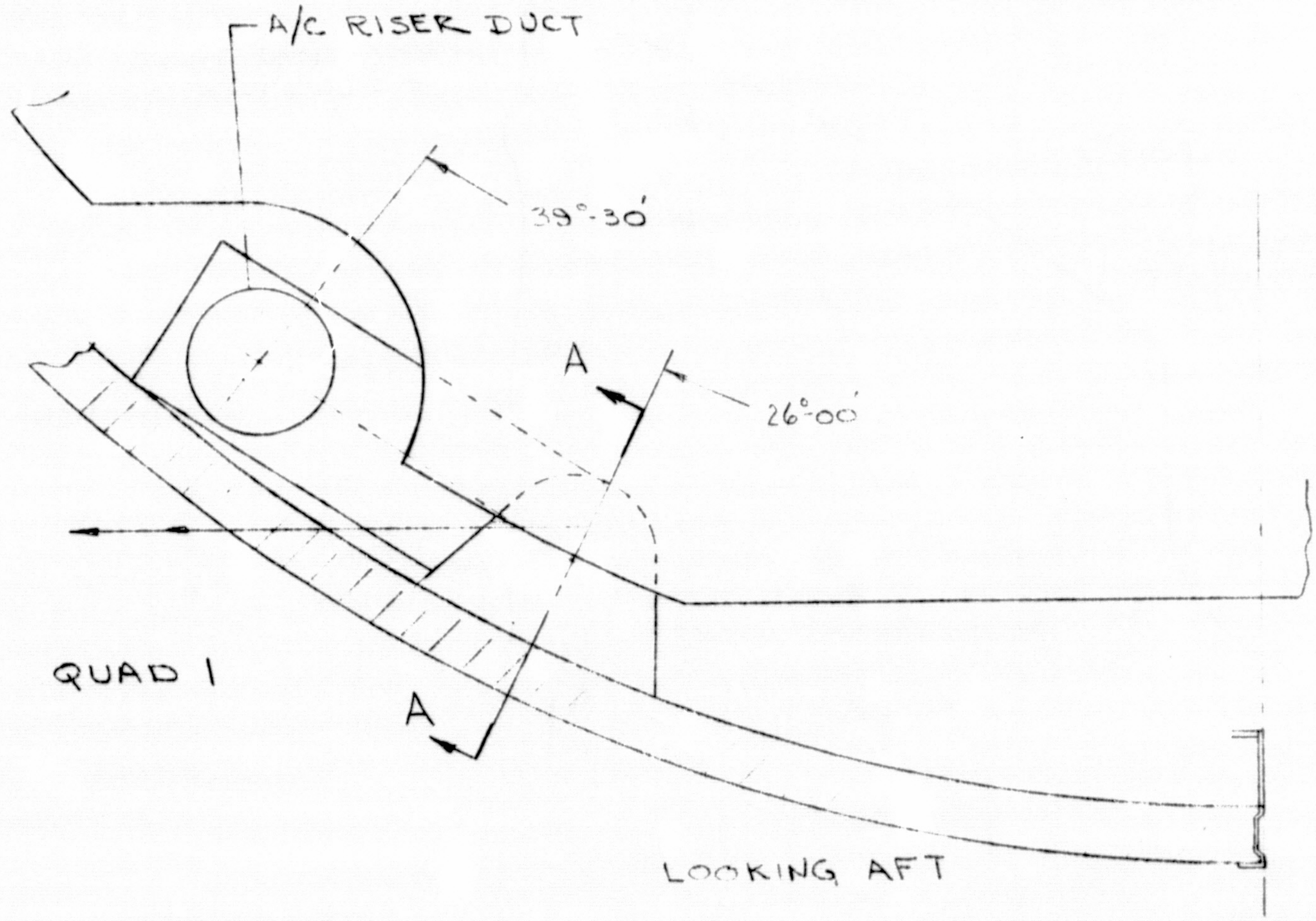

ROTATION ANGLE	MEASUREMENT
0°-00'	1.3" VERT.
1°-54'	.8" VERT.
2°-57'	.7" VERT
3°-27'	.7" NORMAL

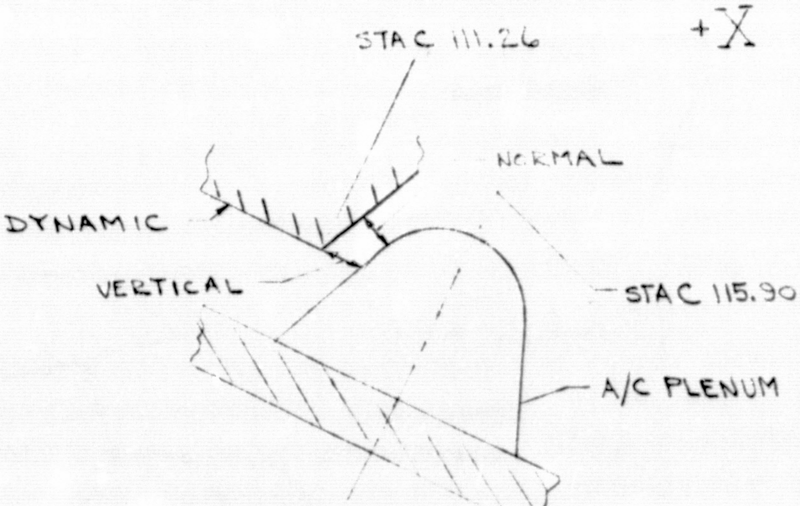

STATIC ROTATION TEST

SECTION A-A

NOSE FAIRING A/C INLET PLENUM
CLEARANCE WITH DYNAMIC ENVELOPE

FIGURE 46 (MVM)

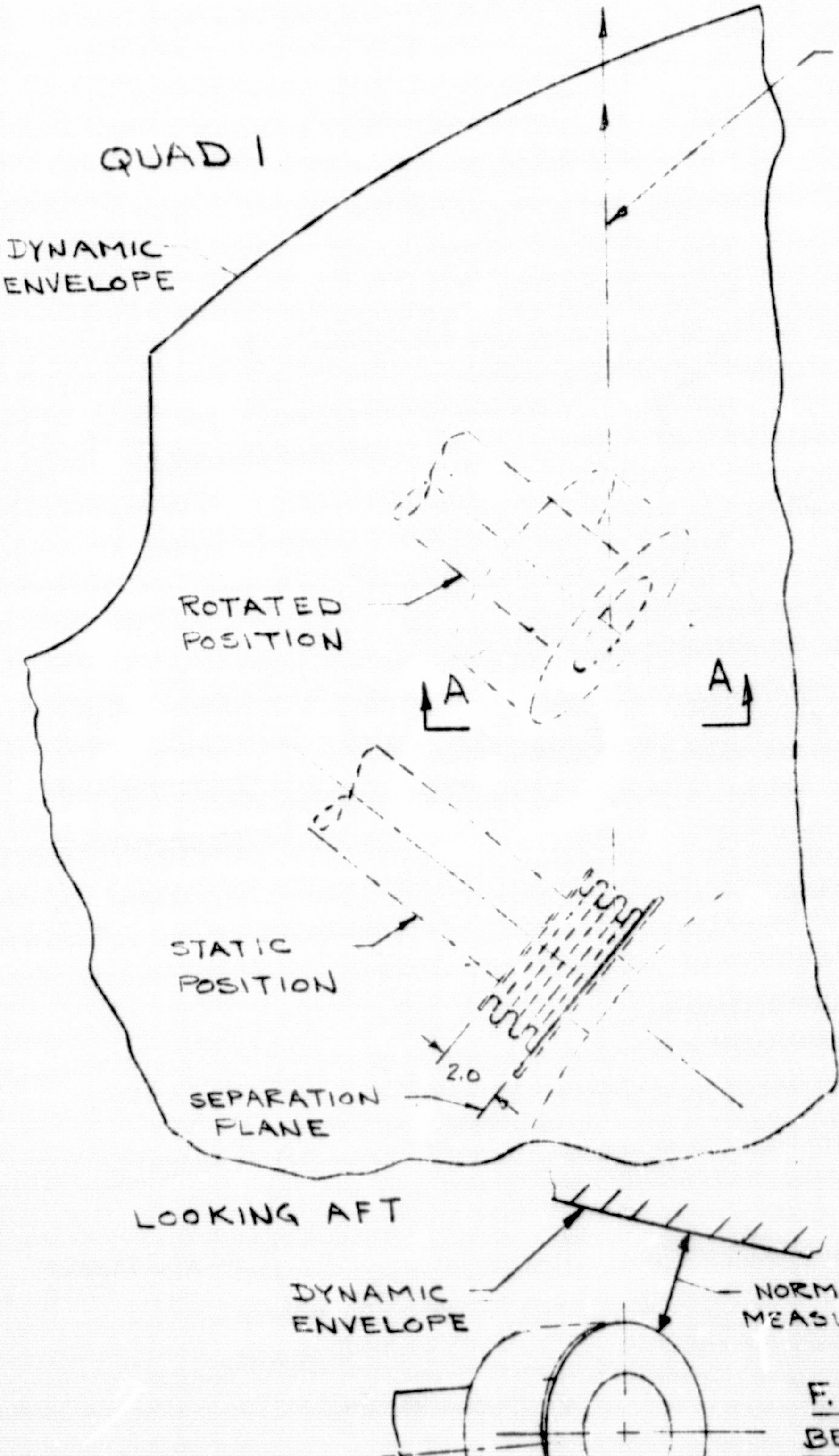

ROTATION ANGLE	NORMAL MEASUREMENT
7°-17'	5.1"
12°-37'	4.5"
18°-49'	4.5"

F.P.A. AIR CONDITIONING BELLOWS CLEARANCE

STATIC ROTATION TEST

FIGURE 47 (MJM)

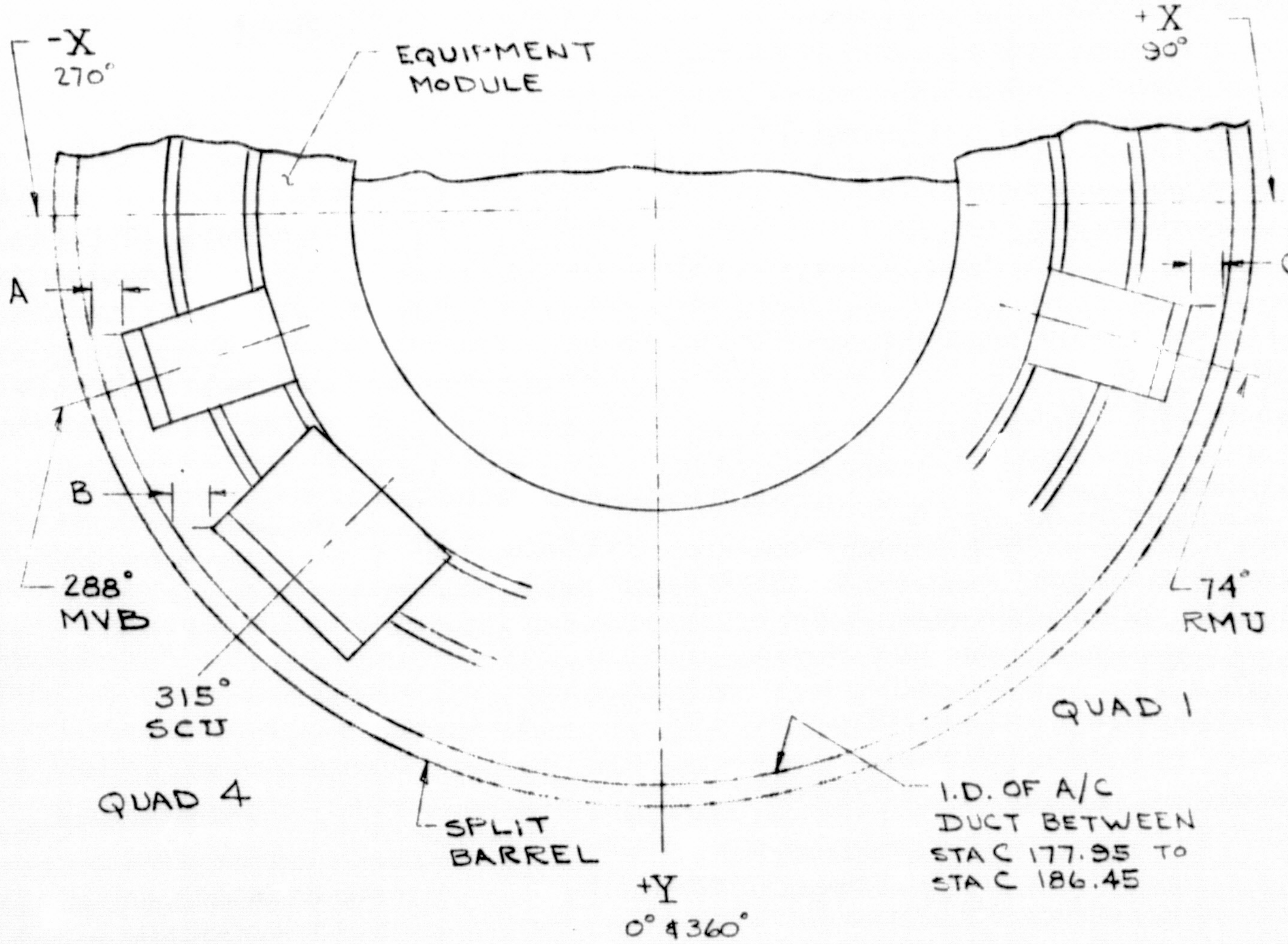

MVB PACKAGE

ROTATION ANGLE	A
4°-32'	2.3"

SCU PACKAGE

ROTATION ANGLE	B
4°-52'	2.8"

RMU PACKAGE

ROTATION ANGLE	C
3° 44'	4.55"

PACKAGE CLEARANCES STATIC ROTATION TEST

FIGURE 48 (MVM)

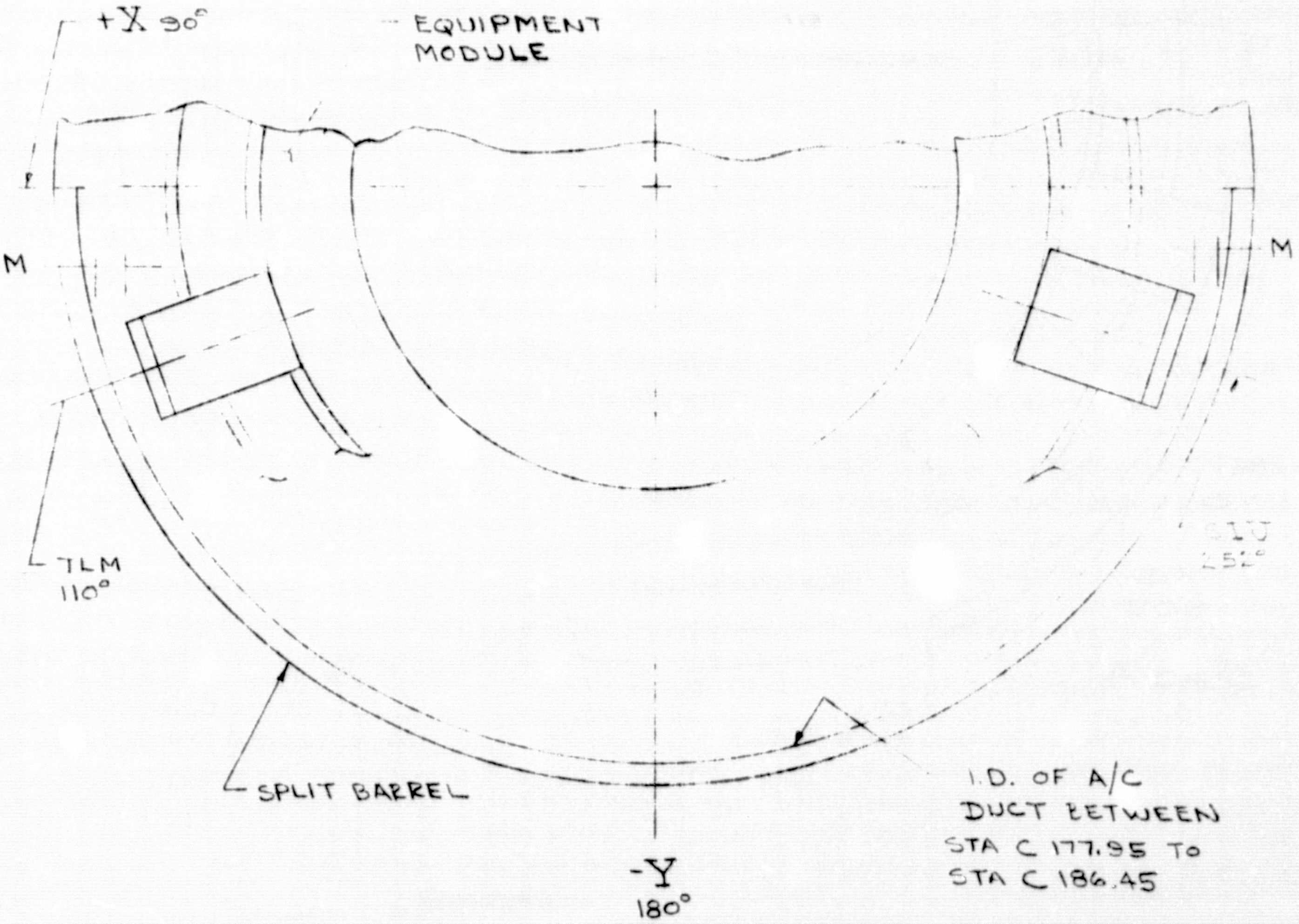

TLM PACKAGE

ROTATION ANGLE	M
1°-55'	2.75"
11°-22'	3.0"

SIU PACKAGE

ROTATION ANGLE	M
1°-55'	2.6"

PACKAGE CLEARANCES STATIC ROTATION TEST

FIGURE 49 (MVM)

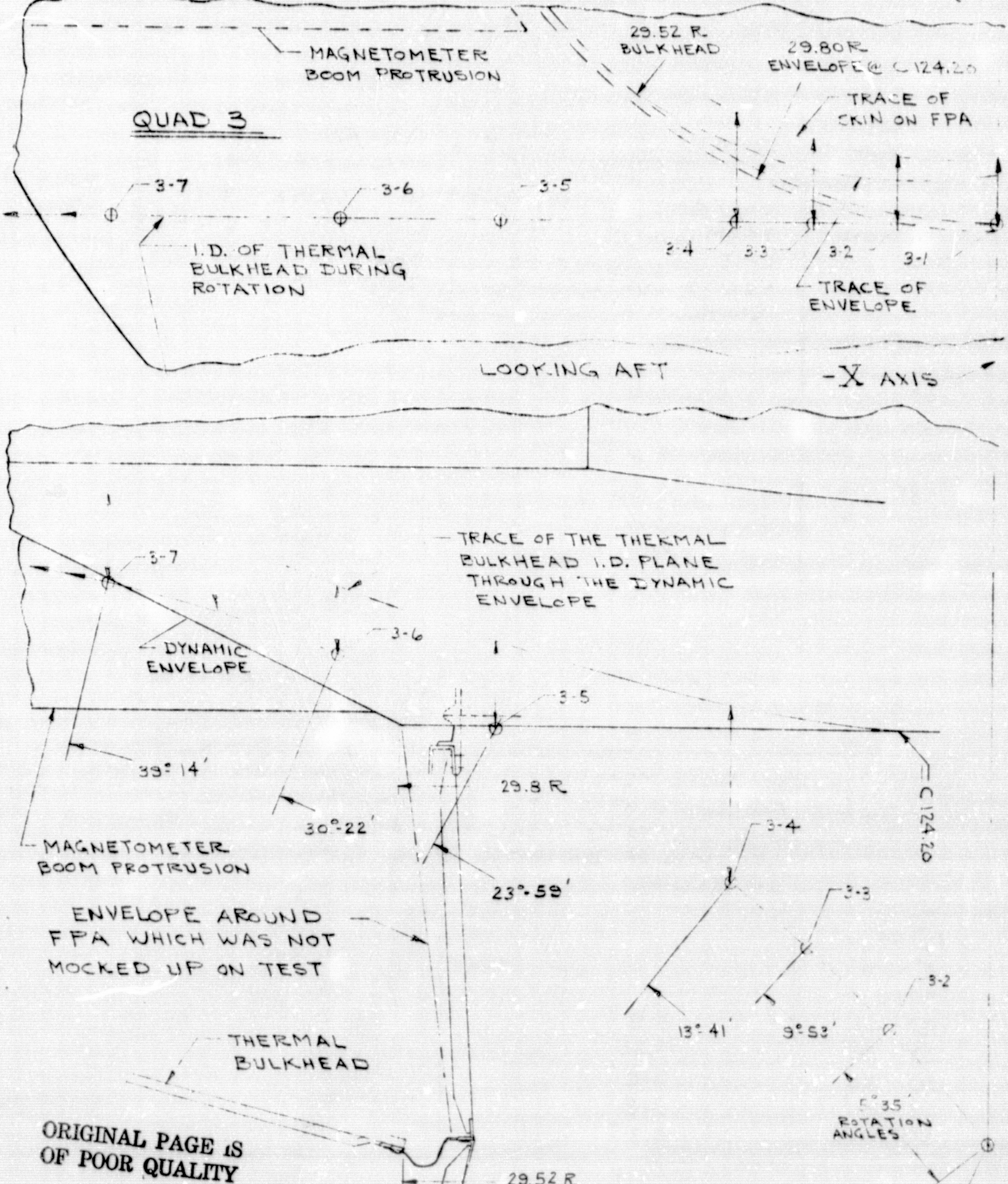

ORIGINAL PAGE IS OF POOR QUALITY

BULKHEAD SPLIT LINE I.D. TO ENVELOPE

FIGURE 50 (MVM) STATIC ROTATION TEST

THERMAL BULKHEAD SPLIT LINE I.D. TO DYNAMIC ENVELOPE CLEARANCES

QUAD 3 ~ SEE FIGURE 50

ANGLES OF ROTATION	VERTICAL MEASUREMENTS FROM BULKHEAD SPLIT LINE I.D. TO CONICAL SECTION OF DYNAMIC ENVELOPE	HORIZONTAL & PARALLEL WITH SPLIT LINE (X-X AXIS) MEASUREMENTS TO F.R.A SKIN
0°-00'		3.25"
5°-35'		3.50"
9°-53'		4.3"
13°-41'	9.0"	5.5"
23°-59'	4.25"	
30°-22'	3.3"	
39°-14'	4.3"	

QUAD 2 ~ SAME AS QUAD 3 FIGURE EXCEPT OPPOSITE HAND

ANGLES OF ROTATION	VERTICAL MEASUREMENTS FROM BULKHEAD SPLIT LINE I.D. TO CONICAL SECTION OF DYNAMIC ENVELOPE	HORIZONTAL & PARALLEL WITH SPLIT LINE (X-X AXIS) MEASUREMENTS TO F.R.A. SKIN
0°-00'		3.25"
5°-35'		3.50"
9°-53'		4.4"
13°-41'	8.9"	5.7"
23°-59'	4.35"	
30°-22'	3.3"	
37°-01'	3.8"	
39°14'	4.2"	

FIGURE 51 (MVM) STATIC ROTATION TEST

QUAD 3 (AS SHOWN)

ROTATION ANGLES	HORIZONTAL MEASUREMENTS
0°-00'	5.1"
3°-03'	5.15"
5°-35'	5.15"
13°-41'	5.2"
*15°-56'	4.5"

QUAD 2 (SAME AS QUAD 3 EXCEPT OPPOSITE HAND)

ROTATION ANGLES	HORIZONTAL MEASUREMENTS
0°-00'	5.25"
3°03'	5.27"
5°-35'	5.32"
13°41'	5.25"
*15°-56'	4.5"

*NOTE:
LONGERON IS DEEPER AT THE AFT END OF N/F

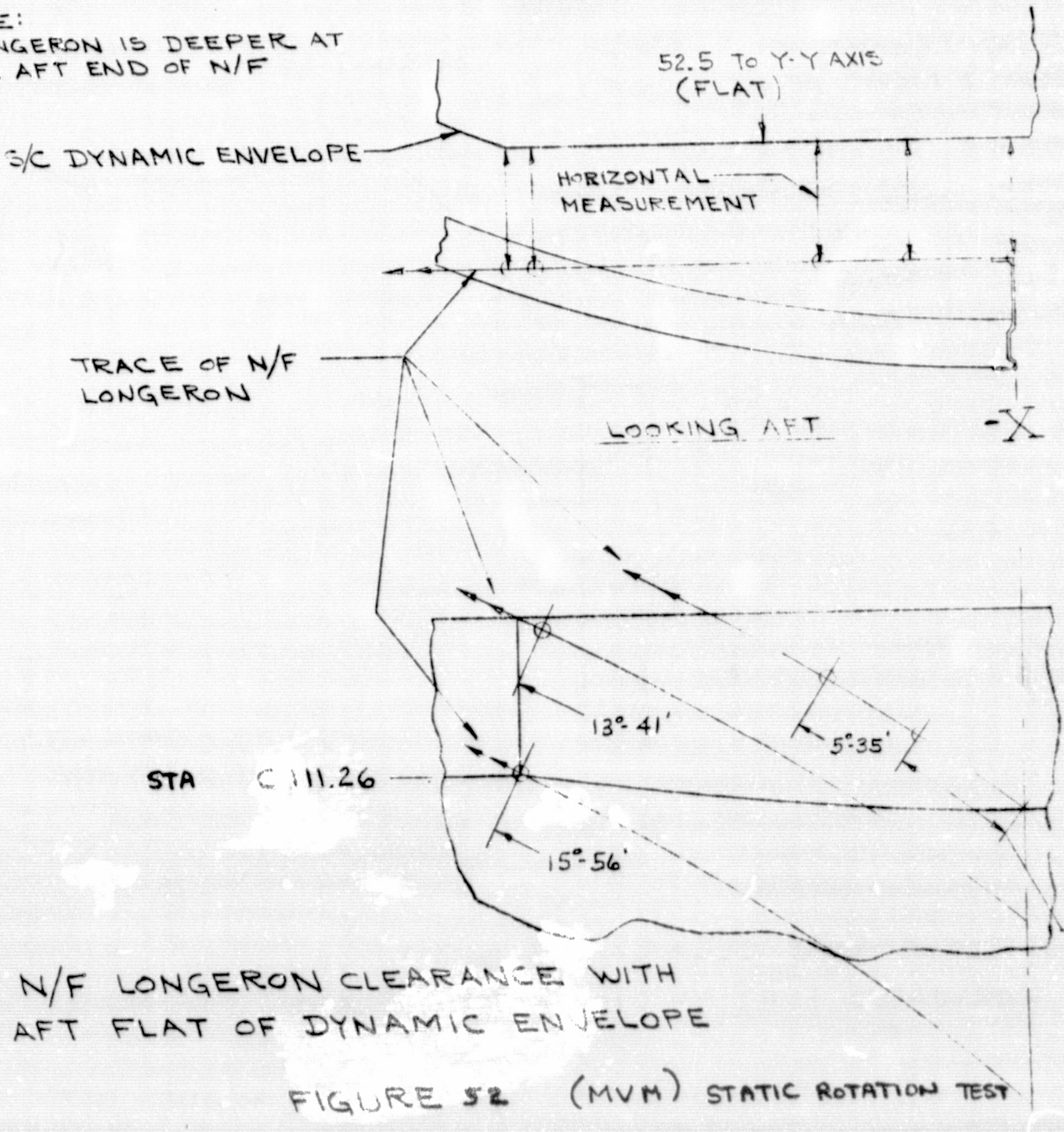

N/F LONGERON CLEARANCE WITH AFT FLAT OF DYNAMIC ENVELOPE

FIGURE 52 (MVM) STATIC ROTATION TEST

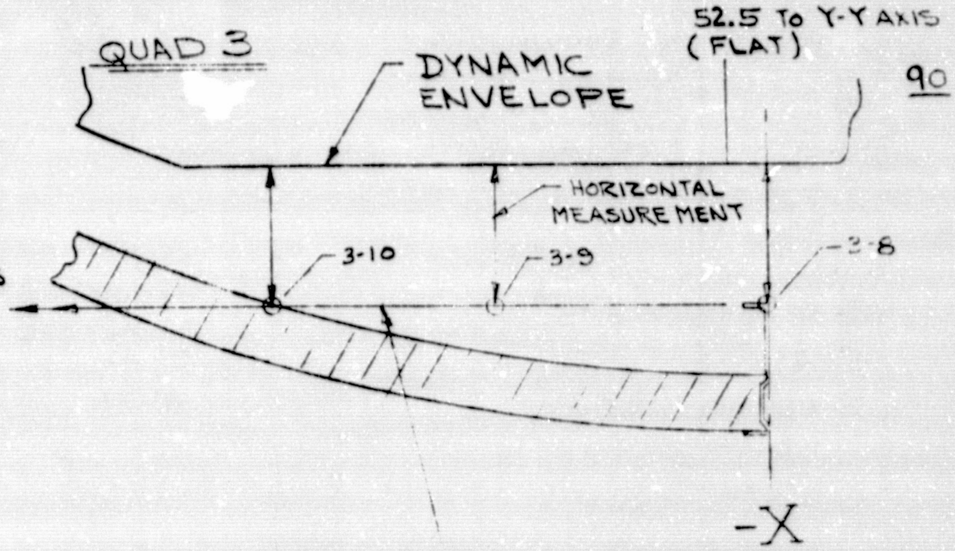

QUAD 3 (AS SHOWN)

ROTATION ANGLES	HORIZONTAL MEASUREMENTS
0°-00'	5.42"
3°-03'	5.46"
5°-35'	5.54"

QUAD 2 (SAME AS QUAD 3 EXCEPT OPPOSITE HAND)

ROTATION ANGLE	HORIZONTAL MEASUREMENTS
0°-00'	5.38"
3°-03'	5.48"
5°-35'	5.36"

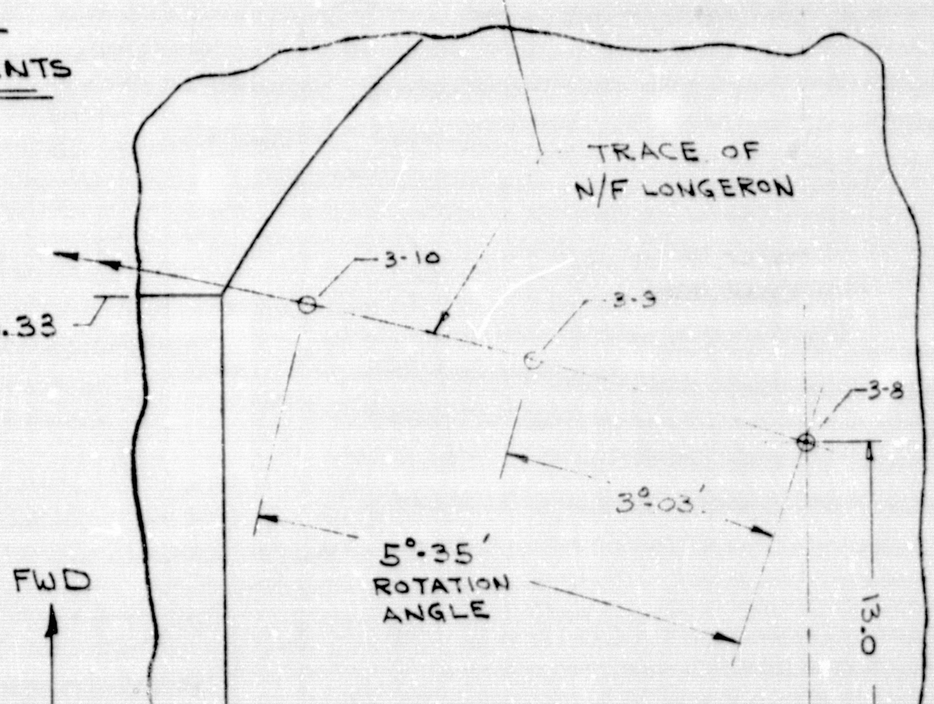

N/F LONGERON CLEARANCE WITH FORWARD FLAT OF DYNAMIC ENVELOPE

FIGURE 53 (MVM) STATIC ROTATION TEST

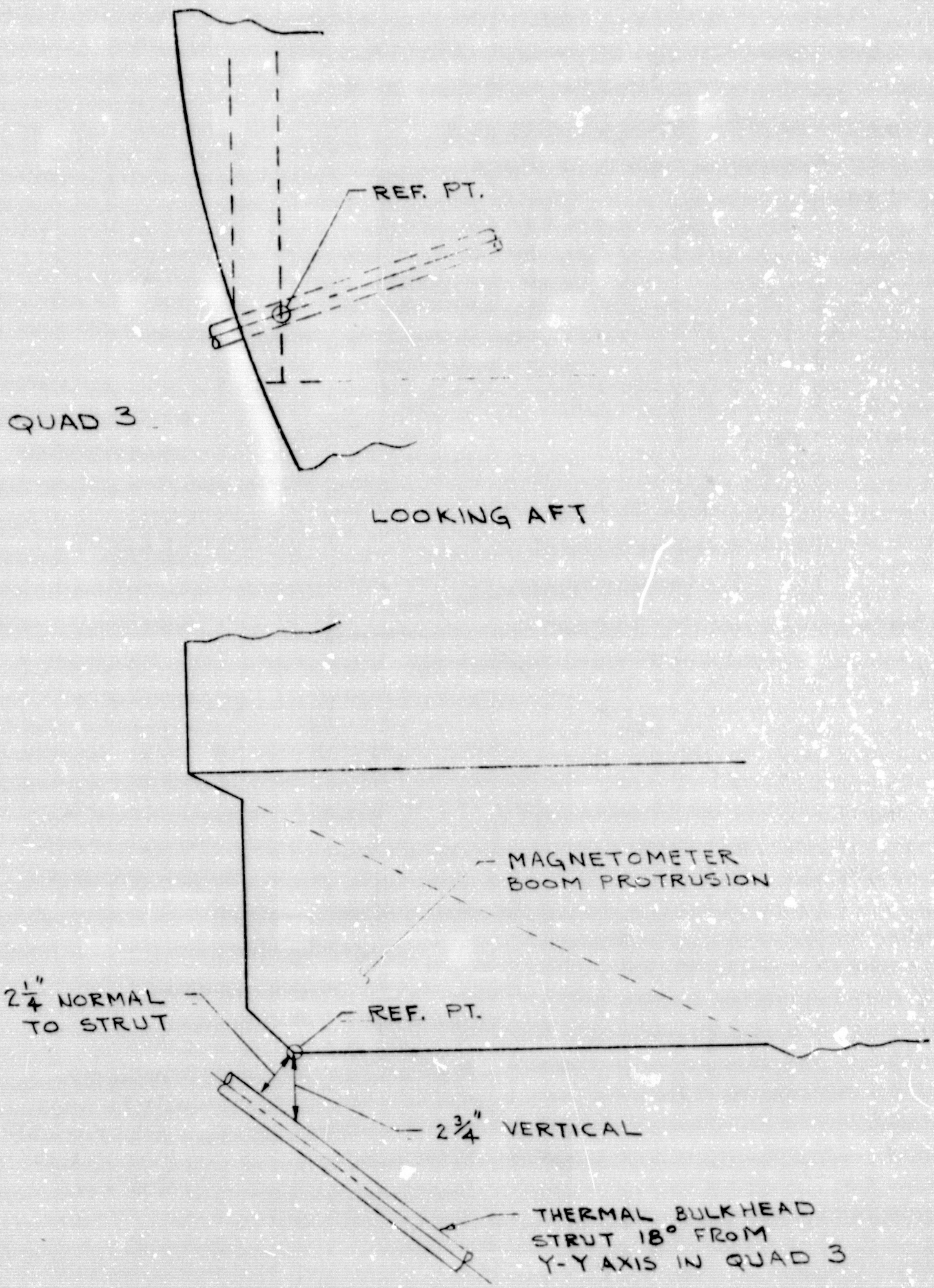

STATIC POSITION CLEARANCES

FIGURE 54 (MVM) STATIC ROTATION TEST

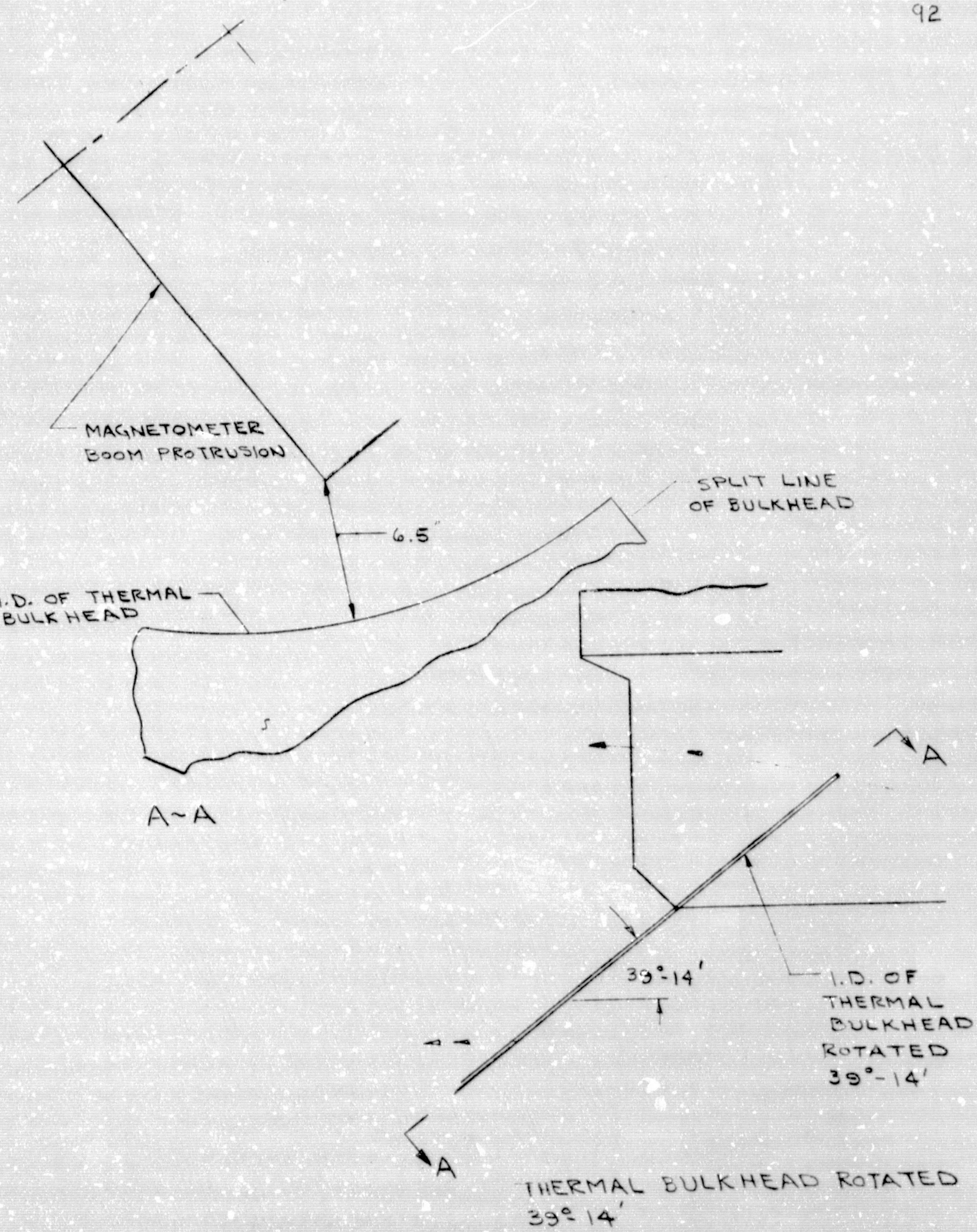

FIGURE 55 (MVM)

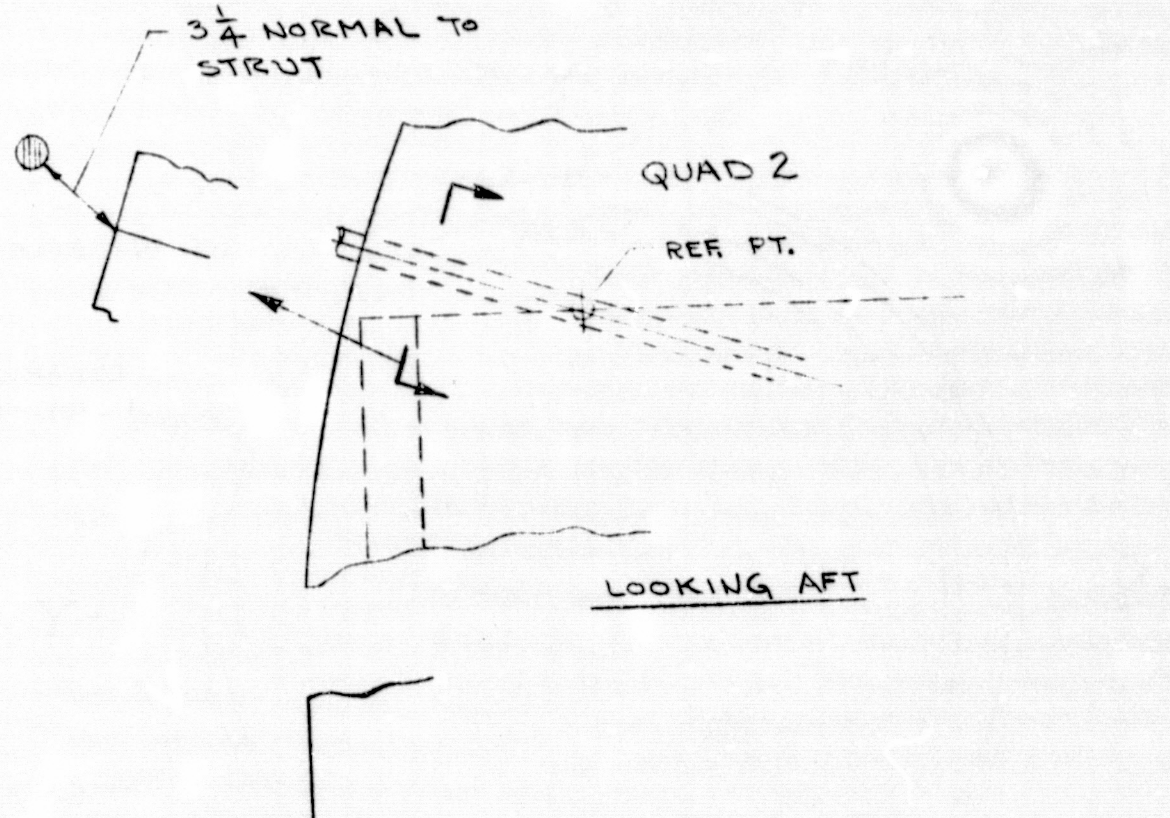

STATIC POSITION CLEARANCES

FIGURE 56 (MVM)

C.2

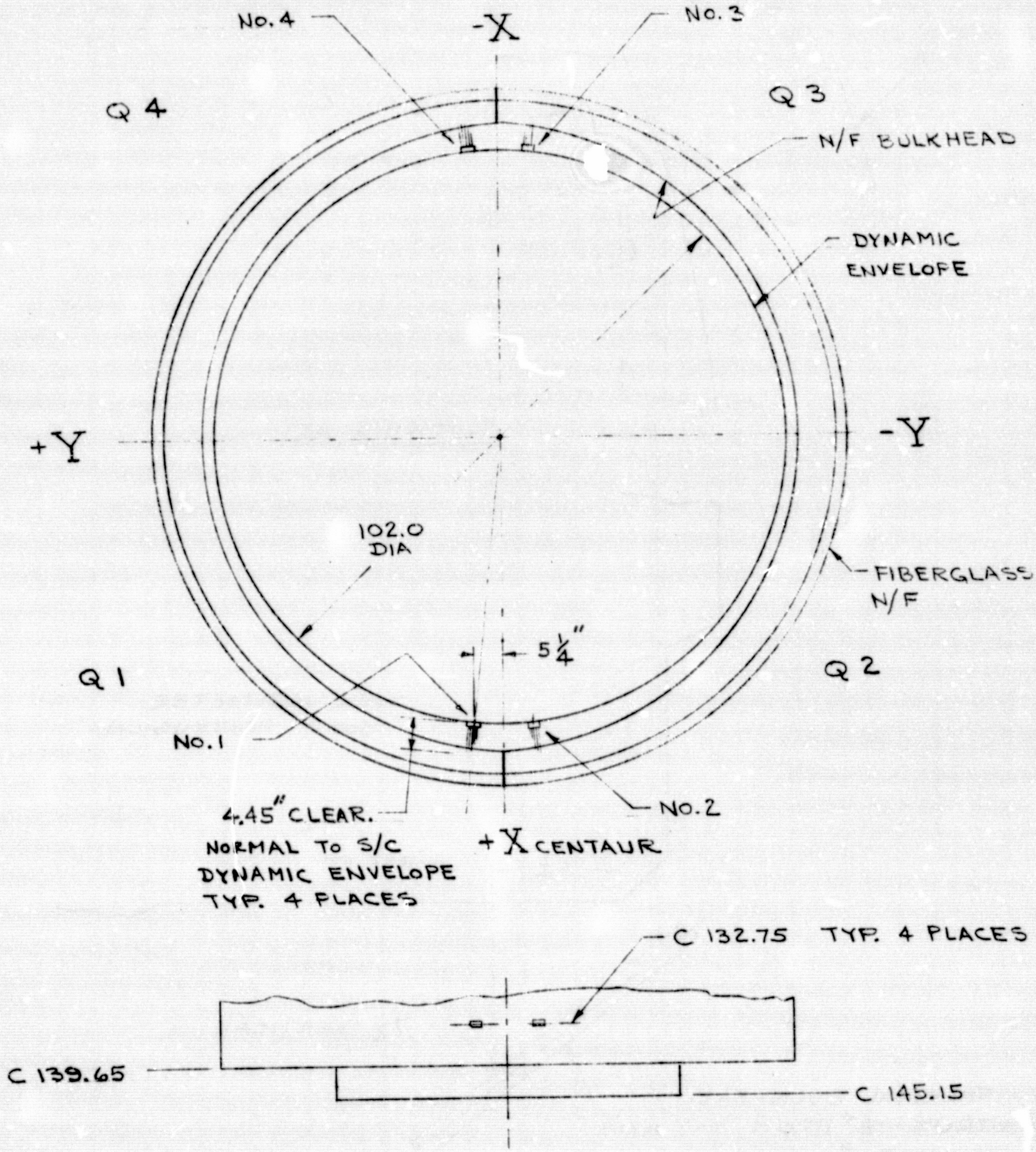

CLEARANCE TO N/F BULKHEAD

FIGURE 57 (TEST #1

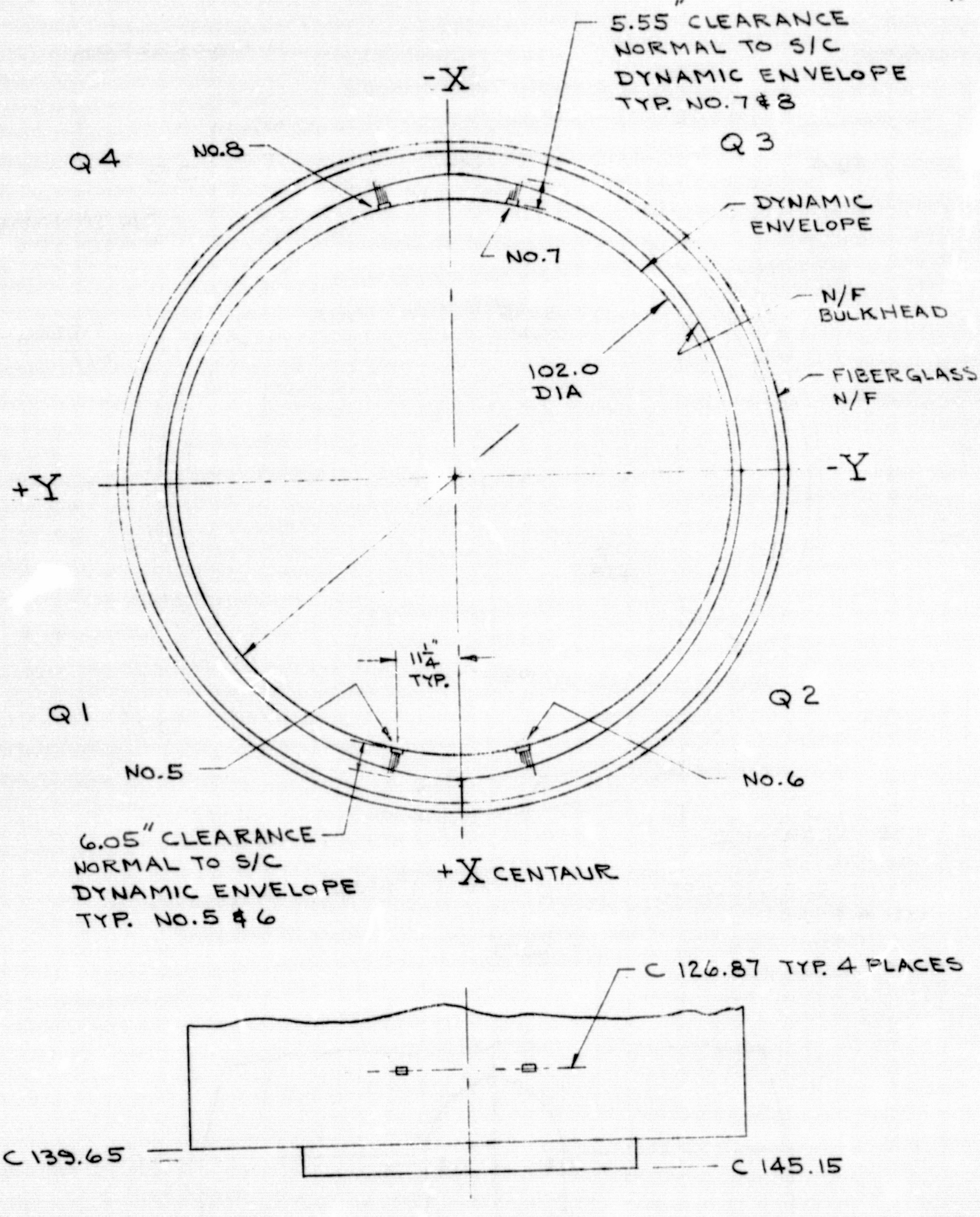

CLEARANCE TO N/F BULKHEAD (TEST #1)

FIGURE 58

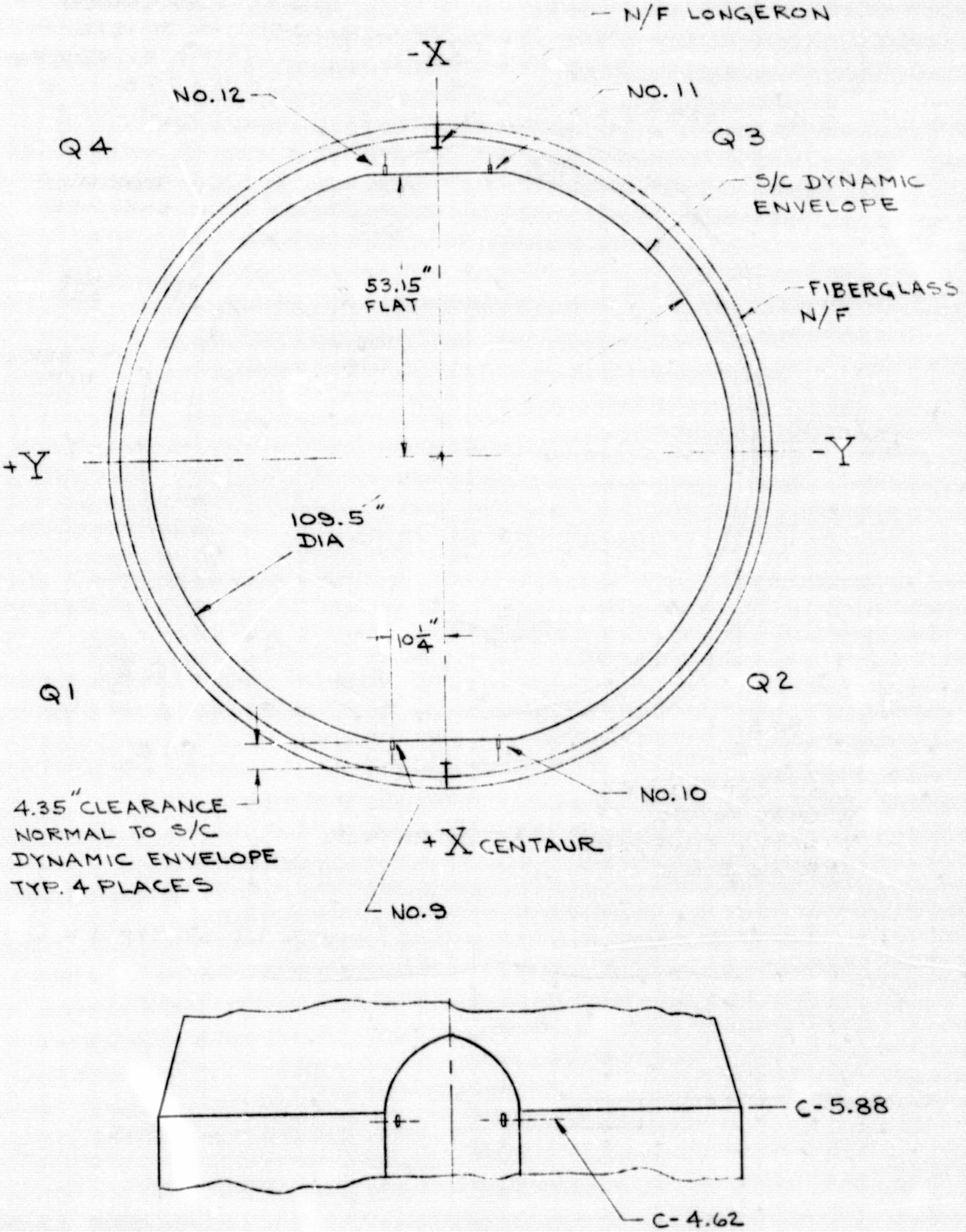

CLEARANCE TO N/F LONGERON
FIGURE 59 (TEST #1)

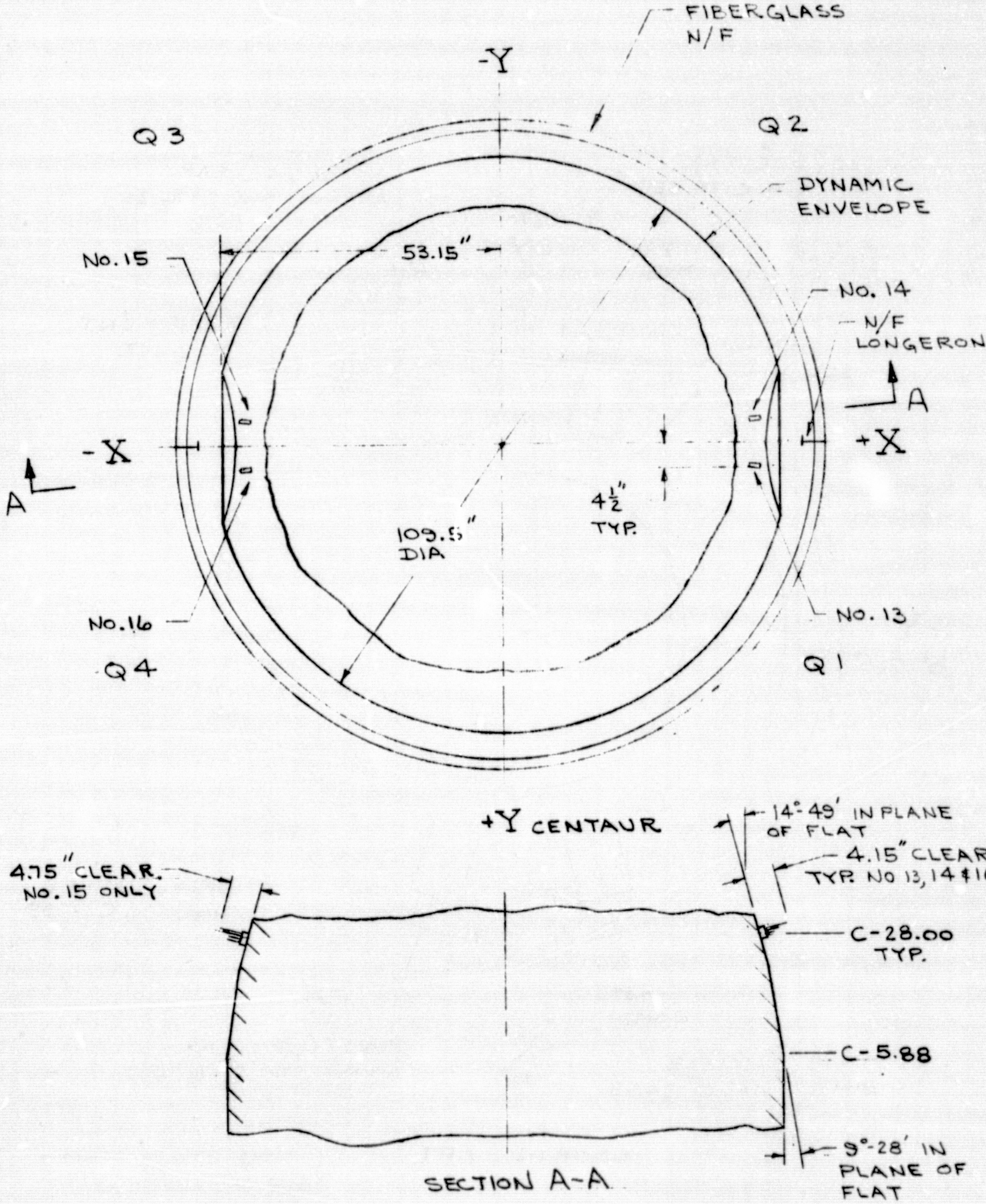

CLEARANCE TO N/F LONGERON (TEST #1)

FIGURE 60

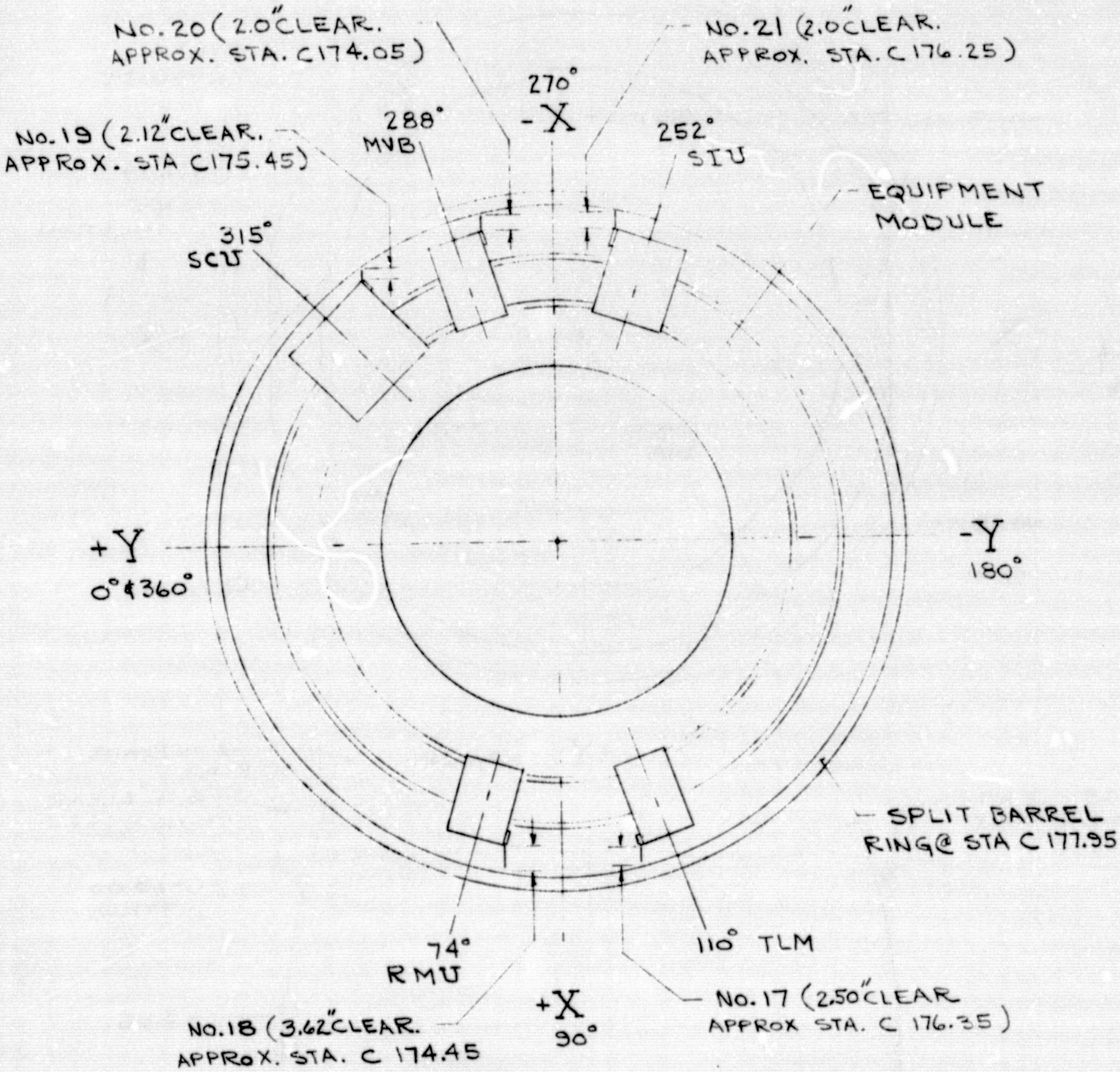

LOOKING AFT

CLEARANCES TO EQUIPMENT MODULE PACKAGES (TEST #1)

FIGURE 61

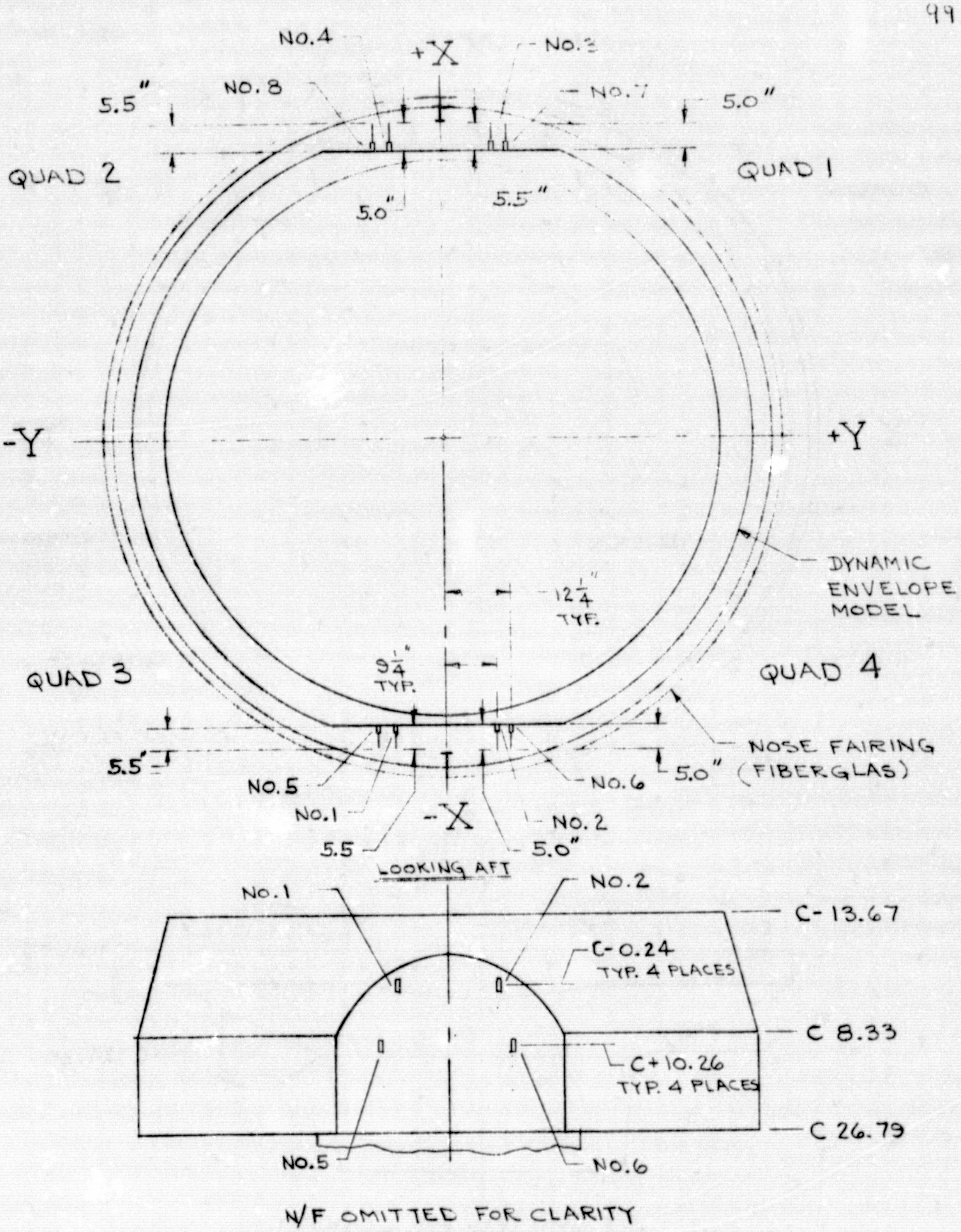

CLEARANCE TO NOSE FAIRING LONGERON (TEST #3)

FIGURE 62

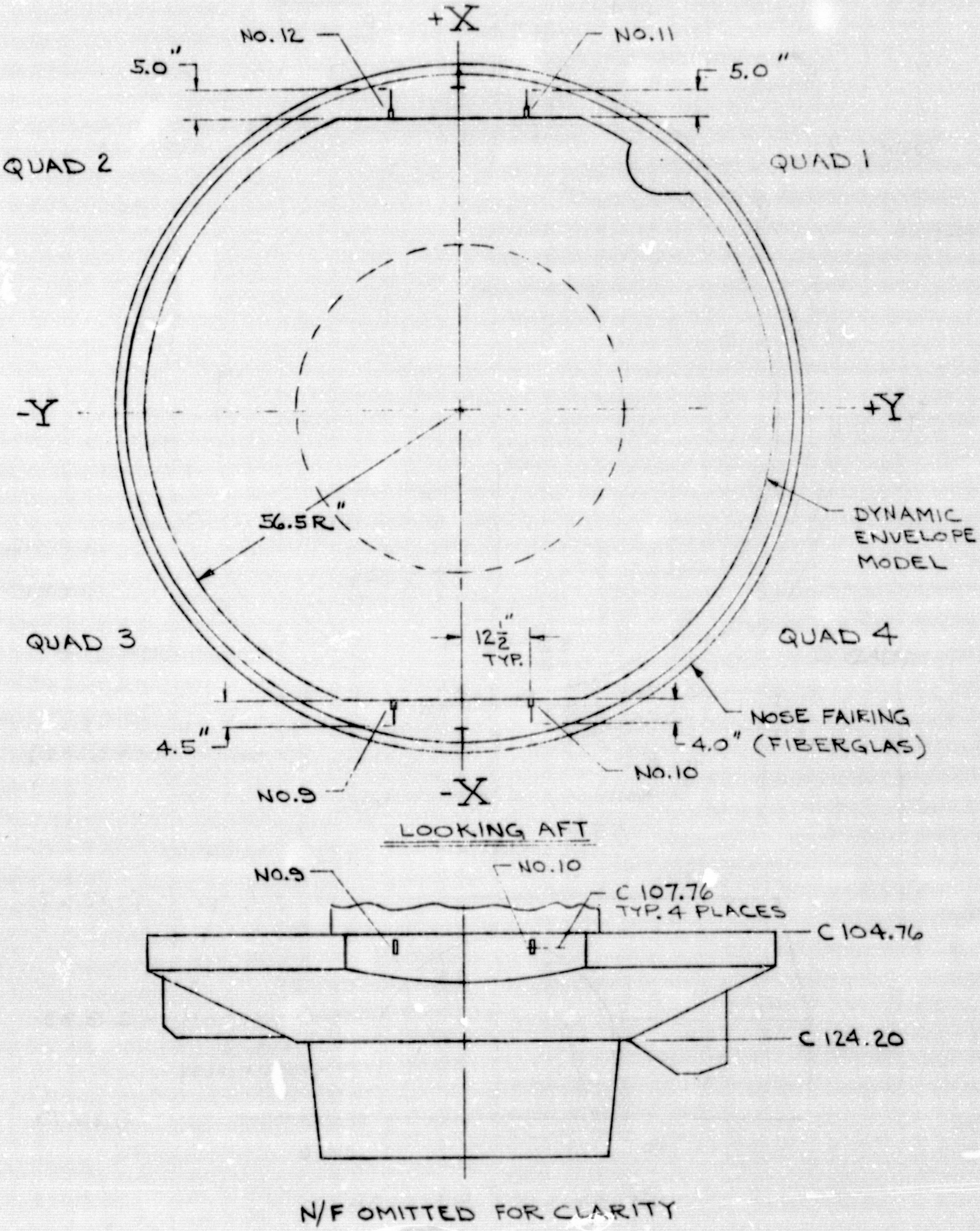

CLEARANCE TO NOSE FAIRING LONGERON (TEST #3)

FIGURE 63

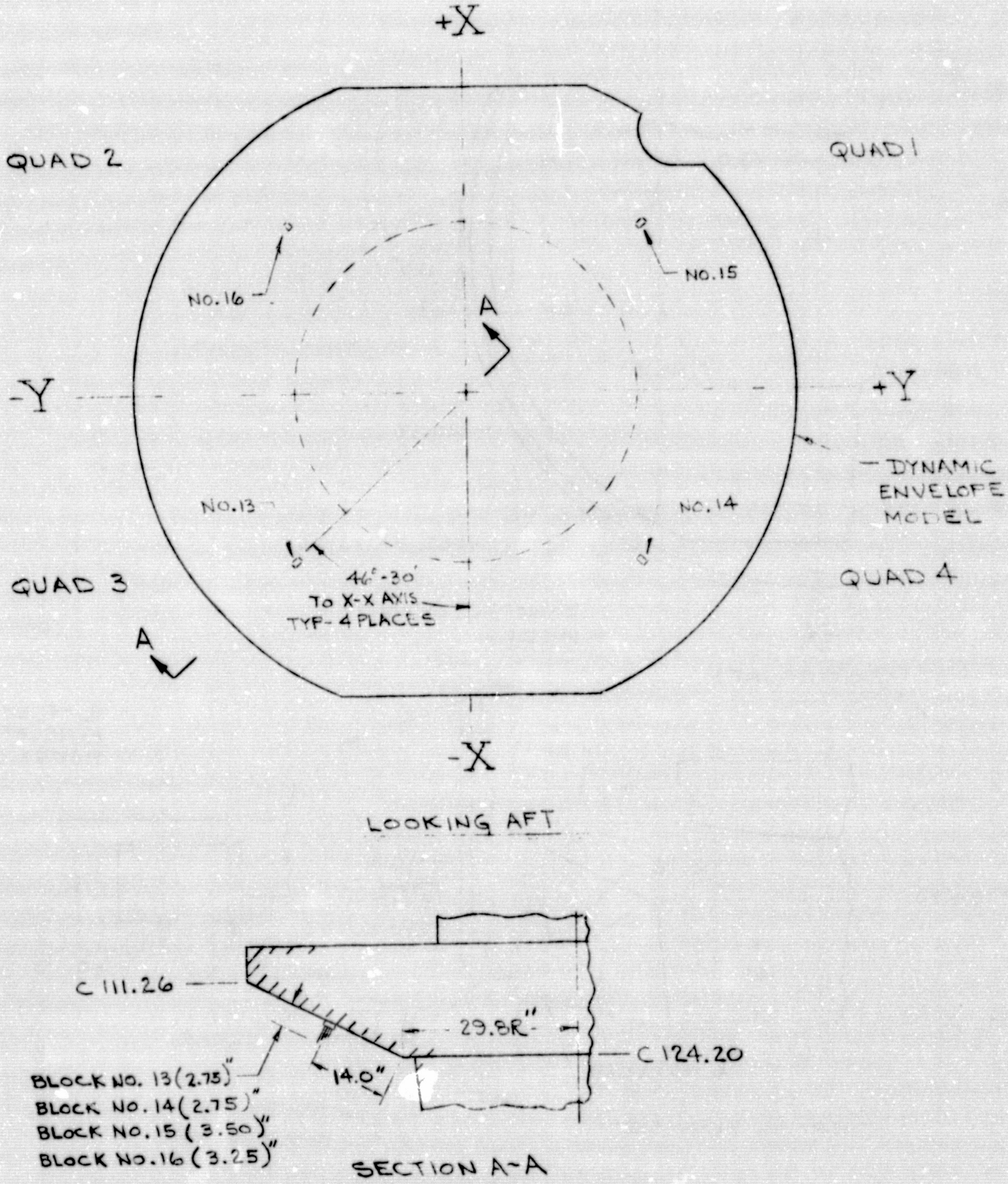

CLEARANCE TO THERMAL BULKHEAD I.D. (TEST #3)

FIGURE 64

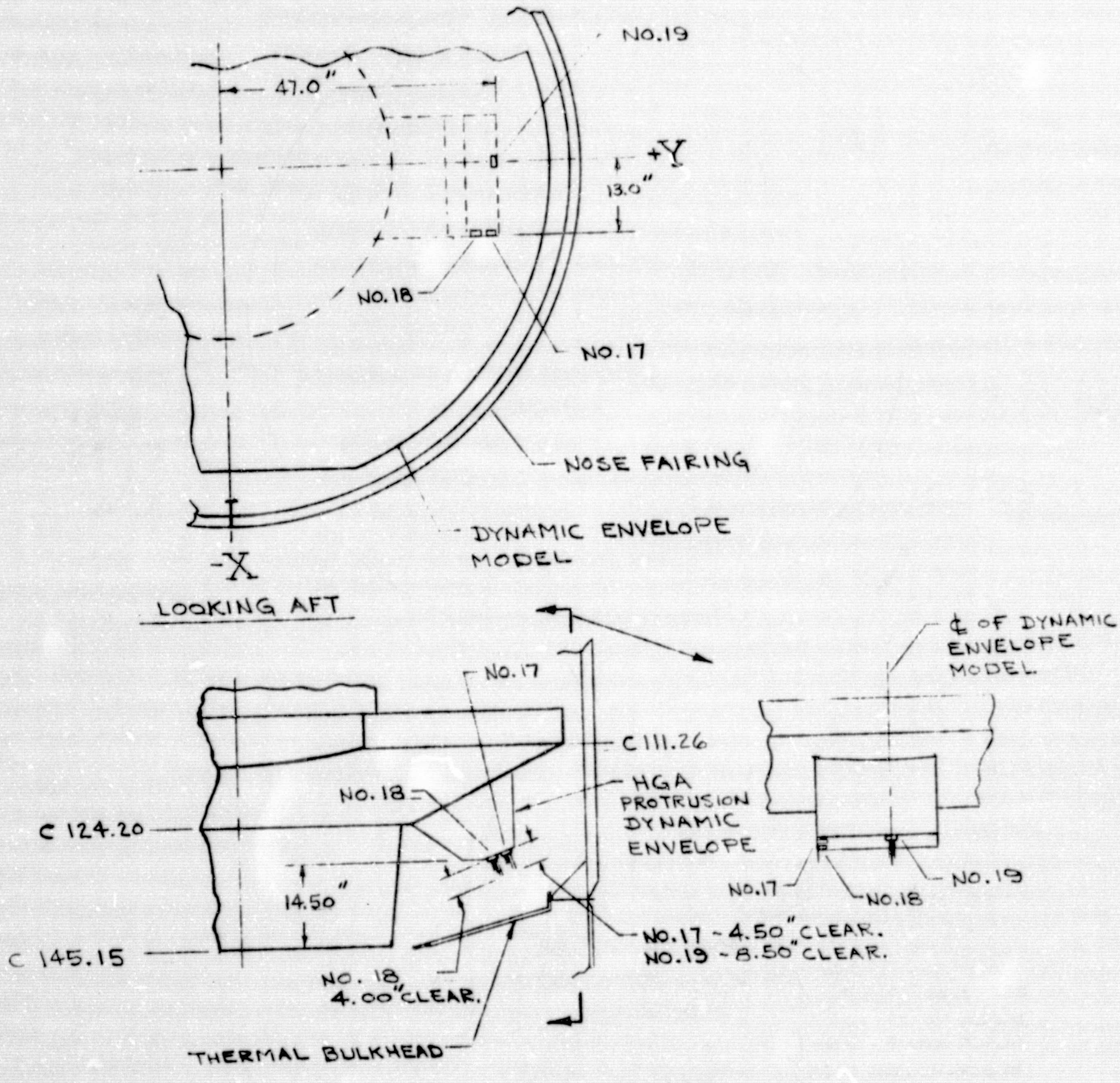

CLEARANCE TO THERMAL BULKHEAD I.D. & STRUTS (TEST #3)

FIGURE 65

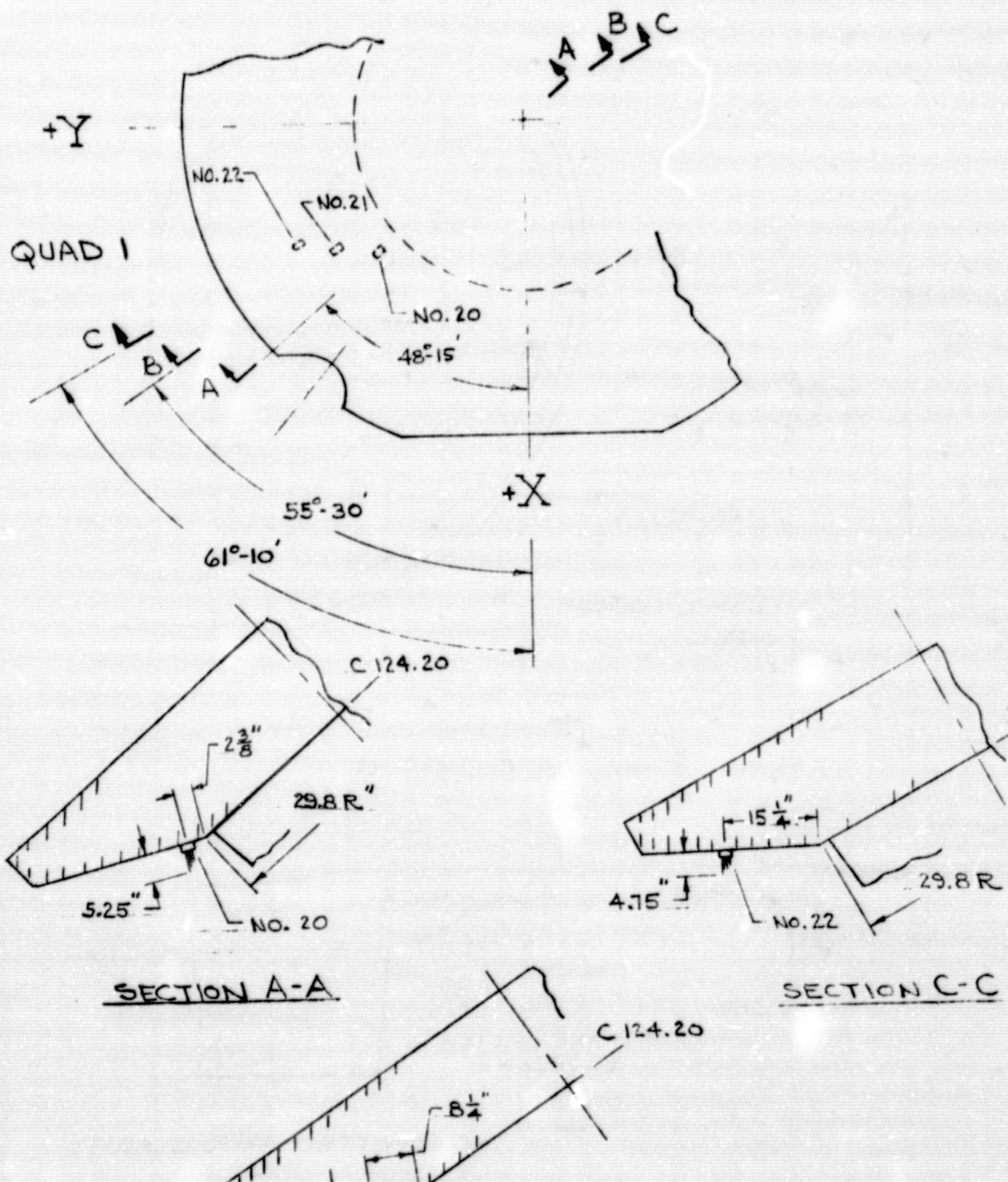

CLEARANCE TO F.P.A. AIR CONDITIONING BELLOWS (TEST #3)

FIGURE 66

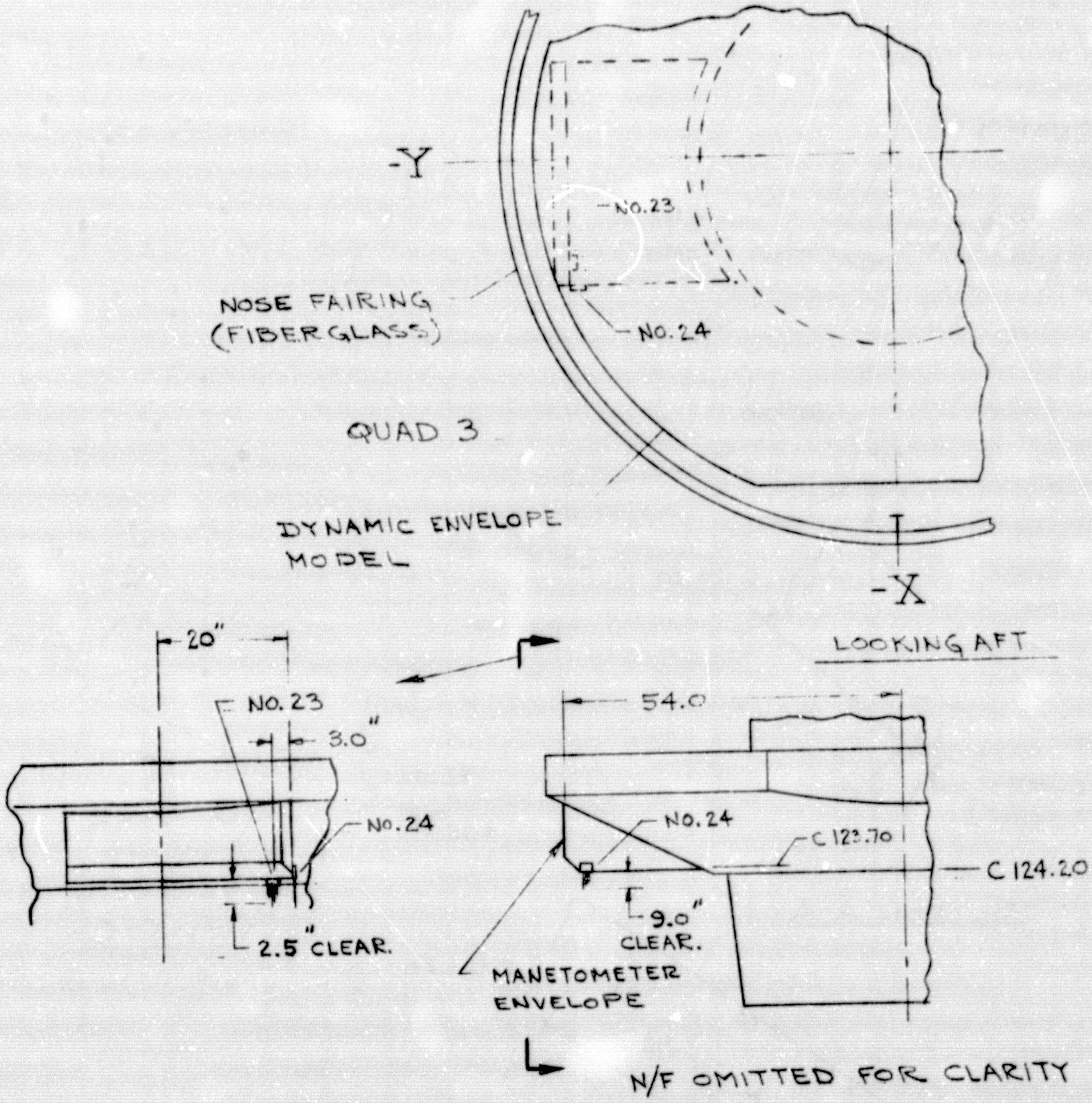

CLEARANCE TO THERMAL BULKHEAD I.D. & STRUTS (TEST #3)

FIGURE 67

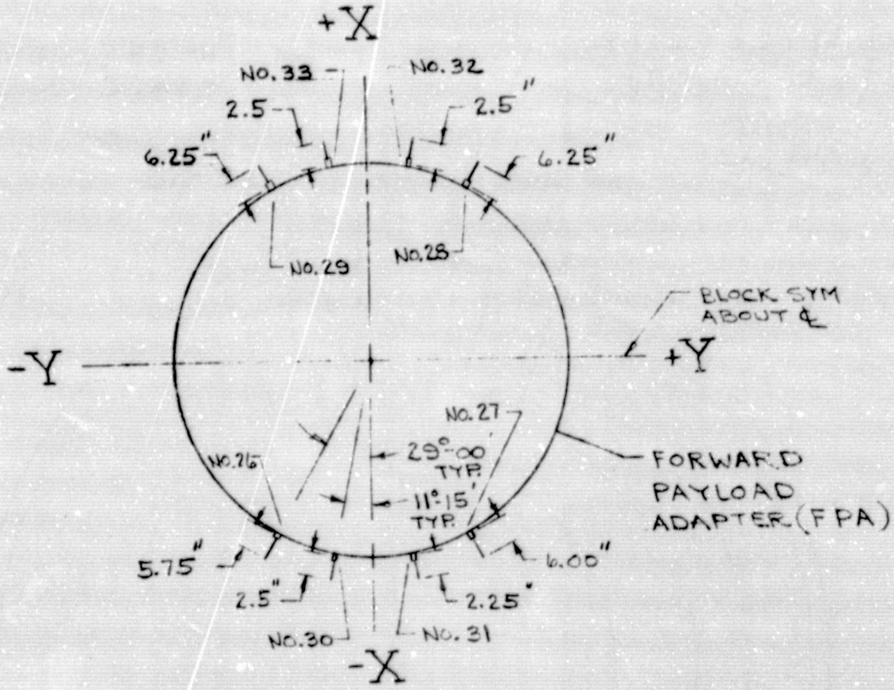

SECTION A-A
LOOKING AFT

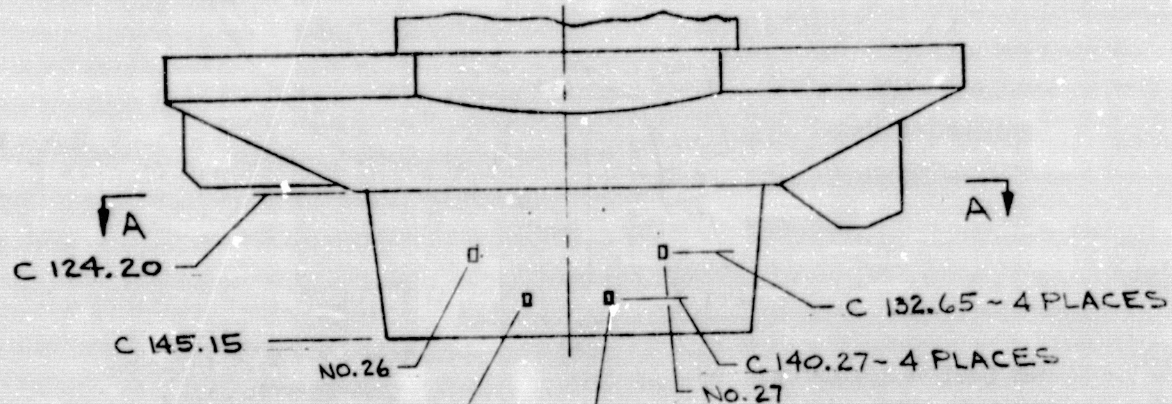

CLEARANCE TO THERMAL BULKHEAD I.D. (TEST #3)

FIGURE 68

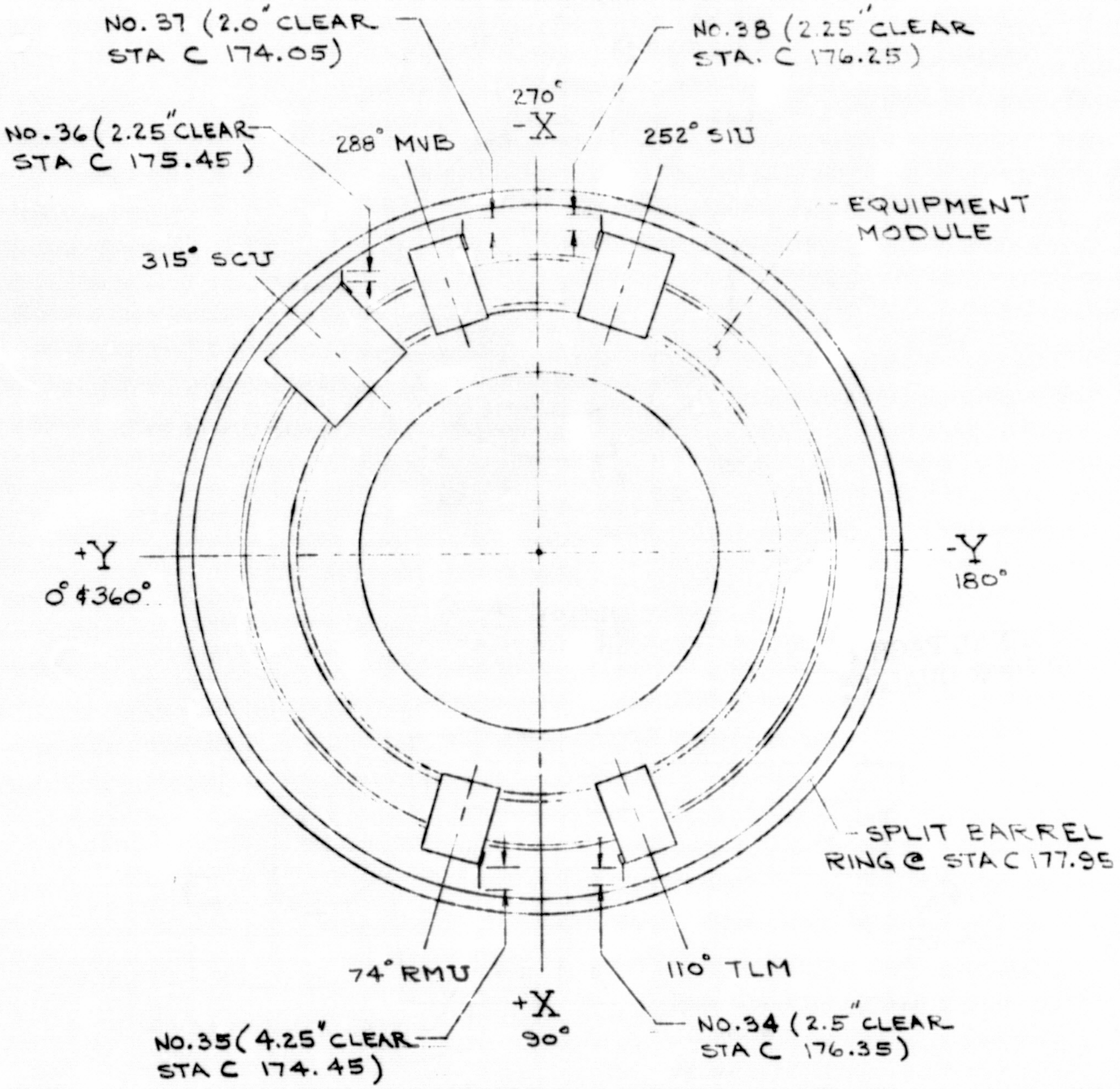

CLEARANCE TO SPLIT BARREL INTERNAL RINGS (TEST #3)

FIGURE 69

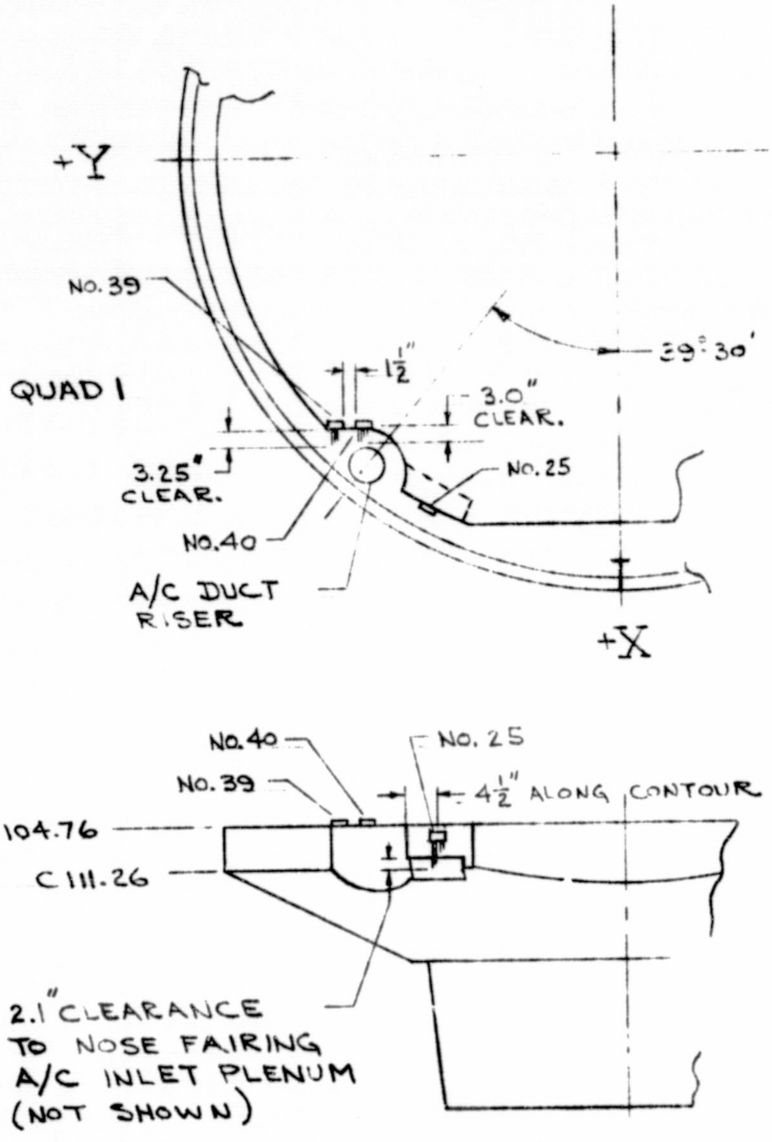

N/F OMITTED FOR CLARITY

CLEARANCE TO NOSE FAIRING A/C PLENUM & RISER (TEST #3)

FIGURE 70